# SCALABLE INDOOR LOCALIZATION USING ULTRA-WIDEBAND RADIOS

---

A Dissertation Presented to
the Faculty of the Department of Computer Science
University of Houston

---

In Partial Fulfillment
of the Requirements for the Degree
Doctor of Philosophy

---

By

SeyyedHessamAldin Mohammadmoradi

May 2019

# SCALABLE INDOOR LOCALIZATION USING ULTRA-WIDEBAND RADIOS

SeyyedHessamAldin Mohammadmoradi

APPROVED:

Dr. Omprakash Gnawali, Chairman
Dept. of Computer Science

Dr. Jaspal Subhlok
Dept. of Computer Science

Dr. Edgar Gabriel
Dept. of Computer Science

Dr. Sirajum Munir
Bosch Research & Technology Center, USA

Dr. Kyungki Kim
Dept of Construction Management

Dean, College of Natural Sciences and Mathematics

# Acknowledgment

Firstly, I would like to express my sincere gratitude to my advisor Prof. Omprakash Gnawali for the continuous support of my Ph.D study and related research, for his patience, motivation, and immense knowledge. His guidance helped me in all the time of research and writing of this thesis. I could not have imagined having a better advisor and mentor for my Ph.D study.

Besides my advisor, I would like to thank the rest of my thesis committee: Prof. Jasphal Sublhok, Prof. Edgar Gabriel, Prof. Kyungki Kim, and Dr. Sirajum Munir, for their insightful comments and encouragement, but also for the hard question which helped me to widen my research from various perspectives.

My sincere thanks also goes to Dr. Sirajum Munir at Robert Bosch research and technology center at Pittsburgh, Pennsylvania, and Dr. Dan Jiang at Philips Lighting research center at Cambridge, Massachusetts, who provided me an opportunity to join their teams as intern, and who gave access to the laboratory and research facilities and work on topics related to my PhD research. Without they precious support it would not be possible to conduct this research.

I thank my fellow labmates, Milad Heydariaan, Shengrong Yin, Nour Smaoui,and Nacer Khalil in Networked System Laboratory for the stimulating discussions, for the sleepless nights we were working together before deadlines, and for all the fun we have had in the last six years. In particular, I am grateful to Milad Heydariaan for his continued support and collaboration during my PhD research.

The accomplishment of this study would not have been possible without the unconditional love and support of my family, to whom this dissertation is dedicated: my honorable father, my precious mom, and my supportive brother.

# Previously Published Material

Chapter 3 revises a previous publication [62]: H. Mohammadmoradi, M. Heydariaan, O. Gnawali. UWB Physical Layer Adaptation for Best Ranging Performance within Application Constraints, Proc. ACM ICSDE, 2018.

Chapter 4 revises a previous publication [64]: H. Mohammadmoradi, M. Heydariaan, O. Gnawali, K. Kim. UWB-Based Single-Anchor Indoor Localization Using Channel Impulse Response, Proc. IEEE CNC, 2019.

Chapter 5 revises a previous publication [61]: H. Mohammadmoradi, O. Gnawali. Study and Mitigation of Non-Cooperative UWB Interference on Ranging, Proc. ACM EWSN, 2019.

Chapter 6 revises a previous publication [63]: H. Mohammadmoradi, M Heydariaan, O Gnawali. SRAC: Simultaneous Ranging and Communication in UWB Networks, Proc. to IEEE DCOSS, 2019.

# SCALABLE INDOOR LOCALIZATION USING ULTRA-WIDEBAND RADIOS

An Abstract of a Dissertation

Presented to

the Faculty of the Department of Computer Science

University of Houston

In Partial Fulfillment

of the Requirements for the Degree

Doctor of Philosophy

By

SeyyedHessamAldin Mohammadmoradi

May 2019

# Abstract

The recent advances in the Internet of Things (IoT) technologies have started a new era in sensor networks and smart assistant systems. Various types of sensing platforms are being deployed to understand the in-depth behavior of people while maintaining human comfort. Technology that tracks people inside buildings could become a key enabler for many applications in this space.

Indoor localization is a process to find the exact location of devices, objects or people inside buildings in which GPS service is mostly unreliable. Existing indoor localization and tracking solutions can be divided into two main categories: passive and active solutions. Passive asset tracking systems are scalable, but their accuracy is limited to a few meters (Room Level). On the other hand, in active tracking scenarios, the target has to carry a tacking device, which makes the location estimation more accurate and robust. In this dissertation, we improve the scalability and robustness of indoor tracking solutions.

Ultrawideband (UWB)-based indoor localization techniques are one of the well-known and popular active indoor tracking systems. Large bandwidth of UWB signals makes them resilient to multipath fading problem and brings the ability to estimate the location of a target with a few centimeters error. Despite the recent advancement of the accuracy of UWB based indoor tracking systems, the scalability of these systems did not receive enough attention from the research community until the last few years.

In this dissertation, we focus on four primary challenges in scalability of UWB systems: adaptively finding optimum UWB physical layer setting to achieve best ranging performance while maintaining application requirements, reducing deployment constraints by proposing single anchor UWB indoor localization, studying and mitigating the impact of multi-user interference on UWB ranging, and combining ranging traffic with non-ranging traffic to increase the applicability of UWB networks for non-ranging applications.

# Contents

# List of Figures

# List of Tables

# Chapter 1

# Introduction

Recent advances in the Internet of Things (IoT) technologies have started a new era in sensor networks and smart assistant systems. Various types of sensing platforms are being deployed to understand the in-depth behavior of the people. Technology that tracks people inside buildings could become a key enabler for many applications in this space.

Indoor localization is a process to find the exact locations of devices, objects or people inside buildings in which GPS service is mostly unreliable. Existing indoor localization and tracking solutions can be divided into two main categories: passive and active solutions. Passive asset tracking systems are scalable, but their accuracy is limited to a few meters (Room Level). The key idea in passive indoor localization techniques is utilizing existing sensing infrastructure for monitoring activities and movements inside the buildings. Each activity has some impact on the sensing environment, and by continuously monitoring the environment, those techniques can locate activities.

Passive indoor localization techniques are not able to achieve high levels of accuracy in estimating the locations of people. On the other hand, active localization techniques are very accurate in terms of location estimation. In such systems, the target carries a device that communicates with the infrastructure, and the location of target can be estimated using communication link properties. Ultra-wideband (UWB)-based indoor localization systems are state-of-the-art active solutions that, on average, can achieve less than 5 cm error in locating devices [60]. The most common active localization system measures its distance to 3 other anchors, which are devices with known locations, and using trilateration, the target can locate itself inside the building.

## 1.1 Scalability Challenges

Despite the existence of very accurate UWB-based indoor localization techniques, the scalability of such systems is under question. Through our studies, we identified four primary challenges in UWB networks which need to be addressed to pave the way for UWB radios to become scalable indoor localization solutions.

- UWB physical layer, as defined in IEEE 802.15.4, has several parameters which can be configured to control the tradeoff between energy efficiency and ranging performance. Finding the optimal setting for UWB physical layer considering the application constraints is a challenge.

- Existing UWB localization solutions rely on line of sight access to anchors to be able to locate the target. This requirement increases the deployment constraints and reduces the scalability of such systems.

- To the best of our knowledge, multiuser interference is not properly addressed in UWB-based indoor positioning systems. State-of-the-art solutions use random back off, or TDMA approaches to avoid interference between users, but these approaches are not scalable. UWB-based systems suffer from the unreliable access control mechanism, and multi-user interference can degrade the performance of such systems.

- Alongside with ranging capabilities, UWB radios have communication capabilities. Today's indoor localization techniques rely on separate protocols for ranging and communication which increases the complexity of these systems.

## 1.2 Dissertation Contribution

In this dissertation, we study and address all four above mentioned scalability related challenges in UWB Networks.

- We study the impact of changing different parameters at UWB physical layer on ranging performance and propose our proposal to adaptively search and find optimal physical layer setting to minimize the ranging error while maintaining application requirements in terms of energy and delay. We evaluated the performance of our framework in real-world environment scenarios, and our results show an average 20% reduction in range errors achieved by our proposed method through proper setting of UWB physical layer parameters. We published the results of our work as a conference paper at IEEE ISCDE'18 conference.

- To relax the minimum 3 line of sight (LoS) anchors constraint from UWB based indoor localization solutions, we investigate the feasibility of fingerprinting for indoor localization to reduce the number of required anchors. We propose our novel single anchor UWB based indoor localization technique which is based on generating unique fingerprints using UWB signals received in each spot. Our results show using previously generated fingerprints, our solution can locate moving target inside the square of 20 cm $\times$ 20 cm with the accuracy of 96%. We published our proposed technique as a workshop paper at IEEE CNC'19 workshop.

- To make UWB-based tracking systems more robust, we study the likelihood of UWB interference in indoor localization applications. We quantify the possibility of interference in such solutions and show the impact of such interference on ranging performance. We also propose simple yet effective techniques to detect packets impacted by interference and also mitigate ranging error caused by interference. We observe 30% to 40% reduction in ranging error caused by interference after applying our proposed technique. We published the results of our study as a conference paper at ACM EWSN 2019 conference.

- To improve the scalability of UWB networks, we utilize the communication capabilities of UWB radios. In all the existing UWB based indoor localization techniques, the UWB radio is used only for ranging. We study the possibility of running non-ranging applications over UWB networks and analyze the co-existence of ranging traffic alongside with non-ranging traffic. We show the feasibility of piggybacking the information required for ranging (timestamps) on top of non-ranging traffic and vice versa. We propose our adaptive scheduler which monitors both ranging and non-ranging traffic and piggybacks either ranging traffic over non-ranging traffic or vice versa. Our results show that our adaptive scheduler can reduce 40% of network traffic. We published this work as a full paper in IEEE DCOSS 2019 conference.

In summary our focus in this dissertation can be divided to two major problem on scalability of the UWB-based indoor localization. First challenge is minimum number of required anchors for locating the target in which we proposed single anchor indoor localization to reduce the number of anchors from three to one. The second challenge is contention in UWB networks. In our first attempt to reduce contention in UWB networks, we decrease number of packets by piggybacking information which reduces the network traffic by 30% to 40%. On the second work in this area, we propose adaptive physical layer configuration in which we minimize the length of the packet while preserving ranging performance. We also propose using random pulse shapes to be able to recover packets distorted by interference and our results indicates 50% reduction in error caused by collision. Based on the results we achieved in this dissertation, we can estimate that the combined solution is able to handle network of 20 to 30 nodes with localization error below 30 cm.

## 1.3 Dissertation Organization

We organize the rest of the dissertation as follows. In Chapter 2, we present background information about UWB signals and UWB-based ranging and localization techniques. In Chapter 3, we propose a novel approach to adaptively tune UWB physical layer setting to improve ranging performance while maintaining application energy and time constraints. Chapter 4 describes our fingerprinting technique to reduce the number of required anchors for indoor localization to just one anchor. We explain our measurement campaign and modeling techniques used for generating fingerprints. Chapter 5 presents the detailed UWB interference analysis and provides detailed information about our proposed interference detection and mitigation techniques. Chapter 6 introduces our proposed network traffic scheduler alongside with our novel technique for combining ranging and non-ranging traffic. Finally, chapter

7 concludes our contributions in this dissertation.

# Chapter 2

# UWB Ranging/Localization Basics

IEEE 802.15.4-11 standardized the use of low power UWB signals in wireless sensor networks. In this chapter, we briefly explain basics of UWB communication and UWB physical layer parameters defined by this standard.

## 2.1 UWB Wireless

Wireless signals with the bandwidth higher than 20% of their central frequency are called Ultra-wideband (UWB) signals. Although this general definition can be applied to many frequency ranges but most popular center frequencies for UWB signals are in the range of 3 GHz to 10 GHz and according to the IEEE 802.15.4 standard [41], the minimum bandwidth for each UWB channel is 500 MHz.

### 2.1.1 Physical Layer Modulation

IEEE 802.15.4-11 [9] standardized the use of low power UWB signals in personal area networks (PAN). In this standard, a specific format has been defined for UWB packets. It begins with a synchronization header consisting of the preamble and the start of frame delimiter (SFD) after which the PHY header (PHR) defines the length (and data rate) of the data payload part of the frame. The UWB used in 802.15.4 is sometimes called impulse radio UWB because it is based on high-speed pulses of RF energy. The PHR and Data parts of the frame, use burst position modulation (BPM) in which position of the burst is utilized to modulate the bits. In addition, binary phase-shift keying (BPSK) is used to shift the phase of the burst by calculating a parity bit.

Forward error correction (FEC) is also included in the PHR and Data parts of the frame. The PHR includes a 6-bit single-error-correct double-error-detect (SECDED) code and the data part of the frame has a Reed Solomon (RS) code applied. These features increase the resilience to interference in the receiver.

In contrast to the BPM/BPSK modulation used for the PHR and data, the synchronization header consists of single pulses. Preamble code defines the actual sequence of pulses sent on each symbol interval. The preamble sequence has a property of perfect periodic autocorrelation which helps a coherent receiver to estimate precise impulse response of the radio channel (CIR).

In summary PHR and Data parts of UWB frame are more resilient to interference compared to synchronization header due to the difference in modulation schema used in these sections compared to synchronization header.

### 2.1.2 UWB Physical Layer Parameters

UWB communication link has to be configured properly before being used for localization or communication purposes. Fundamental factors in UWB links are explained in this section. In this section, we focus on the parameters which are supported by

DW1000 chip [3], a widely used UWB platform.

- Center Frequency: The IEEE 802.15.4 standard UWB PHY defines 16 different channels; the ones supported by DW1000 have been summarized in Table 2.1. Since different channels face different levels of ambient noise, proper selection of center frequency has a critical role in the robustness of the system.

- Preamble Length: UWB packet begins with a synchronization header which contains the preamble and Start of Frame Delimiter (SFD). During the message reception phase, the receiver searches channel to observe the preamble, and once the preamble is detected, the receiver looks for SFD symbols. The moment the receiver detects the first SFD symbol is timestamped as the time of arrival (ToA) for the message. Higher robustness in longer ranges after increasing the length of preamble comes at the price of consuming more energy and spending more time sending each message.

- Pulse Repetition Frequency (PRF): The PRF is one of the basic characteristics of radio systems. In simple terms, PRF defines the amount of time interval between sending two consecutive pulses. After sending the first pulse, the transmitter is not sending new pulses for a time period which gives the receiver enough time to hear the reflections of the first pulse. The required time between sending of each pulse is a function of the system's desired range. Higher PRF values generate more pulses in the constant amount of time, and thus higher radio energy, which are detectable in longer distances. UWB standard defines 16 MHz and 64 MHz as standard PRF values for communication.

- Preamble Code: Depending on the channel and PRF, IEEE 802.15.4 standard defines a choice of two or four preamble codes. These preamble codes are designed in a way that they have a low cross-correlation with each other with

Table 2.1: UWB Physical Layer Parameters (Supported by DW1000)

| Parameter | Values |
|---|---|
| Frequency Channel (MHz) | 1(3494.4), 2(3993.6), 3(4492.8), 4(3993.6), 5(6489.6), 7(6489.6) |
| Bandwidth (MHz) | 1(499.2), 2(499.2), 3(499.2), 4(1331.2), 5(499.2), 7(1081.6) |
| Pulse Repetition Frequency (PRF) | 16 MHz, 64 MHz |
| Preamble Length (symbols) | 64, 128, 256, 512, 1024, 2048, 4096 |
| Date Rate | 110 Kbps, 850 kbps, 6.8 Mbps |

the intention that separate channels with different preamble codes can work simultaneously without interfering with each other.

- Data Rate: IEEE 802.15.4 standard has defined three different data rates (110 kbps, 850 kbps, and 6.8 Mbps) for UWB communication.

Table 2.1 summarizes all UWB physical layer's adjustable parameters and their potential values.

## 2.2 UWB-based Localization Procedure

The procedure in UWB based localization techniques is similar to GPS approaches. In a 2D localization setting, there are at least 3 anchor points with the known positions and the fourth node (Tag) which can locate itself by measuring its distance to each anchor and finding the intersection of the circles with the centers at anchor locations and the radius of distance to each anchor as shown in Figure 2.1a.

To measure the distance between the Tag and each anchor at least 2 messages needs to be exchanged between them. In the simplest scenario Tag sends the first message to the anchor and puts the time of sending inside the message (T1). The

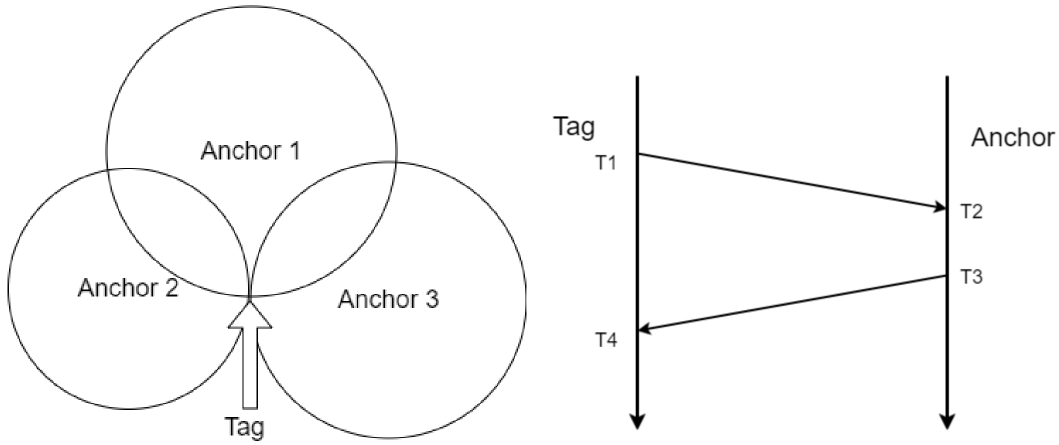


(a) Intersection of circles is the location of Tag

(b) Ranging technique in UWB

Figure 2.1: UWB-based localization procedure

anchor receives the message and marks the reception time (T2) and replies back with the second message which contains sending time from the anchor (T3) alongside with reception time (T2). Upon the reception of the second message at Tag (T4), signals travel time can be calculated using formula 2.1:

$$SignalTravelTime = \frac{(T4 - T1) - (T3 - T2)}{2} \tag{2.1}$$

This process is called two-way ranging and is illustrated in Figure 2.1b.

### 2.2.1 Time of Arrival Measurement in UWB

Perfect auto-correlation between preamble codes allows UWB receiver to accurately estimate channel impulse response (CIR). The accurate CIR helps the receiver to resolve the channel in detail and determine the arrival time of the first (most direct) path, even when attenuated.

Accurate ranging using UWB requires the ability to precisely detect first path's time of arrival. The challenging part in time of arrival estimation is proper selection of the threshold for the minimum gap between signal's power and noise. If the gap

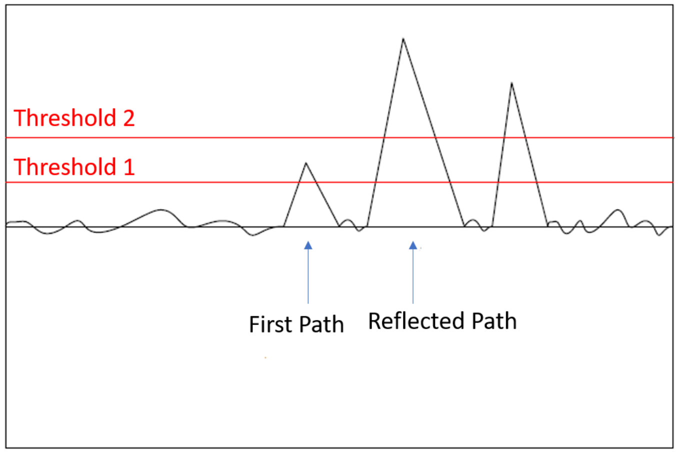


Figure 2.2: Energy-based first path detection

between the power of the first path and the noise floor is small, the chance of misclassification of noise signal as the first path signal (false positive) increases. On the other hand, higher threshold value increases the chance of not finding the first path signal which is buried in the noise (false negative).

### 2.2.2 First Path Detection Challenge in UWB Ranging

The challenging part in ToA calculation is proper selection of the threshold for the minimum gap between signal's power and noise. The smaller gap between first path power and noise floor increases the chance of misclassification of noise as the first path signal. On the other hand, higher threshold values, increase the chance of not finding the firth path signal. This phenomenon is shown in Figure 2.2 where *Threshold 2* is not a suitable choice but *Threshold 1* is able to detect proper first path.

Another problem in UWB systems is that the Non-Line-of-Sight (NLoS) signal is indistinguishable from LoS on the receiver side. For instance in Figure 2.2, in the case that the system is using *Threshold 2* value, the receiver can not spot the real first path and will consider reflected signal (second peak) as the first path. There is no practical way for the receiver to realize that the measured distance is wrong due to detection of NLoS signal as LoS.

# Chapter 3

# UWB Physical Layer Adaptation for Best Ranging Performance

Despite very accurate results achieved by UWB-based techniques to track objects with errors less than 5 cm [60], building a robust UWB-based indoor localization system is challenging. The accuracy of localization with UWB technology depends on the propagation characteristics of the unique circumstances of the deployment. To achieve best ranging performance one can set the transmission power and frame length to the maximum possible but that approach is not suitable in some applications. For instance, increasing frame length decreases the location update rate (due to interference) which is not desired in most of the tracking applications. There are no tools or methodologies to determine the best configuration for UWB communication to increase ranging quality while limiting power consumption and air utilization within application constraints. Without those tools and methodologies, it is difficult to achieve accurate and efficient UWB-based localization while meeting application constraints in power and latency. Dynamics in wireless propagation environment requires re-discovery of best settings, thereby making the problem of robust indoor localization even more challenging.

One of the major problems that threatens the robustness of UWB based indoor localization systems, is short coverage due to noise interference and attenuation from obstacles. In our work, we propose a framework to make UWB localization more robust and resilient to attenuation and noise. We implement an efficient algorithm to find the best setting for the UWB channel which gives the best ranging performance while it meets power consumption and air utilization requirements. Our solution changes the parameters of the UWB channel to improve the quality of ranging which makes the whole localization system more reliable and robust. The proposed method can be used during the deployment phase to find the best channel setting and also during online ranging once the quality of ranging drops due to changes in the environment. We proposed a simple technique to monitor the ranging performance and trigger the proposed method to change the UWB channel setting if the quality of ranging drops below a certain threshold.

Our contributions in this work can be summarized as the following:

- Investigate the impact of changing UWB communication channel configuration on accuracy and robustness of UWB-based indoor localization system.
- Design a framework to monitor the quality of ranging and change the configuration of UWB physical layer to improve the ranging accuracy while maintaining power consumption and frame duration restrictions.
- Evaluate the performance of the system in a real-world environment using DW1000 UWB transmitters.

## 3.1 Related Work

The literature on UWB based indoor localization techniques can be divided into two major topics: First path detection techniques and error detection techniques. The following paragraphs elaborate on both areas in more details and cover state-of-the-art work in UWB indoor localization.

### 3.1.1 First path detection in UWB

Time-of-Arrival (ToA) is a critical concept in wireless indoor positioning systems. The general idea here is that considering the constant speed of the signal through the air, accurate measurement of signal's flight time provides an accurate estimation of the distance between sender and receiver nodes. The challenging part is accurately timestamping signal's ToA. Even one nanosecond error in ToA measurement may cause in the order of 30 cm error in estimated range. Two most common categories of previous work to identify ToA are maximum likelihood (ML) techniques and energy-based methods.

#### 3.1.1.1 ML-based First Path Detection

Correlation between sent and received signals is utilized in ML techniques. The goal is finding the optimum propagation time which maximizes the correlation between sent and received signals. Experiments have shown that ML estimators can achieve to the Cramer Rao Lower Bounds (CRLB) in the high-SNR region [22]. In addition to the correlation between sent and received signals, the similarity between uplink and downlink also has been utilized to estimate the most likely propagation time for the signal [69]. However, ML estimators require processing the signal at very high sampling rates which makes them inapplicable in most of the low power embedded system implementations.

#### 3.1.1.2 Energy-based First Path Detection

Energy-based ToA detection algorithms utilize the power of the received signal as an indicator to leading edge of the signal [27]. The basic idea is sampling the received signal and detecting the first sample which has higher power than a particular threshold as the leading edge of the signal. Although the accuracy of energy-based first path detection techniques is not as good as ML estimators, they are much easier to implement. The first sample that passes the threshold is considered as the first path and is used to measure ToA.

The real challenge in energy based leading edge detection techniques is selecting the proper threshold. There are many research work that tried to propose a suitable threshold based on the signal and noise characteristics. The lowest complexity approach is monitoring a massive amount of data and finding the best threshold value to set for deployment [39]. Threshold also can adaptively change based on the maximum and minimum energy level in the signal [42], [55]. A proper threshold value should be designed depending on the received signal characteristics, the operating condition, and the channel characteristics. The ambient noise floor is an important factor in detecting the first path. SNR can be utilized [57] to find the best threshold to mark the leading edge of the signal. Due to their simplicity and excellent performance, energy detection-based first path detection algorithms are used in current UWB-based indoor localization systems including DW1000 chip which is most dominant UWB-enabled chip used in indoor localization [3].

The general rule of thumb in UWB ranging is that higher power UWB frames provide more accurate ranging since the gap between the first path and ambient noise will be bigger which means it would be easier for the receiver to detect the first path. IEEE 802.15.4-11 [41] which standardizes the low power UWB communication suggested a few adjustable parameters for UWB physical layer which provides the capability of changing transmitted frame's power and duration. The effectiveness of changing these UWB physical layer settings to improve communication quality has been investigated before [37] and the results show 30% to 40% of improvements in packet reception rate under interference by changing the UWB physical layer settings.

To the best of our knowledge, there is no previous study on the impact of different UWB physical layer settings on ranging performance and quantization of each configuration's ranging improvements. Our solution finds the optimum physical layer setting which meets the power consumption and frame duration requirements of the application and at the same time minimizes the ranging errors.

### 3.1.2 UWB Localization in the Real World

Recent advances in embedded system design and development have made the inexpensive UWB transmitters available for public usage. Despite the huge body of work in UWB system design, in most cases, evaluations have been done through simulations. There are few works [40, 43, 50, 71] that tried to deploy UWB systems in the real world and report their performance. Overall, based on those reports, in the situations with clear Line-of-Sight (LoS) between two nodes, the UWB indoor localization systems are very reliable with centimeter-level accuracy in locating objects, but in the locations with high levels of noise floor or crowded areas where LoS signals are not available, there is a huge performance drop in localization performance including lots of blind spots (places where a Tag cannot determine its location) even in short ranges.

In summary, the research community has been successful to propose highly accurate UWB-based wireless indoor localization, but robustness and reliability of such systems still require a lot of attention.

## 3.2 Design

To make UWB-based indoor localization systems more robust, the best configuration for UWB channel which meets accuracy, power consumption, and air utilization requirements is selected through an efficient search algorithm. Features like preamble length and frequency channel have a significant impact on the robustness of the UWB positioning system. Higher preamble length means better robustness but with the cost of consuming more energy and having higher air utilization. In addition, reducing the receiver's threshold for received signal power, will increase coverage of the system but at the same time increases the chance of detecting noise as the first path signal in the environments with higher levels of noise. The effectiveness of changing these settings is directly related to the power in the reflected signal. In this section, we study the impact of changing each of the above mentioned UWB physical layer settings on the accuracy of localization solution.

### 3.2.1 Building the Dataset

UWB physical layer has several adjustable parameters which are listed in Table 2.1 alongside with the list of their potential values. Overall, the DW1000 chip supports 252 different configurations ($6 channels \times 2 PRFs \times 7 preamblelengths \times 3 datarates$) for UWB physical layer. To estimate ranging error associated with each configuration,

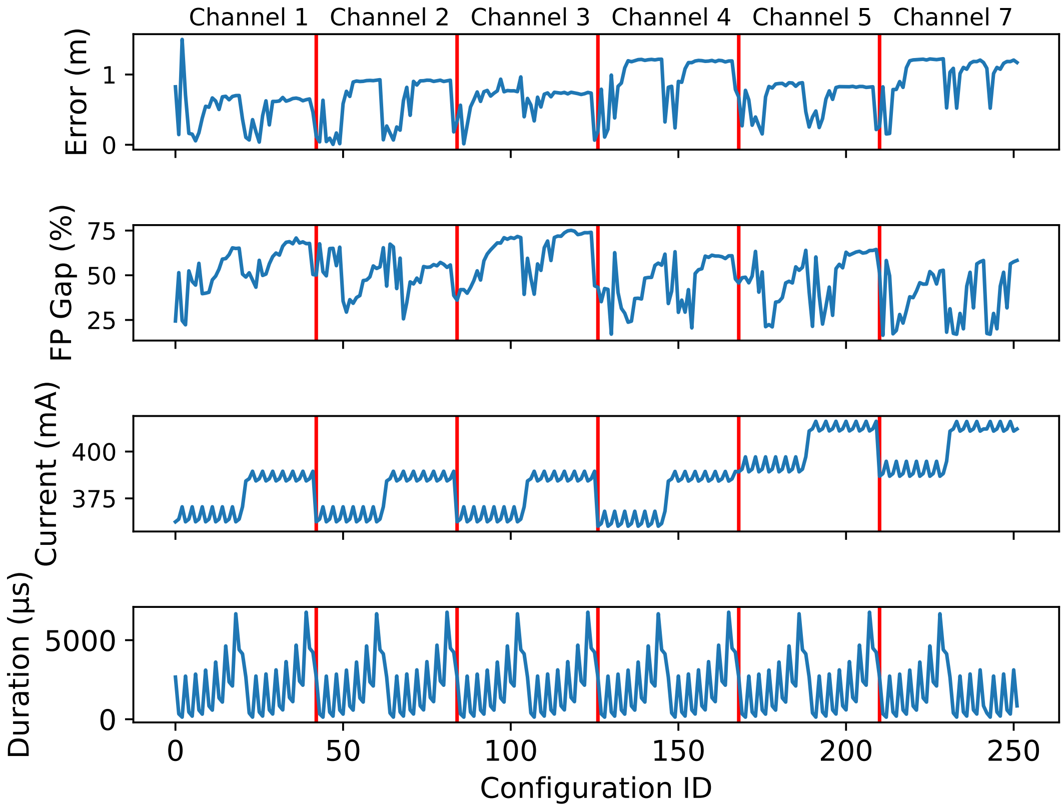


Figure 3.1: Average ranging error, first path gap, current consumption and frame duration across all 252 UWB physical layer configurations (Each configuration ID represents one combination of physical layer parameters)

we conducted experiments in 2 different locations (inside an academic building and also a coffee shop with lots of furniture). In each experiment, a pair of UWB nodes (Decawave EVB1000) are placed in the distance of 10 m from each other. The sender and transmitter both set their physical layer parameter to one setting at a time from the 252 possible settings, and under each configuration, the two-way ranging is done for 200 times. Figure 3.1 shows the ranging error, the gap between the first path signal and ambient noise ($(firstpathpower - ambientnoise)/firstpathpower$), transmission and reception current ($mA$) and frame duration ($\mu s$) for all the 252 configurations averaged based on the data collected in both of the locations.

The main purpose of Figure 3.1 is to show the impact of changing configuration of UWB channel on ranging accuracy. We use error values measured in this phase to assign an error to each of the configurations. Later on, our algorithm uses this information to find the best configuration for UWB communication and ranging. All the frame duration and power consumption measurements in this work are based on the tool [29] provided by Decawave company which measures current consumption and duration for each packet based on the channel's setting. Power consumption is a general limitation in wireless sensor networks including UWB based indoor localization. Also, there are regulatory restrictions on maximum transmission power in UWB communication. Frame duration is also important since it impacts the interference and reliability of communication.

We performed a simple experiment to determine the optimal inter-node distance for our empirical study. In this experiment, we use 2 nodes (Tag and Anchor). We configure our UWB radios to use channel 2 and increase the distance between Tag and anchor (2 m, 5 m, 10 m, 16 m, and 25 m) and measure error reported by them in different distances. We repeat the same experiment with channel 5. Figure 3.2 summarizes the results.

Figure 3.2 shows that the ranging error does not increase significantly as we increase the distance between nodes to 20 m. Based on this observation, we decide to put 2 nodes in 10 m distance during data collection phase to build our dataset.

As shown in Figure 3.1, changing the physical layer has some impact on ranging performance but what could be the reason? As mentioned in the previous section, energy detection algorithm is used inside DW1000 chips to mark the first arriving path, which means the difference between the first arriving path's power and ambient noise has direct relationship with the accuracy of ranging. In Figure 3.3, we focus on the relationship between the first path gap and ranging error across different channels.

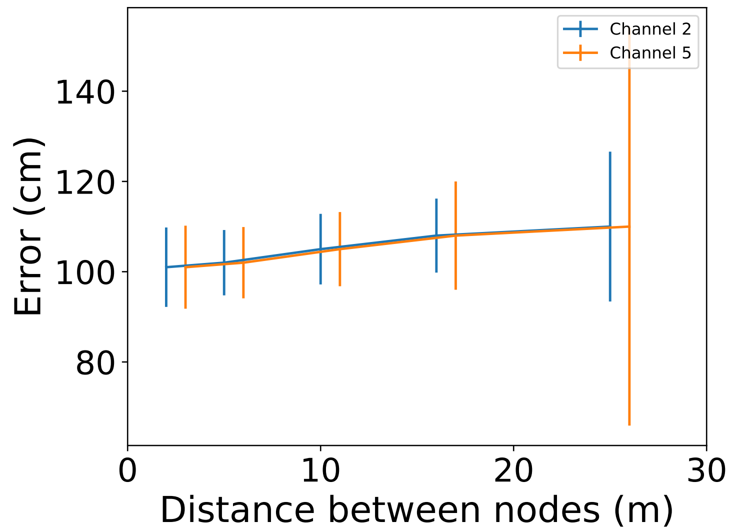


Figure 3.2: Ranging error across different distances. Below 20 m distance, ranging performance is consistent.

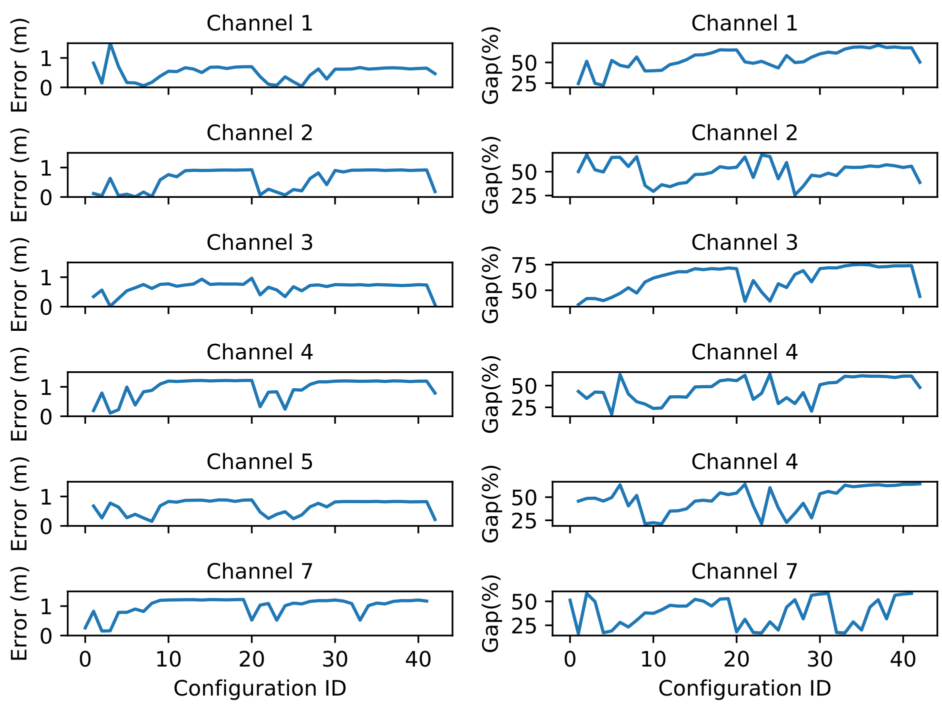


Figure 3.3: Gap between first path and noise has a direct relationship with observed ranging error

Figure 3.3 supports our earlier hypothesis. Across different channels, ranging error increases once the gap between first path and the ambient noise decreases. This observation gives us the idea of improving the ranging performance by changing the channel setting. For example noise pattern is different across different channels which means changing the center frequency can reduce the ranging error. Also, longer preamble length provides more power in the received signal which means higher first path power gap.

### 3.2.2 UWB Physical Layer Parameter's Impact on Ranging

In the following paragraphs, the impact of changing each of the factors on the final accuracy of UWB-based localization system has been investigated using the data we collect in our dataset. In all the experiments, off-the-shelf EVB1000 chips [30] are utilized as anchor and Tag nodes.

#### 3.2.2.1 Frequency Channel

The first analyzed factor is frequency channel. Figure 3.4 shows the average error measured in estimating the distance to the Tag node using different frequency channels (average of 4000 ranging per channel). As shown in Figure 3.4, higher frequencies provide more accurate and reliable (with less variation) results.

Figure 3.5 shows the gap between the noise floor and the first path signal in different frequency channels. As it is shown in Figure 3.5, the amount of noise floor in different frequency channels varies a lot which is reasonable considering the distribution of noise in different frequency channels. This observation helps us to justify different ranging performances across different frequency channels.

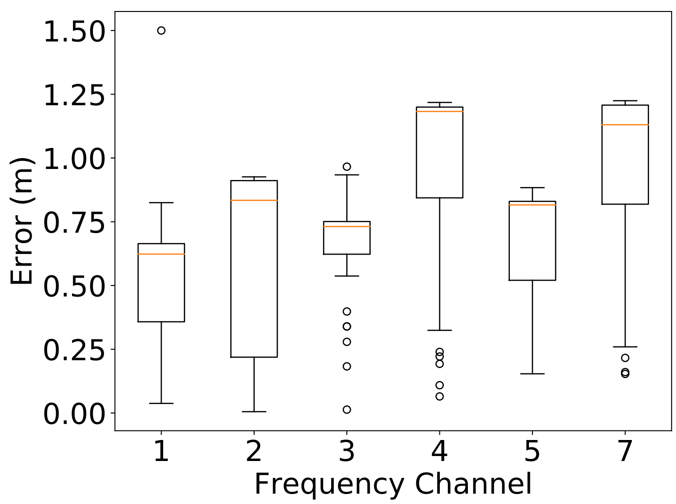


Figure 3.4: Ranging error across different frequency channels. Higher frequency channels have more reliable ranging performance. On channel 4 and 7 larger bandwidth (1 GHz) increases the error.

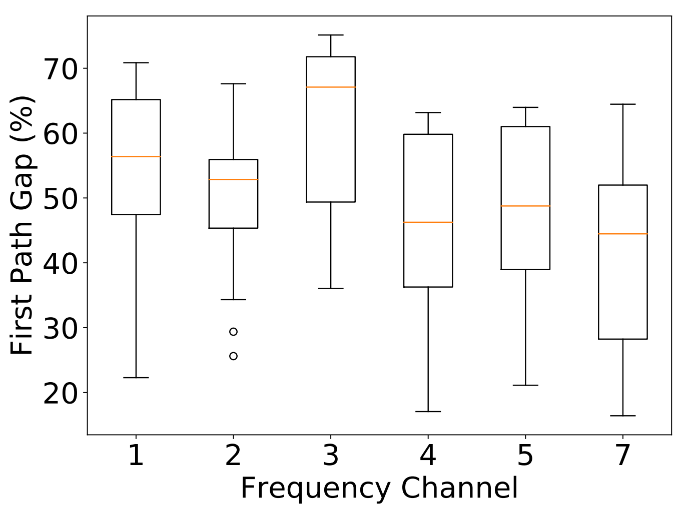


Figure 3.5: Gap between first path power and noise across frequency channels

#### 3.2.2.2 Preamble Length

The second parameter to be considered to change in UWB physical layer is the preamble length. Figure 3.6 shows the average error (more than 4000 ranging measurements per preamble length) in estimating the distance to the Tag node while changing the

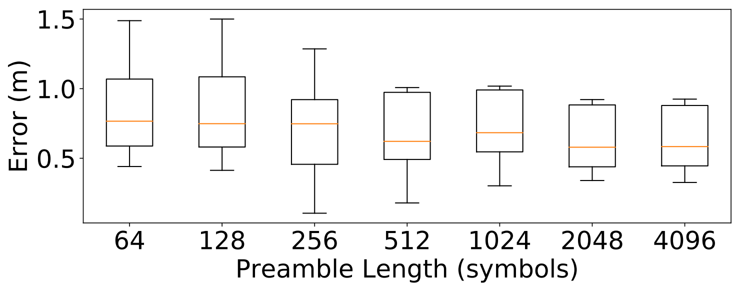


Figure 3.6: Ranging error across different preamble lengths. Increasing the preamble length significantly improves ranging performance

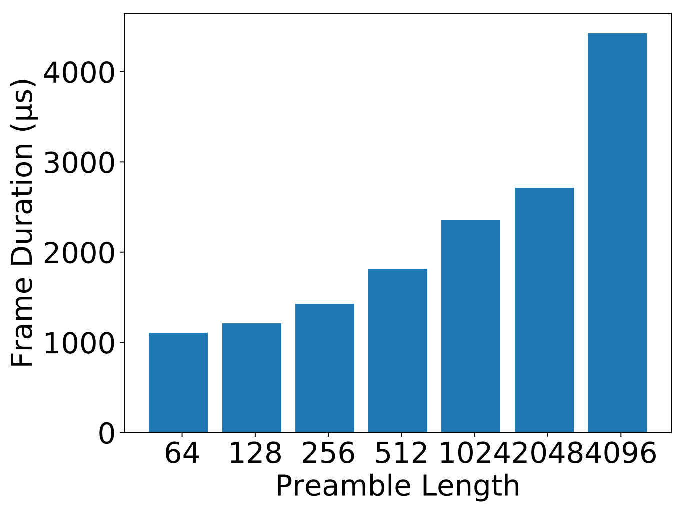


Figure 3.7: Frame duration across different preamble lengths. Longer preamble length increases air utilization

preamble length. As we expect, increasing the length of the preamble from 128 symbols to 1024 symbols significantly decreases the error but after 1024 symbols, increasing the preamble length does not have a noticeable impact on reported accuracy. On the other hand, increasing preamble size increases the length of message which means it will increase the amount of time required for the system to transmit the message (higher energy consumption and lower location update rate). Figure 3.7 shows the amount of time required for sending messages with different preamble lengths (with 30 bytes of data payload). Based on the results from these two experiments, changing

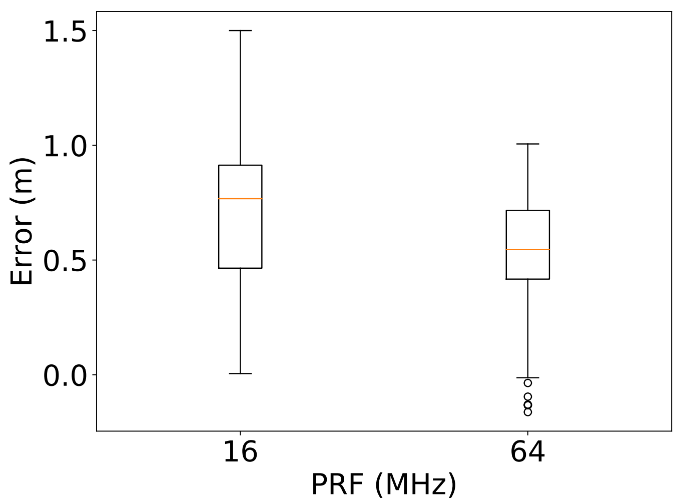


Figure 3.8: Ranging error across different PRFs. Higher PRF has better ranging performance.

preamble length is one of the key features of the designed solution to increase the robustness of the system. We need to mention, looking at Figure 3.7, increased ranging performance comes with the price of increased frame duration which means higher air utilization. To emphasize the importance of air utilization in UWB communication, we need to mention that, in IEEE 802.15.4-11 standard, the default Medium Access Control (MAC) for UWB communication is ALOHA [20] which is based on random access to the medium (UWB signals are very low power compared to background noise which makes CSMA protocols impractical in UWB communications [41]). In the case of long frames, the chance of collision and interference increases which reduces the robustness of the UWB based localization and communication technique.

#### 3.2.2.3 Pulse Repetition Frequency

The third channel configuration parameter is PRF value. Figure 3.8 shows significant improvement by changing the PRF value from 16 MHz to 64 MHz in estimating the distance to a Tag.

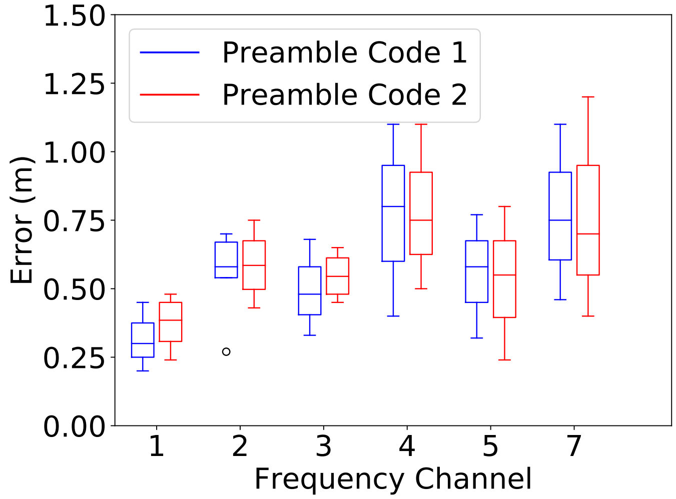


Figure 3.9: Ranging error across different preamble codes. Preamble code does not have signification impact on ranging performance.

#### 3.2.2.4 Preamble Code

Preamble code is another configurable parameter in UWB communication link. As it can be seen in Figure 3.9, changing the preamble code in the same frequency channel does not have a significant impact on the accuracy of estimated location.

#### 3.2.2.5 Data Rate

The last configurable parameter is data rate. Figure 3.10a shows the impact of changing the data rate on final accuracy of ranging. As shown in Figure 3.10a, changing the data rate does not have a noticeable impact on the final accuracy of the system but on the other hand, Figure 3.10b indicates the fact that increasing the data rate will significantly decrease the frame duration which means reduced air utilization in higher data rates.

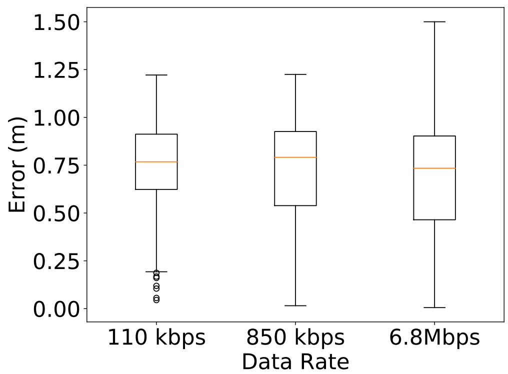


(a) Ranging error across different data rates

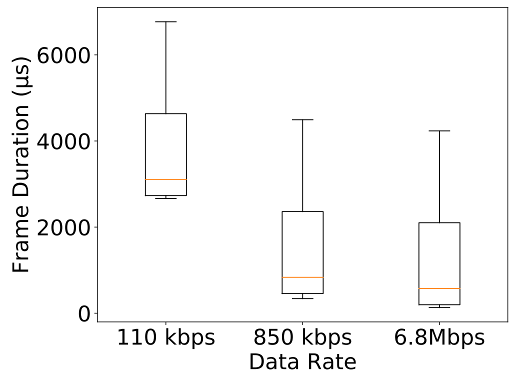


(b) Frame duration across different data rates

Figure 3.10: Impact of data rate on ranging error and air utilization. Higher data rate reduces air time but does not significantly change the ranging performance.

#### 3.2.2.6 Frequency Channel Vs. Preamble Length

As mentioned in previous sections, frequency channel and preamble length have high impacts on average error. In order to compare the impact of each of them, we designed a simple experiment. A pair of Tag and anchor points were placed in the distance of 20 m, in non-line of sight condition. We changed channel setting (preamble length and frequency channel) and measured average error. Figure 3.11 shows the impact of changing the frequency channel and also preamble size on the reported accuracy. Figure 3.11 shows that increasing preamble length has a lower impact on accuracy of measurements (25% error reduction) compared to increasing the frequency channel (50% error reduction). In all the cases, increasing preamble length makes the measurements more stable. On the other hand, channels with higher frequencies have more accurate results but with higher chances of NLoS measurements.

### 3.2.3 Detecting Low Quality Ranging

The environment has a significant impact on the UWB ranging error. Interference and attenuation change the UWB channel characteristics which leads to different ranging

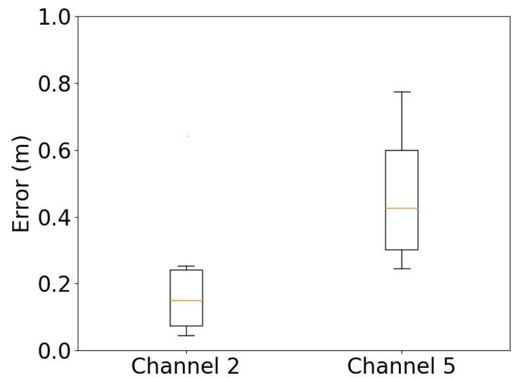


(a) Preamble Length = 128

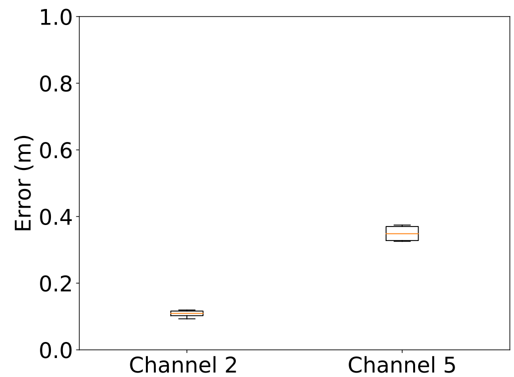


(b) Preamble Length =1024

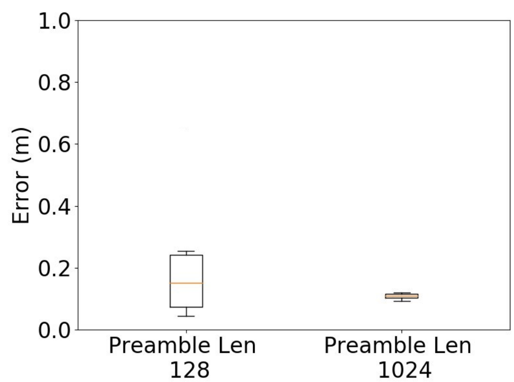


(c) Channel = 2

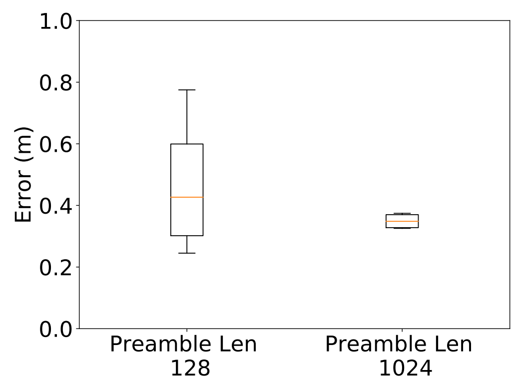


(d) Channel = 5

Figure 3.11: Impact of frequency switching compared to increasing the preamble length on ranging

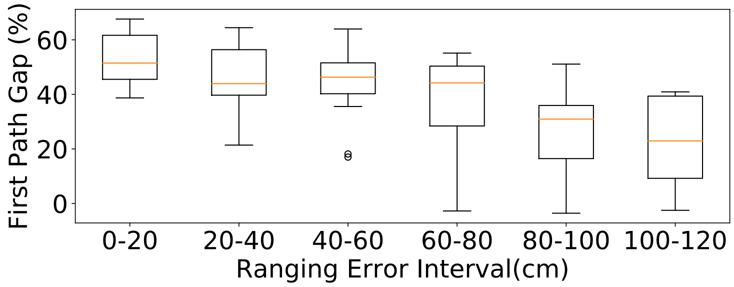


Figure 3.12: Observed gap between first path power and noise in different ranging error intervals.

performance. As mentioned earlier, our proposed solution can improve the ranging performance by changing the channel setting, but, we need to have an indicator of low quality ranging to trigger the search algorithm. DW1000 chips utilize energy detection algorithm to find the first path which means the distance between the first path's power and ambient noise can be used as ranging quality indicator. Figure 3.12 shows the amount of gap between the first path power and noise in different ranging error ranges from our dataset. It is shown in Figure 3.12 that if we want to keep the error range below 20 cm, the gap between first path and noise should be bigger than 50%. We decided to use threshold of 50% as an indicator of low quality ranging. In other words, if the gap between first path power and ambient noise is smaller than 50% of first path power, our framework marks the ranging as low quality ranging and in the case of seeing multiple consecutive low quality ranges, it will trigger the search algorithm to change the UWB physical layer setting.

### 3.2.4 Proposed Search Algorithm to Find Best Physical Layer Configuration

Impact of changing each of the configuration parameters on the final accuracy of the system has been investigated in previous sections. The simplest way to change the channel configuration is running a brute-force search algorithm and test the error based on all the possible combinations of values for configuration parameters. In this case, the search space would be 252 different settings. In our framework, considering the impact of each factor on final robustness, accuracy, energy consumption and delay, an efficient search algorithm proposed. Based on our measurements, we proposed Algorithm 1 to change the setting of the channel to improve the robustness considering trade-offs between data rate, power consumption, error rates, and robustness.

**Algorithm 1** Find The Best Physical Layer Configuration

$Configs \leftarrow AllAvailableConfigurations$
$P_{th} \leftarrow MaxAllowedPower$
$D_{th} \leftarrow MaxAllowedFrameDuration$
$PC \leftarrow PotentialConfigurations$
$PC_{filtered} \leftarrow \{Config \in PC, Config_{power} \leq P_{th}$ **and** $Config_{length} \leq D_{th}\}$
**for all** $C \in PC_{filtered}$ **do**
    $C_{error} \leftarrow$ Extract ranging error associated with current configuration from the dataset
**end for**
$C_{min} \leftarrow \{C, C_{error} \leq allConfigs \in PC_{filtered}\}$
**return** $C_{min}$

The proposed algorithm first finds the configurations which satisfy energy and time constraints. As we showed in previous sections, changing channel settings will change power consumption and frame duration. Based on the desired application, user can define thresholds for maximum power consumption preferred per ranging activity and also the maximum duration of time per packet. Packet length has two direct impacts on the ranging. First, the packet length identifies the power consumption. It is obvious that longer packets require longer transmission and reception which leads to higher power consumption. Frame duration also is important in air utilization. If the packets are too long, the air utilization increases and causes interference problem among the UWB nodes. We need to find a configuration which meets both the requirements and also minimizes the error rate. Since the size of the whole search space is 252, the total time to execute the proposed algorithm is negligible.

## 3.3 Evaluation

In this section, we first evaluate the effectiveness of the proposed algorithm on reducing ranging errors and next, we study the impact of changing UWB physical layer configuration on 2D localization (3 anchors and 1 Tag).

### 3.3.1 Ranging Quality in Proposed Solution

To evaluate the effectiveness of the suggested technique, we perform simulations using our collected dataset from 2 nodes. In each round, we randomly select a configuration to be the starting configuration, then run proposed search algorithm over all the 252 settings in our dataset, to find best configuration in which power consumption and frame duration are below the power consumption and frame duration of current configuration and ranging error is the minimum among the rest of configurations. Figure 3.13 shows reductions achieved by running our proposed search algorithm to find the best possible configuration which satisfies either power consumption or frame duration thresholds. The results are achieved by running the simulation for 100 times. Figure 3.13a shows the reductions in ranging error by only considering power consumption threshold and Figure 3.13b illustrates error reductions happened by only considering frame duration threshold.

Figure 3.13, shows as much as we have higher power consumption or frame duration thresholds, there is more room for error reduction. Another interesting fact is that increasing power consumption threshold has more potential to reduce ranging errors compared to frame duration threshold.

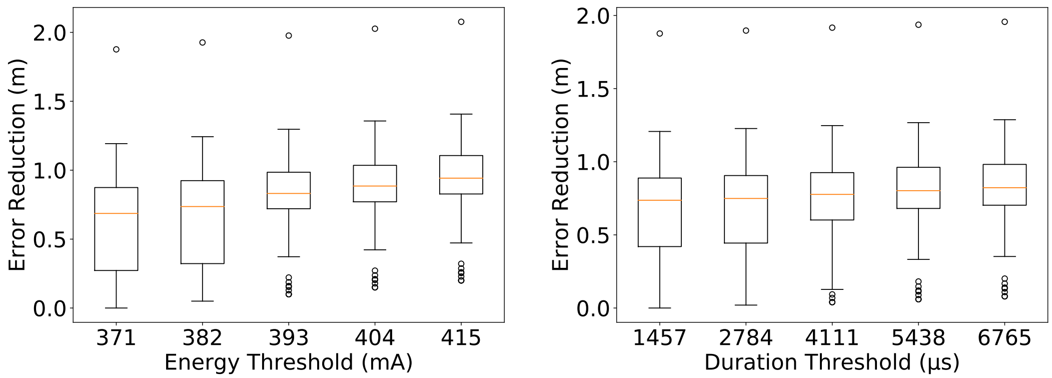


(a) Only consider power consumption threshold

(b) Only consider frame duration threshold

Figure 3.13: Effectiveness of proposed search algorithm on ranging

### 3.3.2 Localization with Different Physical Layer Configurations

In this section, we conduct few experiments to evaluate the effectiveness of the proposed algorithm on accuracy and robustness of UWB-based indoor localization technique. In our experiments, we used TREK1000 [80] system provided by Decawave. The system contains four DW1000 based modules (EVB1000) providing UWB transmissions conforming to IEEE 802.15.4a standard. We deployed three nodes as anchor nodes inside an academic building and tracked the fourth node (Tag) carried by a person moving across a predefined path inside a corridor ($12m \times 6m$). There were no other obstacles or moving objects around the data collection area. We conducted the experiment with 4 different configurations to show the impact of changing physical layer configuration on the ranging performance. The four configurations are summarized in Table 3.1. As mentioned in earlier sections, preamble size and PRF are the two most important factors which have direct impact on accuracy and coverage of UWB localization system. In these experiments, we change both PRF and preamble size to evaluate their impact on final accuracy and robustness of system. Figure 3.14a shows the trajectory as green lines and reported locations for each configuration. We

Table 3.1: "UWB Physical Layer Configurations Selected for the Evaluation of mobile Tag Localization

| Config # | Frequency (MHz) | PRF | Preamble Length | Data Rate |
|---|---|---|---|---|
| 1 | 3493.6 | 16 MHz | 128 | 110 kbps |
| 2 | 3493.6 | 64 MHz | 128 | 6.8 Mbps |
| 3 | 3493.6 | 16 MHz | 1024 | 110 kbps |
| 4 | 3493.6 | 64 MHz | 1024 | 6.8 Mbps |

find that by increasing the preamble length, the location update rate is reduced but the reported locations are more accurate.

Figure 3.14a also shows that configuration 4 which has 1024 symbols as preamble length and 64 MHz as PRF value, increases the robustness of the system by covering more places. Figure 3.14b shows average reported error in locating the object with each of the configurations. We calculated the minimum distance of each point to the trajectory and considered it as the error in estimating the location. Figure 3.14b shows the average error for each configuration. As expected, configuration 4 has the smallest value of the error.

Finally, Figures 3.14a and 3.14b prove that changing configuration of the channel will improve the robustness of indoor localization system.

## 3.4 Discussion

UWB wireless technologies can be used both for localization and data communication. The optimal setting for localization application may be different from the optimal setting for communication application of UWB. In our current work, we focused on indoor localization and changing the channel setting in a way to increase the

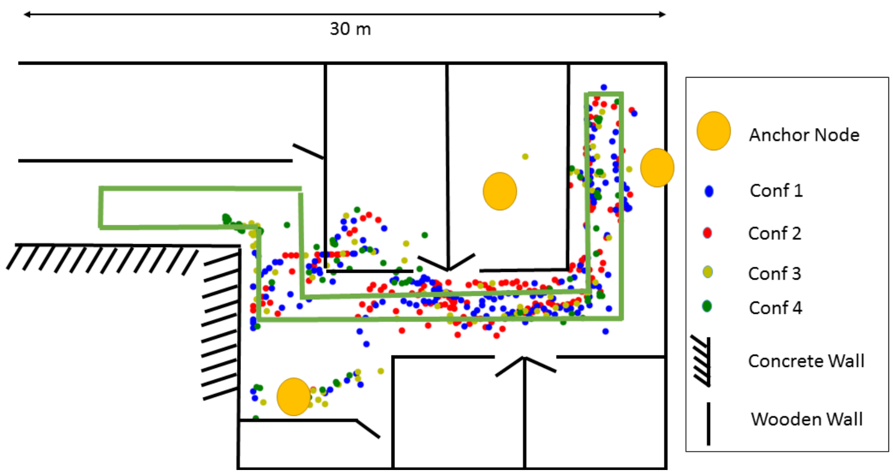


(a) Tracking moving target with different physical layer configurations

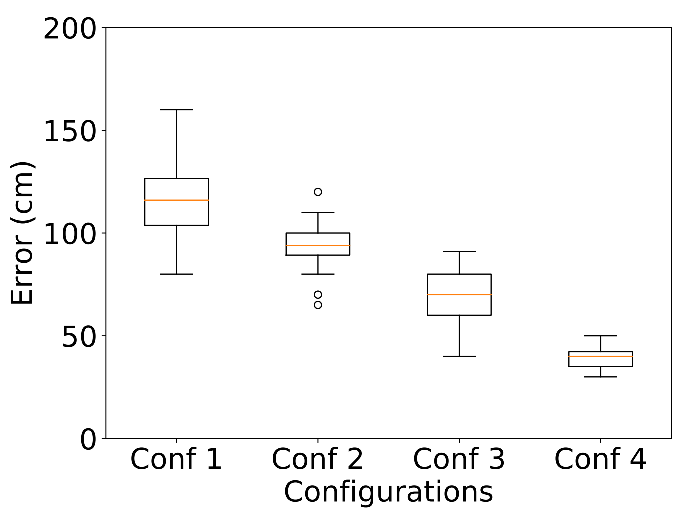


(b) Error in each configuration

Figure 3.14: Localization with different physical layer configurations (The configuration parameters are shown in table 3.1)

robustness of localization at the cost of reducing the efficiency and speed of data communication. Different UWB applications may make different tradeoffs in settings depending on their combination of localization and data transfer goals.

The designed framework will be executed during deployment of the system and it finds the best performing settings. It also can continue monitoring the performance of the localization and update the setting during runtime via a central or distributed protocol. In the localization algorithm, Tag communicates with each anchor in a separate message which means it can utilize different setting to communicate with each anchor node. The channel setting can be exchanged between Tag and anchor during a simple handshaking protocol, in fact, we used this technique in our evaluations.

## 3.5 Conclusion

Wireless indoor localization using ultra-wideband signals is one of the promising technologies to solve problem of locating moving objects inside the buildings. In this work, we propose a novel framework to improve the robustness of UWB localization systems by changing the UWB channel setting in an efficient and quickly. Through extensive real-world implementations using DW1000 UWB transmitters, we verified the effectiveness and robustness of our proposed framework. We showed the impact of different UWB channel settings on the ranging performance and proposed an algorithm to utilize these differences to increase the robustness of UWB-based indoor localization systems. Utilizing proposed technique, UWB localizations can adapt to changes in the environment and also support more challenging scenarios which overall increases the scalability of UWB localization systems.

# Chapter 4

# UWB Localization Using Single Anchor

The recent studies in UWB-based indoor localization have reported errors of less than 40 cm for 3D localization [60]. Most of UWB-based indoor localization techniques need to process LoS signals to accurately locate the target. However, in indoor environments, the reception of LoS signals is not guaranteed in every location e.g. LoS either is blocked by obstacles or is not distinguishable from NLoS signals. Recent work in UWB-based positioning approached this challenge either by increasing the chance of receiving LoS signal through addition of extra antennas and channels, or utilizing NLoS signals to improve the robustness of the localization system. Despite these improvements, creating a UWB-based indoor localization solution that is robust, reliable, scalable, and accurate remains unsolved. Most of the existing works require at least three anchors in the line of sight condition to be able to locate the target which means robustness of them is dependent on the number of LoS anchors.

In this work, we increase the robustness of UWB-based indoor localization by reducing the number of required anchors. Our approach requires only one node with known location (anchor) to locate the target node. Our main idea is utilizing the unique features of UWB signals by extracting high-resolution estimations of Channel Impulse Response (CIR) to accurately estimate the location of the target node. The shape of CIR is dependent on the location of the sender and receiver of the signal. Our hypothesis is that the differences in CIR patterns in different places can be utilized as reliable fingerprints to locate targets based on previously seen patterns. We study the characteristics of CIR samples in each location and use statistical features of those components as fingerprints. Later on, to find the location of a target, CIR samples in the received signal are compared with a list of previously seen clusters in the same area and the location corresponding to the best match is selected as the estimated target location.

We designed and implemented our single anchor UWB-based indoor localization system on Decawave platform and evaluated its performance in different indoor environments. Our results show that the proposed system can locate the target within a $20cm \times 20cm$ area with an accuracy of 96% using only one anchor node. Our contributions are:

- Propose a robust single anchor UWB-based indoor localization technique by utilizing differences in statistical characteristics of Channel Impulse Response in different locations using only one anchor node.
- Generate fingerprints using statistical characteristics of amplitude and phase information for each CIR sample which increases the resilience of generated fingerprints to temporal changes in the environment and also significantly reduces the model size.
- Evaluate the reliability and accuracy of using CIR as fingerprints in different environments with frequent temporal changes.

## 4.1 Related Work

Literature in NLoS handling area can be categorized in two groups: Avoiding NLoS signals [26, 45, 58] and utilizing NLoS signals [28, 38]. In avoiding NLoS category, the key idea is increasing the chance of receiving LoS signal by adding more channels and links and try to avoid NLoS situations. In utilizing NLoS category, the main idea is estimating the error caused by the presence of NLoS signals then correcting it in range measurements. Despite the accurate results achieved by approaches in both categories, the scalability of such techniques is under question. These approaches require at least 3 anchors to work. To reduce the number of required anchors to make indoor localization system more robust, the idea of using virtual anchors has been explored in the literature [38, 50]. These techniques hold a lot of assumptions about the environment, such as prior knowledge about room geometry, highly reflective surfaces, and insignificance of the effects like diffraction and diffuse scattering. Although as shown in [40], other effects like diffraction and attenuation can severely impact the ranging accuracy and consequently, the overall performance of such systems.

Our proposed solution as a single anchor localization solution utilizes the unique shape of the combination of NLoS and LoS signals received in each location to generate reliable and robust fingerprints. Feasibility of using information from wireless links (Bluetooth and WiFi) to generate fingerprints has been studied before [31, 82]. Features like the Received Signal Strength Indicator (RSSI), Channel Frequency Response (CFR), and Channel Impulse Response (CIR) have been utilized previously. CFR is an estimation of the impact of environment on wireless signals across their bandwidth while they travel from sender to receiver. CIR is the equivalent of CFR in the time domain. CIR information contains multipath components (MPC) which can be used to generate fingerprints. The advantage of using CIR compared to CFR is that CFR is very dependent on temporal frequency fading and simple changes in one of the sub-carriers change the CFR model, but CIR information is more resilient to temporal changes, since each impulse response is based on response across all the bandwidth [83]. Existing wireless fingerprinting techniques can locate the target within $75cm \times 75cm$ spot with 90% accuracy [79]. The key benefit utilized in our approach to improve accuracy is the larger bandwidth and the shorter wavelength of UWB signals compared to WiFi and Bluetooth.

Feasibility of using UWB signals to generate fingerprints has been studied before [24, 56], but the evaluation focused on signals with very large bandwidth (3 GHz to 7 GHz), and high sampling rates in the lab environment. Studies [25] showed that the bandwidth of UWB signals has a huge impact on the reliability of fingerprinting approaches. To the best of our knowledge, no prior work in the literature evaluates the reliability of CIR information, captured from UWB signal (IEEE802.15.4-11 standard) with the bandwidth of 500 MHz using commercial off-the-shelf DW1000 chips, to generate reliable and persistent fingerprints.

## 4.2 System Design

Multipath reflection is a serious challenge in wireless communications. Reflected multipath components can cancel out each other and make it difficult for the receiver to decode the packet [78]. UWB signals have a unique feature. They are sent as a sequence of short pulses (2 ns) [9] which makes reflections from different paths to arrive at the receiver with enough time gap which enables the receiver to distinguish them. This characteristic is a key enabler for accurate distance measurements since the receiver can accurately timestamp the reception of the first path (LoS) signal. In this work, we utilize this capability to increase the robustness of the indoor localization

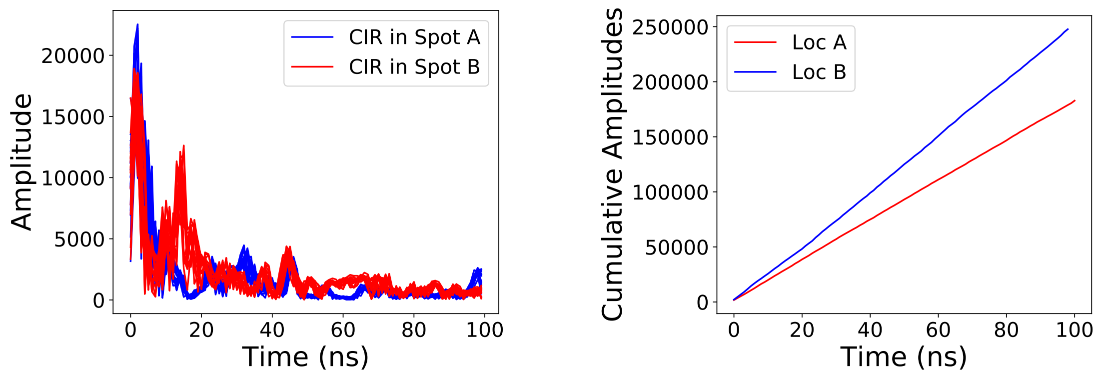


(a) CIR collected from 2 different spots (30 cm distance)

(b) Cumulative amplitudes of CIR

Figure 4.1: CIR distinguishability across spatial change. Changing the location changes the CIR pattern

systems in challenging scenarios in which LoS signals either do not exist (buried in the noise floor) or are not distinguishable from NLoS signals. Different locations or environments have different patterns of multipath components (MPC) which means MPCs can be considered as fingerprints of locations. In this section, the design choices we have for converting MPCs to reliable fingerprints are explained in detail.

### 4.2.1 Channel Impulse Response in UWB

In UWB communication, accurate estimation of CIR is possible due to the unique shape of UWB signals (sequence of short pulses). The CIR contains high-precision information about how UWB signals are propagated which includes first (direct) arriving path and other reflected or scattered paths. We analyze the CIR information in different locations to generate unique fingerprints. CIR contains information from both LoS and NLoS signals and we utilize uniqueness of this combination as a key feature for generating unique fingerprints.

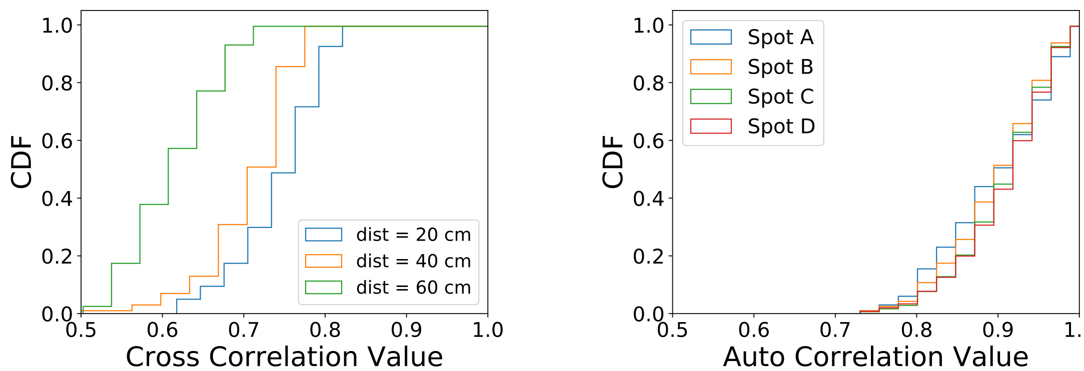


(a) Cross correlation of CIR samples in different spots

(b) Autocorrelation of CIR samples in same spot

Figure 4.2: Correlation of CIR across spatial and temporal change. CIR is consistent over time but changes by changing the location

### 4.2.2 CIR Distinguishability across Spatial Changes

To have a reliable fingerprinting system we have two basic assumptions which we need to verify. Our first assumption is CIR information in different locations is different enough and this difference can be utilized to generate unique fingerprints per location. Our second assumption is CIR information at the same location is relatively stable across time which means it is resilient to temporal changes. We perform several experiments to validate our assumptions. In all the experiments, there is a pair of sender and receiver nodes. The location of the sender (anchor) is fixed but the receiver (target) is placed at different locations. Figure 4.1a shows the amplitude values for the first 100 CIR samples collected from two different locations (400 packets in each location) which are 30 cm away from each other. Figure 4.1b is the cumulative amplitude of CIR samples. From Figure 4.1 two clusters of CIR are clearly distinguishable. This observation supports our first assumption about the distinguishability of CIR over short spatial changes.

To validate our second assumption, we collected CIR samples at 4 different locations (each location for 1 hour). The CDF of autocorrelation between amplitude values seen for first 50 CIR samples is reported in Figure 4.2b and the CDF of cross-correlation between amplitudes of first 50 CIR samples in pairs of spots (distance > 20 cm) are reported in Figure 4.2a. As shown in Figure 4.2, cross-correlation between CIR in two different locations is much lower compared to autocorrelation across the samples collected from one location which means our second assumption is also valid in these datasets. It is also shown in Figure 4.2a that cross-correlation between CIR decreases as the distance between the spots is increased. In conclusion, CIR samples are reliable sources to generate unique fingerprints per location.

### 4.2.3 CIR Classification

In this section, we evaluate the feasibility of using standard classification algorithms to generate fingerprints using CIR and accurately distinguish different spots from each other.

#### 4.2.3.1 Feature Extraction

We extract the following features from CIR values:

- **First Path Delay & Power**: The time it takes for the first arriving path to travel from sender to receiver and its received power.
- **Power**: Amount of power in the received signal.
- **Average & Std Deviation of Noise**: Average and standard deviation of the ambient noise.
- **Preamble Count**: UWB packets start with preambles (sequences of 0,1 and -1 determined by preamble code). The accumulative correlation between the

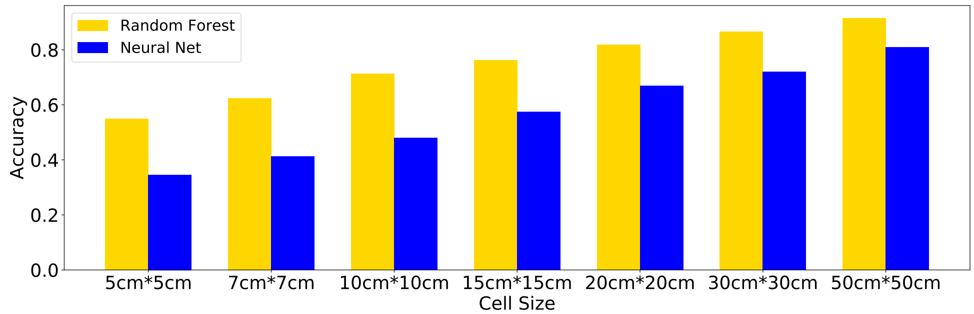


Figure 4.3: Classification accuracy using extracted features from CIR.

received signal and expected preamble is used to estimate the CIR. The number of preambles used to estimate the CIR depends on the quality of the received signal. We utilized the number of preambles used for estimating the CIR, as a feature.

We divided the target area to grids with different sizes ($5cm \times 5cm$ to $50cm \times 50cm$). To perform data collection consistently and systematically, we used a robot (TurtleBot [18]) to move around with a constant speed (0.05 cm/s) while the receiver is mounted on top of it. The sender (anchor) is in a static location and sends beacons every 50 ms. The maximum distance between sender and receiver is 12 m. Figure 4.3 shows the classification accuracies achieved by running neural networks (MLP Classifier with quasi-Newton solver and with network size (5 layers, 5 neurons per layer)) and random forest (number of estimators = 10, criteria = entropy) classification algorithms on the features collected from different spots (15 spots which are at least 30 cm apart) with the same size (in each spot, at least 2000 packets used for training). The accuracies are reported after running 10-fold-cross-validation on the dataset.

As shown in Figure 4.3, the best result which is approximately 84% accuracy is achieved by the random forest algorithm with the spot size of $50cm \times 50cm$. The classification becomes less accurate as we decrease the size of squares. Overall, the

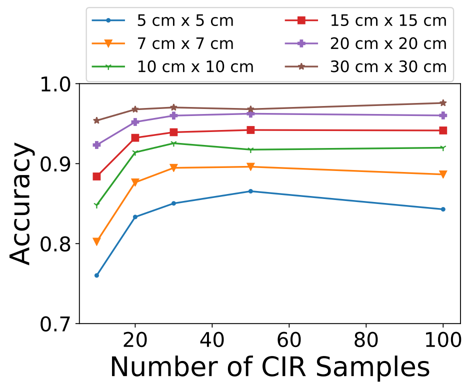


(a) Neural Net

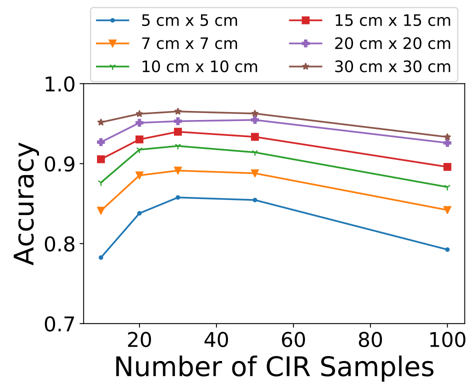


(b) Random Forest

Figure 4.4: Classification accuracy using raw CIR information for localization. Not best performance due to Overfitting problem.

collected features are not reliable enough for generating fingerprints. Using other classification algorithms like SVM and Bayes Nets in scikit-learn 0.19.1 also could not improve the accuracy.

#### 4.2.3.2 Over-fitting with Raw CIR

Next, we study the feasibility of using raw CIR information as classification features instead of extracting general features from CIR samples. Figure 4.4 shows the accuracy reported by the neural net (MLP Classifier with quasi-Newton solver and with network size (5,10)) and random forest (number of estimators = 20, criteria = entropy) algorithms after feeding them with raw CIR values from the previous experiment (15 spots). We also changed the number of CIR samples used in the training phase from 5 samples up to 100 samples.

As shown in Figure 4.4, overall accuracies improved (in average 25%) compared to the previous approach (using extracted features). This observation is expected since CIR information contains more details about each location. Despite improvements in the reported accuracy, Figure 4.4 shows that the classification using raw CIR data

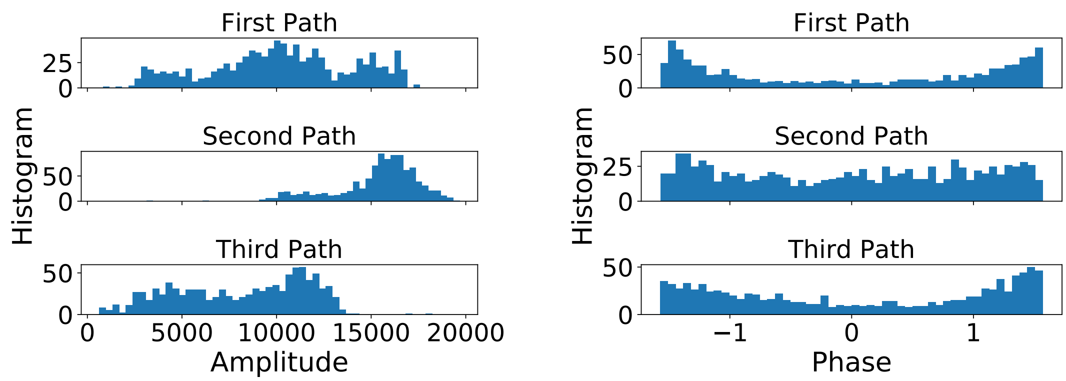


(a) Amplitude Distribution (b) Phase Distribution

Figure 4.5: Histogram of first 3 CIR samples over 400 packets- Gaussian mixture model for amplitude and Beta distribution for phase

suffers from overfitting. As we increase number of reflected components above 50, the accuracy starts decreasing. In other words, those algorithms do not benefit from the rest of CIR samples in the data.

#### 4.2.3.3 Modeling CIR

Up to now, we showed either extracting general features or using raw CIR to generate fingerprints did not achieve either accurate nor robust performance. The former suffers from low accuracies and the later suffers from overfitting and non-resilience to temporal changes. In next step, we extract generalized statistical features of CIR samples in each location. Our hypothesis here is that statistical distributions are more resilient to temporal changes compared to previous approaches and can improve the robustness of localization solution. Figure 4.5 shows the histogram of amplitude and phase for the first three CIR samples calculated from sampling 400 packets while the locations of sender and receiver are fixed. Figure 4.5a shows that the amplitude information on each reflected component follows a mixture of Gaussian distributions. Also, the collected phase information (Figure 4.5b) follows the Beta distribution which is reasonable due to the nature of UWB signals. They are sent as sequence of 0,+1 and -1 values [9] which means the phase values are mostly around +90 degrees and -90 degrees phases.

We observe the same pattern in the rest of the CIR samples across different locations. Amplitude values for each CIR sample is modeled as Gaussian Mixture model when observing 400 packets. Variational Bayesian Gaussian Mixture [68] is used to find optimum number of Gaussian components for each CIR sample. In summary, the proposed fingerprinting approach works as follow. For each location CIR is collected across several beacon packets sent from the nearby anchor; for each CIR sample, the amplitude is modeled as a Gaussian Mixture model and phase is modeled as Beta distribution with $\alpha$ and $\beta$ parameters when observing 400 packets. We store these models for each CIR sample as fingerprints. For instance, if we decide to use information for 50 CIR samples as fingerprint, at each location, we store set of 50 pairs of models (amplitude model and phase model). Later, in the online phase, to locate the target, after receiving beacon message from a specific anchor, the CIR information from test packet is investigated to find its best match with previously seen clusters which are associated with same anchor. To measure the similarity, we define the following metric:

$$S(P, U^t, V^t) = \sum_{i=1}^{N} LogLK(U_i^t, Amp_i) + \sum_{i=1}^{N} LogLK(V_i^t, Phase_i) \tag{4.1}$$

in which, P is the received test packet, $U^t$ is set of Gaussian Mixture models for amplitude values in location t (one Gaussian mixture model (GMM) per CIR sample), $V^t$ is the set of Beta distributions for phase values at location t (one Beta distribution per CIR sample), LogLK stands for log likelihood function, $Amp_i$ and $Phase_i$ are amplitude and phase values of $i^{th}$ CIR sample at test packet P respectively and N is number of CIR samples considered for generating fingerprint. By searching through all the clusters which are associated with the sending anchor, the most similar one to the test packet is the estimated location of target. It is essential to mention that since for each spot the proposed approach only saves distribution parameters and not the raw data, the approach has low memory overhead and faster to search for the matching location.

## 4.3 Performance Evaluation

To evaluate the accuracy and robustness of the proposed fingerprinting approach, we collected data from different locations and evaluated the accuracy of correctly identifying the locations. Following sections cover various aspects of our evaluation process.

### 4.3.1 Experiment Setting

We used EVB1000 [7] nodes which are evaluation kits manufactured by Decawave company and include DW1000 chips. DW1000 chips estimate CIR with 1 ns resolution. We collected data from different locations including office space in (*i*) our lab ($12m \times 6m$), (*ii*) a crowded coffee shop on campus ($18m \times 12m$) and (*iii*) a large ($40m \times 30m$) dining hall with lots of furniture. In each experiment, we compared the performance of proposed solution in accurately classifying the signature into 15 classes corresponding to the 15 different spots. In each location, we collected data from up to 3 different anchors. As expected results from anchors with LoS condition outperform results from NLoS anchor; We focus on the results with the NLoS anchor. Our dataset contains 223366 packets collected from 200 different spots. The target node is placed on top of a robot which moves with constant speed (0.05 cm/s). The anchors broadcast beacons every 50 ms. The target node estimates and saves the

CIR information from received beacon messages. In each environment, we made sure one of the anchors is in the NLoS condition (no visual Line-of-Sight, error in distance measurement at least twice the error in LoS condition with the same distance). In all of the following sections (except those in which source of data is clearly mentioned) reported results are average performance results over all three tested environments. The anchors are deployed at the height of 160 cm and the target is deployed at the height of 70 cm. Knowing the start location and speed of the robot, ground truth information can be extracted.

### 4.3.2 Impact of Contributing Factors

#### 4.3.2.1 Number of CIR Samples and Spot Size

There are two main factors which determine the accuracy of the proposed system: number of used CIR Samples and spot size. Figure 4.6 shows the $F1$ score (Formula 4.2) calculated from

$$F1 = \frac{precision \times recall}{precision + recall} \tag{4.2}$$

test data collected in the coffee shop. As shown in Figure 4.6, as we increase the number of used CIR Samples in fingerprint, the score goes higher but this trend stops after using 100 CIR samples which is due to over-fitting. Also, increasing spot size improves performance. With spot size of $5cm \times 5cm$, the maximum score is around 0.8 which is not good enough but if we increase the spot size to $15cm \times 15cm$, the score increases to 0.95. Another interesting observation is the fact that the best classification score happens at spot size $7cm \times 7cm$. The data were collected while the nodes were communicating over channel 2 with center frequency of 3.993 GHz. The wavelength of this frequency is approximately 7 cm which is the reason spot size

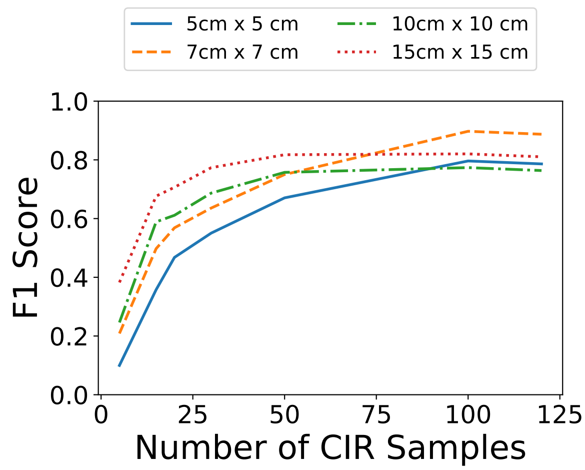


Figure 4.6: Impact of increasing number of CIR samples and spot size on accuracy of spot detection using our proposed technique (Modeling CIR)

of $7cm \times 7cm$ has very high classification scores (0.88 with 100 CIR samples in use). We verified that in average, the difference between power level of 100th CIR sample and noise is greater than 10 dB in our dataset.

#### 4.3.2.2 Minimum Spot Size

Instead of using just one packet, we evaluated the possibility of using multiple packets and considering the majority vote (to increase the resilience to outliers) as the final detected location. Figure 4.7 shows the $F1$ scores reported from window sizes of 3 and 5 packets. As we expected, the score increases to 0.96 after considering the last 3 samples for deciding the location with the spot size of $7cm \times 7cm$. Average human walking speed is 130 cm per second [23] and we are collecting data every 50 ms which means to receive 3 samples, the target has moved around 20 cm. In other words, our solution locates the target within the spot of $20cm \times 20cm$ with the $F1$ score of 0.96.

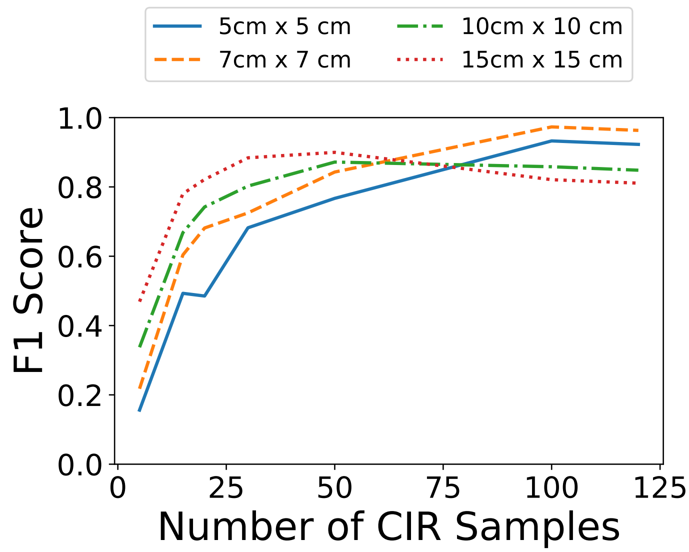


(a) Window size = 3

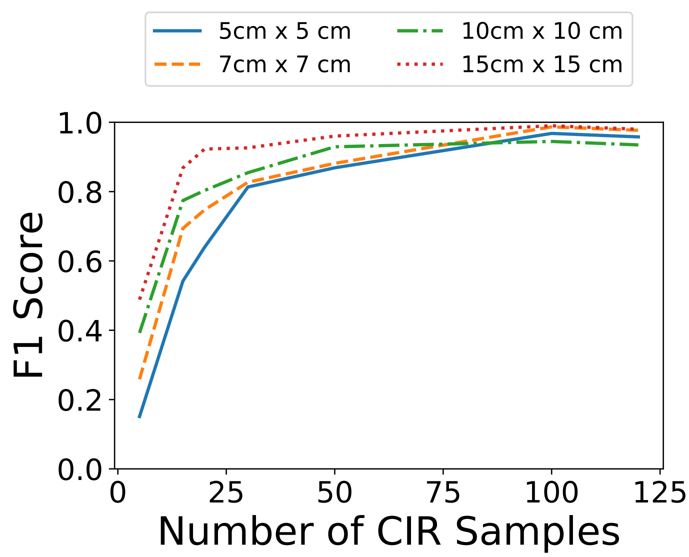


(b) Window size = 5

Figure 4.7: Minimum reliably distinguishable spot size using proposed technique (Modeling CIR)

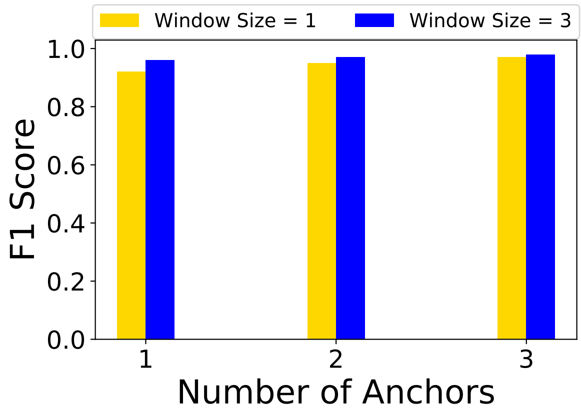


Figure 4.8: Impact of increasing number of anchors on accuracy of proposed solution. Increasing the number of anchors increases classification accuracy.

#### 4.3.2.3 Number of Anchors

We collected data in each location from 3 different anchors but in all the previous sections, the reported results are average scores calculated from just 1 anchor. In this section, we evaluated the impact of combining results from more than 1 anchor. Figure 4.8 shows the evaluation results. As expected, combining data from more anchors increases the robustness. Figure 4.8 shows that if we combine data from 3 anchors, using just 1 sample (window size of 1), we can detect the spot size of $7cm \times 7cm$ with an F1 score of 0.97.

#### 4.3.2.4 Training Size / Time

One of the important aspects of every classification problem is the amount of training data. In this section, we evaluate the amount of required training data to adequately estimate the location. In this experiment, we change the amount of packets used to generate fingerprints and report the final $F1$ score to classify 15 spots with the size of $7cm \times 7cm$. The results are reported in Figure 4.9. Figure 4.9 shows that

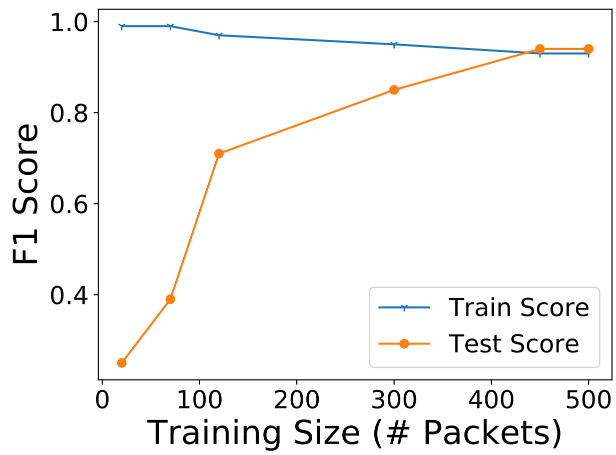


Figure 4.9: Impact of changing training size on accuracy of proposed solution.

after increasing number of training packets to more than 450 packets, the training score does not change that much and test score becomes higher which is an indicator of overfitting. We observed the same behavior in other locations (dining hall and office space) as well. Since the anchors broadcast beacons every 50 ms, collecting 450 packets for training requires at least 22 seconds of data collection in $7cm \times 7cm$ area.

#### 4.3.2.5 Wireless Link Properties

DW1000 chip supports up to 7 channels with different central frequencies. In this section, the impact of using different frequency channels on the accuracy of the solution is shown. In this experiment, we collected data in two rounds. In the first round, the nodes communicate in channel 2 with frequency of 3.993 GHz and in the second round we collected data from the same spots but this time nodes communicate in channel 5 with central frequency of 6.489 GHz. As it is shown in Figure 4.10, the results are more reliable in channel 2 compared to channel 5. It is reasonable considering the fact that higher frequency channels have lower penetration capabilities and loose power faster than lower frequency channels.

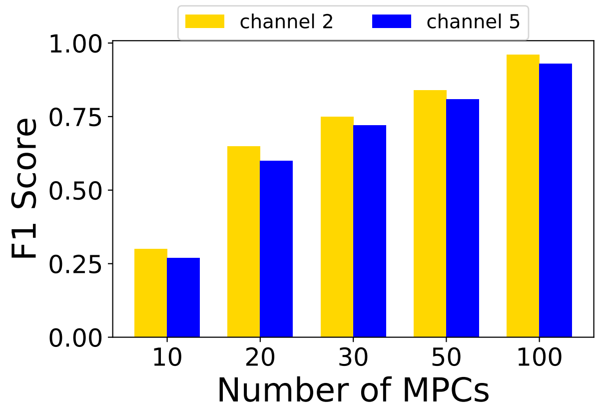


Figure 4.10: Impact of different frequency channels on accuracy- lower frequencies generate more reliable fingerprints

### 4.3.3 Overall Accuracy

#### 4.3.3.1 Compared to Time-of-Arrival Ranging

We also run two-way ranging application provided by Decawave company in the coffee shop area ($15m \times 10m$) with 3 anchors and measured its accuracy over 12 test points. The average error was approximately 45 cm.

#### 4.3.3.2 Maximum Localization Error

There are cases in which the system misclassifies the target's location. Now we study, how far is the detected location from the real location. Figure 4.11 shows the CDF of maximum errors. As shown in Figure 4.11, in 92% of the times the maximum error is below 6 cm and in 97% of times, the maximum error is below 10 cm making the system useful in indoor localization applications.

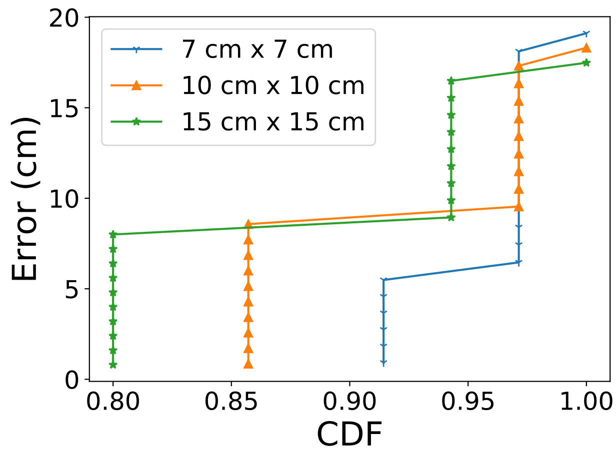


Figure 4.11: Maximum localization error observed by proposed solution(CDF). In 92% of the times the error is less than 6 cm.

#### 4.3.3.3 Resilience to Temporal Changes

To evaluate the resilience of proposed method to temporal changes, we collect data from the coffee shop one week after collecting the training data creating four different scenarios: in each scenario, we reorganized some pieces of furniture like tables and chairs and collected data from the same spots as training data was collected. Figure 4.12 reports $F1$ scores and maximum errors calculated from our proposed method. Despite sometimes $F1$ score going down to 0.6 even with window size of 3, the maximum error remains under 20 cm in all the scenarios. Periodic training could improve the classification score.

## 4.4 Discussion

The smallest spot which can reliably be located with proposed approach is $20cm \times 20cm$ which is comparable with state of the art indoor localization techniques using ToA or TDoA estimation; but those approaches need information from at least 3 anchors in Line-of-Sight view to accurately estimate the location of target. Since

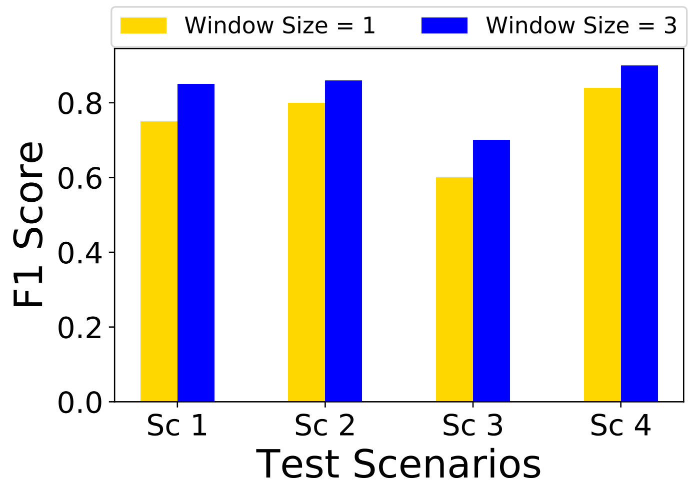


(a) $F1$ Score

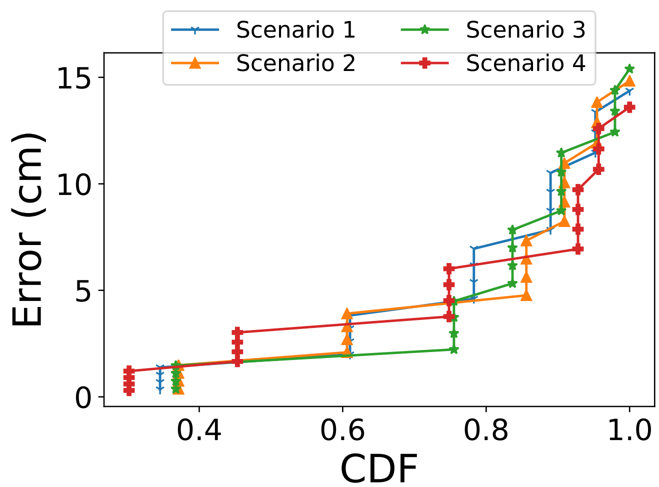


(b) Maximum Localization Error

Figure 4.12: Resilience to temporal changes. Changing the environment does not dramatically degrade the performance of spot detection

the proposed approach uses signal features to generate fingerprints, and does not not measure the time of flight, the path traveled by the signal can be either line of sight or non line of sight. Other single-anchor localization techniques (virtual anchor solutions) in the best case achieve 1 m error in 90% of the times.

In our data collection, we used a robot to move around and collect data. Despite the fact that our evaluations show that the CIR fingerprints are resilient to temporal changes in the environment, to improve the robustness of the system to massive changes in the environment (for instance, movement of big pieces of furniture), the automatic retraining can be done via programming the robot to follow a predefined path on regular basis. The main advantage of proposed approach is reducing the number of required anchors from 3 to 1 while keeping the accuracy reasonably comparable with state of the art solutions. Also, data collected by robot is only used for training; our solution is able to locate the target with 96% accuracy by using only 3 consecutive packets which makes it practical for indoor object/human tracking. In other words, receiving 3 packets only takes 150 ms in which target still is inside the target cell.

## 4.5 Conclusion

In this work, we study the feasibility of using reflected multipath components extractable from CIR information from UWB signals to implement a robust single anchor indoor localization applications. Our evaluations show that the proposed approach can locate a target inside a spot with size of $20cm \times 20cm$ with $F1$ score of 0.96. Our solution uses just one anchor, which is not necessarily LoS, to locate the target which significantly increases the robustness of indoor localization systems.

# Chapter 5

# Study and Mitigation of UWB Interference on Ranging

The 802.15.4-11 standard defines ALOHA as MAC protocol for UWB communication in which interference is considered negligible and nodes use the medium whenever they need to send a message without checking the availability of medium.

If we increase the number of communicating UWB nodes in localization network, ALOHA may not be able to protect UWB communication from interference. In addition, non-cooperative UWB communication may increase ranging errors. Non-cooperative UWB traffic and interference are caused by other UWB nodes in the vicinity but are not necessarily adversarial. As UWB systems become more common, the chances of non-cooperative UWB interference increases. The main question we try to answer in this work is how scalable is the UWB localization given the possibility of interference and its impact on localization accuracy?

In our work, we study the likelihood of wideband interference in different localization scenarios with different UWB physical layer setting and network sizes. We also quantified the impact of interference on ranging accuracy and showed performance drop in UWB-based localization due to the existence of non-cooperative UWB interference.

UWB signals are sent as a sequence of short pulses and the accuracy of UWB-based ranging methods is mostly dependent on the ability to identify the time of the first path's arrival. UWB-based ranging techniques use an accurate estimation of the channel impulse response (CIR) to accurately identify the first path. Non-cooperative UWB traffic can change the CIR which may lead to errors in ranging. In this work, we proposed a simple and practical technique called RAPSI (Random Pulse Shape Identification) to detect the ranging error caused by wideband interference and reduce this error by using unique characteristics of UWB signals. For each node, we use different pulse shapes and we utilize this unique shape of UWB pulses to search the distorted CIR to find the best match for the known pulse shape. Overall, RAPSI reduces 30% to 40% ranging error caused by wideband interference in normal indoor localization applications.

Our contributions in this work are:

- Study the likelihood of wideband interference and its impact on UWB-based ranging
- Design RAPSI, a simple and practical method to detect and mitigate ranging error caused by wideband interference
- Evaluate the effectiveness of RAPSI in real world scenarios

## 5.1 Related Work

Interference is an old research problem in wireless communications including Ultra-wideband signals.

### 5.1.1 UWB Interference Detection & Mitigation

Impact of interference from narrow-band signals on UWB receivers has been studied before. Non-linear filters can improve the performance of UWB receivers by canceling out narrow-band interference [47, 49, 72, 75]. Recently [70] compressed sampling is also used to estimate and remove narrowband interference (NBI). Creative ideas like using direction of UWB waves to detect and remove narrowband interference showed reduction in the bit error rate in UWB receivers [46].

Multi-user interference (MUI) in UWB systems has also been investigated before. Multi-user interference can be modeled with hidden Markov model or Gaussian mixture model [32]. Another work [76], utilizes the received UWB signal cluster sparsity characteristics to mitigate the multi-user interference. These efforts improved decoding performance of energy detection based receivers in UWB communication by adding complexity to the receiver.

Studies show [34] adding randomness to modulation scheme will improve the performance of ranging and reduces the error to a few meters. Using non-linear filters in physical layer also reduces the errors but makes the receiver more complicated and expensive [74]. Perfect autocorrelation characteristic of UWB preambles is used to detect the interference in the physical layer and reduce the ranging error to few meters [33].

One option to prevent multi-user interference is to coordinate medium access,

Table 5.1: Maximum Advised Transmissions per Second If ALOHA used as MAC Layer vs datasheet [3]

| Channel | PRF (MHz) | Date rate | Preamble Length (Symbols) | Payload (Bytes) | TX Time | TX per second at 18% air-utilization |
|---|---|---|---|---|---|---|
| 2 | 64 | 110 kbps | 2048 | 30 | 4.684 ms | 40 |
| 2 | 64 | 6.8 Mpbs | 1024 | 30 | 1.108 ms | 180 |
| 7 | 16 | 110 Kpbs | 256 | 30 | 2.853 ms | 62 |

for instance, with carrier sensing. However, the low power signals, the intermittent characteristics of IR-UWB signals and the possible absence of a carrier make it hardly feasible to reliably perform carrier sensing or clear channel assessment (CCA) with a reasonable complexity.

### 5.1.2 ALOHA Protocol

The ALOHA mechanism is the suggested channel access method in the IEEE 802.15.4 UWB PHY standard. Performance of ALOHA protocol has been evaluated previously and studies [53] showed its performance drops dramatically in dense networks. For ALOHA to work successfully total air utilization has to be less than 18% across all nodes in range of each other [3]. With air utilization above 18%, collision probability is high and system performance degrades quickly. Below the 18% air utilization, 97% of transmissions are likely to succeed without collisions. This 18% air utilization comes into play when deploying a group of Tags. Table 5.1 gives some indications of the blink transmission rates corresponding to some typical data rate/preamble length combinations and with a minimum 12-byte blink frame sending the Tag ID. It is shown in table 5.1 that due to a comparatively long transmission time of typical ranging packets, collision is very likely in dense networks.

Table 5.2: Scalability and Limitations of Commercial UWB Indoor Localization. (Supporting evidence for some of these claims are not available and could be incorrect)

| Company | Localization Technique | Max number of Tags | Max number of Anchors | Update Rate (Hz) | Limitation |
|---|---|---|---|---|---|
| Decawave [2] | TWR | 6 | 4 | 10 | TDMA based MAC |
| CIHOLAS [1] | TDoA | 48 | 10 | $\leq$20 | not evaluated |
| UNISET [19] | TWR | Limited Density | 10 | $\leq$ 20 | Density Unknown |
| UNISET [19] | TDoA | Unlimited (Claimed) | 10 | $\leq$ 20 | Not evaluated |
| POZYX [12] | TWR | 10 | 10 | $\leq$ 40 | Not evaluated |
| RedPoint [14] | TDoA | 65000 (Claimed) | 1000 | Not Specified | Wired Infrastructure |
| Time Domain [17] | TWR | Unknown | Unknown | Unknown | TDMA based MAC |

### 5.1.3 Commercial UWB-based indoor Localization and Interference

After IEEE 802.15.4 standardized the usage of UWB signals in low power wireless networks, there have been a lot of efforts to bring inch-level accurate UWB based indoor localization systems to the real world. There are many companies who design and sell the real time localization system (RTLS) solutions. We did a survey on the most widely used commercial solutions to understand how they handle interference and their scalability. Despite the very accurate results in ranging performance these companies mention in their websites and show in their demos, almost all of them did not evaluate their systems in dense networks. Table 5.2 summarizes the result of our survey.

Table 5.2 shows that two-way ranging solutions support a maximum of 10 nodes in the network since most of them use the time division multiple access (TDMA) protocol to handle the interference. Other solutions suggest using time difference of arrival technique (TDoA) for localization and claim that their solution can support high density networks. TDoA based solutions also have their scalability limitation. First of all, in TDoA, the anchors (nodes with known position) should be synchronized which is a major problem in making these solutions scalable. Also, TDoA solutions are mostly for tracking applications (Localization is done in Anchors) and are not useful for navigation solutions. TDoA requires cooperation between anchors to be able to locate the target which reduces the scalability.

In summary, the impact of multi-user interference in energy detector receiver in impulse UWB ranging has not been studied and addressed properly in the literature. In our work, we study the likelihood of interference in UWB localization applications and the impact of that interference on ranging performance. We also provide a simple yet effective solution to mitigate the impact of interference.

## 5.2 Design

In this section, we describe the basics of UWB communication and ranging, present the results that show UWB interference in different scenarios and their impact on ranging error, and present the design of RAPSI, a technique to detect and mitigate ranging errors caused by interference. Our key idea is using different pulse shapes for different nodes to improve the ability of receiver to extract the intended pulse from CIR which is distorted under interference.

#### 5.2.0.1 Network Traffic in Localization Applications

Generally, localization applications are considered low traffic applications due to the limited number of messages required for ranging. However, factors like location update rate and the number of neighbor nodes may increase the overall traffic leading to a higher chance of wideband interference. There are three major techniques for UWB indoor localization: Two Way Ranging (TWR), Time Difference of Arrival (TDoA), and Direction of Arrival (DOA). The most simple one is TWR since the other two approaches require precise synchronization (with nanosecond granularity) between nodes which decreases the scalability of such approaches.

In TWR, each target node (Tag) needs to estimate its distance to at least three other nodes with known locations (Anchor) and finally, use trilateration to estimate its 2D location. To estimate the distance to each Anchor, at least three messages (double-sided two way ranging [48]) have to be exchanged. Thus, each location estimation requires at least 8 packet transmissions in localization applications and 5 packets in tracking applications even with an optimization: Tag talks with all 3 anchors with one message through broadcast which reduces the total number of packets.

Based on the values reported in table 5.1, if on average each packet occupies the channel for 2 ms, and each Tag updates its location 10 times per second, overall each Tag occupies the channel for 160 ms per second. Such a network with just five Tags would result in 80% channel utilization. Thus, a relatively simple localization application in a small network could lead to high channel contention and interference.

In non-cooperative UWB networks, the probability of packet collision can be surprisingly high as we found from testbed experiments and also quantified under simplifying assumptions: $1 - e^{-2G}$ (G is number of attempts to send packets during twice the time it takes to send one packet). A 10-node network with 10 Hz broadcast of 12 bytes/pkt can lead to collision probability of 46%. Empirically we found this probability to be about 54%.

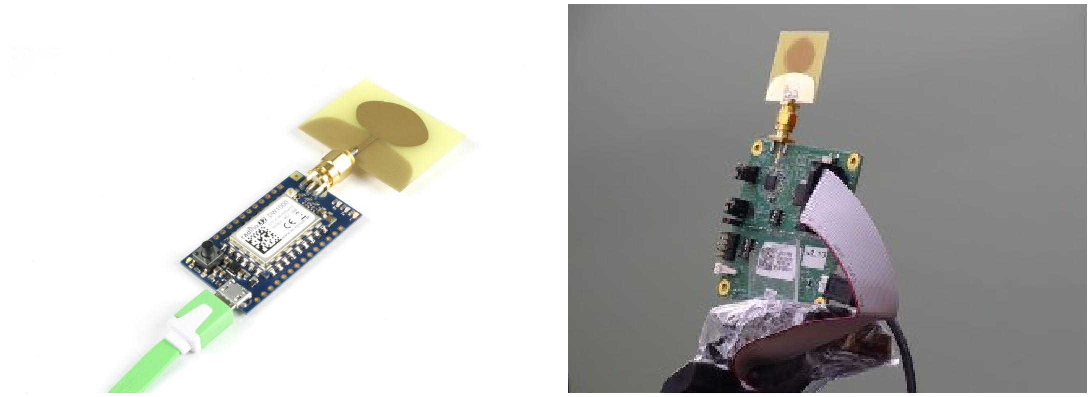

(a) Radino32 (b) EVB1000

Figure 5.1: UWB nodes used in data collection

### 5.2.1 Wideband Interference & Ranging

In this section, we analyze the impact of wideband interference from non-cooperative UWB nodes on the ranging performance.

#### 5.2.1.1 Interference Measurement Setup

Our testbed consists of Radino32 (Figure 5.1a) and EVB1000 (Figure 5.1b) boards which both have DW1000 RF Transceiver, which is IEEE 802.15.4-2011 UWB compliant. Radino32, uses STM32L151CC with 32-bit ARM Cortex-M3 CPU with 256 KB Flash, 32 KB RAM, 8 KB EEPROM and 12 bit ADC and DAC [10]. EVB1000 boards use STM32F105 ARM Cortex M3 processor with 12 MHz external crystal and 32.768 kHz RTC crystal [5].

We deployed 15 Radino32 nodes in a corridor ($6m \times 14m$) (Figure 5.2) while two Decawave EVB1000 nodes are placed 12 meters apart. In all the experiments, EVB1000 nodes are used for distance measurements and we refer to them as ranging nodes. Ranging nodes are placed in constant locations and run two way ranging with 10 Hz.

Figure 5.2: Experimental set up to create interference

To create non-cooperative UWB network traffic, we setup Radino32 nodes to periodically send packets with 30 bytes payload. The sending rate can be configured to 20 Hz, 10 Hz or 5 Hz. Each node uses a random delay value before sending its packet. This random value is selected between 0 up to maximum possible delay based on configured sending intervals (for instance 0 to 50 ms for 20 Hz frequency).

In each experiment, we collect at least 2000 packets and results are averaged over all the collected packets. In total, during our experiments, we collected more than 200000 ranging packets.

Last but not least, in order to improve the visibility of figures and claimed assumptions, in all the experiments, CIR samples are 10 times up-sampled using the Fourier method [8].

#### 5.2.1.2 Likelihood of Wideband Interference

We first study the impact of the non-cooperative wideband interference on communication. We want to know if the nodes can decode messages under interference. How do changing the parameters of UWB physical layer impact the packet drop rates? In this section, we use different settings (Number of Nodes, Physical Layer Setting and

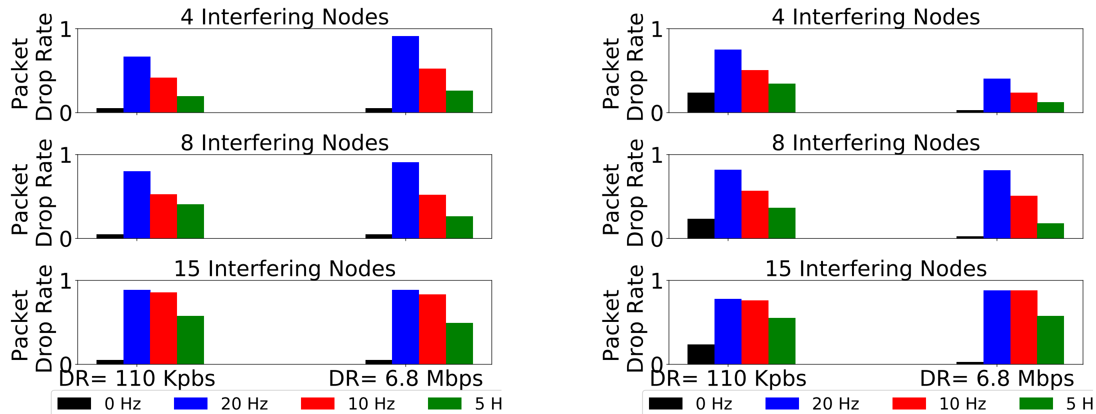


(a) Channel 2, PRF = 64 MHz, Preamble Len = 1024

(b) Channel 7, PRF = 64 MHz, Preamble Len = 1024

Figure 5.3: Packet drop caused by wideband interference under different data rates (110 Kbps and 6.8 Mbps)

Packet Transmission Rate) of UWB nodes and measure packet drop rates in each of those settings. Unless otherwise mentioned, in each experiment, all the interfering nodes (Radino32) and ranging nodes (EWB1000) are configured using the same parameters.

**Data rate & Wideband Interference.** UWB nodes can communicate with three different data rates: 110 Kbps, 850 Kbps and 6.8 Mbps [9]. Generally, lower data rates are preferred for a better ranging performance, but decreasing the data rate will increase the packet transmission time which leads to higher chance of collisions. Figure 5.3 shows the impact of changing the data rate on packet drop rates.

In less dense networks with less traffic, the lower data rate causes more packet drop rates in crowded scenarios. Higher data rates are preferred on more dense networks.

**Preamble Length & Interference.** Another parameter in UWB physical layer which impacts ranging performance is preamble length. Figure 5.4 shows the impact of changing the preamble length on the likelihood of collision and dropping the packet.

In most cases, changing the preamble length does not cause a noticeable increase

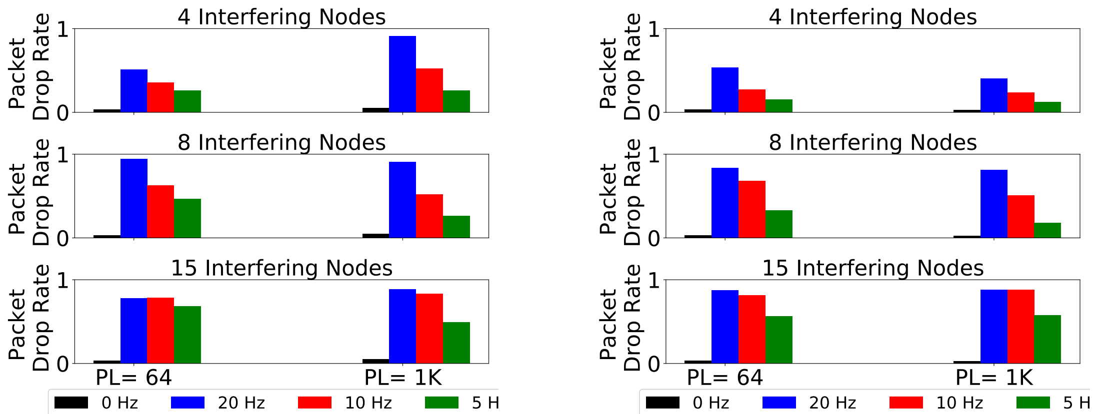


(a) Channel 2, PRF = 64 MHz, Data Rate = 110 Kbps

(b) channel 7, PRF = 64 MHz, Data Rate = 110 Kbps

Figure 5.4: Packet drop caused by wideband interference under different preamble length (64 and 1024 symbols)

in packet drop rates.

**Center Frequency & Interference.** IEEE standard defines 16 different channels for UWB communication which are in the range of 3 GHz to 7 GHz but DW1000 only supports 6 of them (Table 2.1). In this experiment, we kept all the UWB physical layer configurations same (PRF = 64 MHz, Preamble Length = 1024 and Data rate = 110 Kbps) and only changed the center frequency. The results are summarized in Figure 5.5. Channel 7 has higher bandwidth ($\approx$1.3 GHz) compared to channel 2 ($\approx$500 MHz) and that is why the packet drop rates are higher in channel 7.

Results from Figure 5.5 show that wideband interference is a real problem across all the frequency channels and increasing the bandwidth will not significantly improve the ranging performance under interference.

#### 5.2.1.3 Ranging Errors Under Wideband Interference

In previous sections, we showed that even in high density and high traffic networks, nodes still receive some ranging packets. Now, if a node receives a packet under

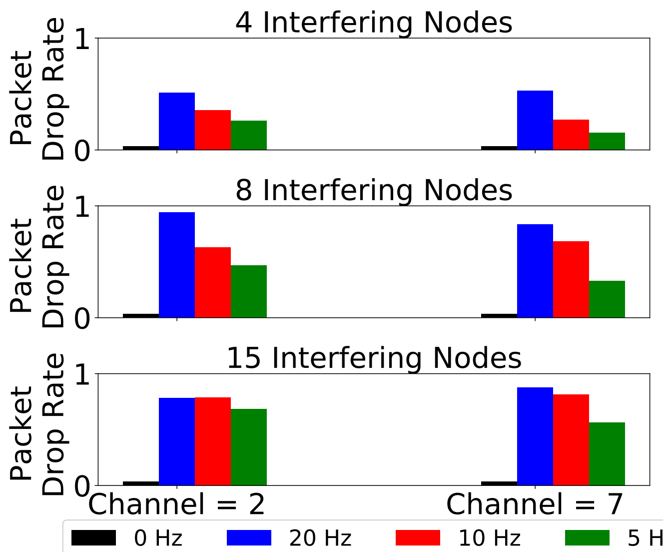


Figure 5.5: Packet drop caused by wideband interference under different frequency channels (Channel 2 and 7)

interference, what happens to the ranging performance. Figure 5.6 shows the CDF of ranging errors under interference happening in different channels.

We find that ranging done with the packets retrieved under interference leads to large errors.

Regardless of the frequency channel, on average the chance of ranging error of more than 40 cm is more than 50%. The error is worse in 2D localizations: at least 3 range estimations are required to locate the target thus leading to higher chances of not being able to locate the target.

### 5.2.2 Design of RAPSI for UWB Interference Detection and Mitigation

In this section, we describe the design of RAPSI, Random Pulse Shape Identification, a technique to detect and mitigate the impact of interference on UWB-based ranging.

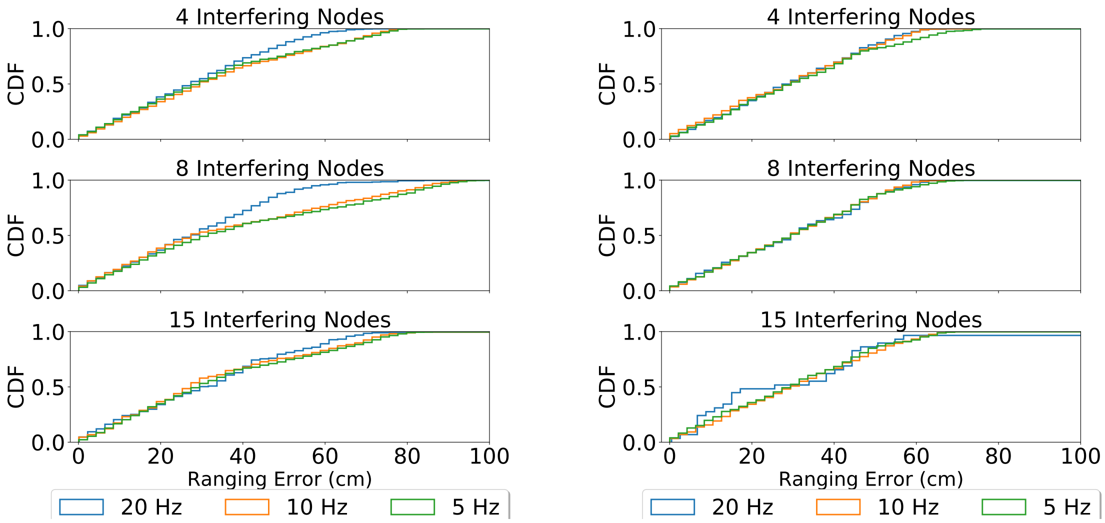


(a) Channel 2, Preamble Length = 1024, PRF=64 MHz

(b) Channel 7, Preamble Length = 1024, PRF=64 MHz

Figure 5.6: CDF of observed ranging errors across different number of interfering nodes and with different traffic

#### 5.2.2.1 Pulse Shape

UWB signals are sent as a sequence of pulses. There is a parameter in DW1000 settings called pulse generator delay (PGDelay). PGDelay sets the width of transmitted pulses which changes the output bandwidth. Previous studies showed that changing the pulse width will not impact the ranging performance but it changes the pulse shape and unique pulse shape can be used as unique identifier for sender nodes [36].

Our hypothesis is if nodes use different pulse shapes, these unique pulse shapes can be extracted from distorted CIR using matched filters (the key idea of our proposed random pulse ranging). In order to validate our hypothesis, we put two EWB1000 nodes in an anechoic chamber (Figure 5.7a) and collected CIR information while nodes were communicating with different PGDelay values. We also created a reflection path by using a reflective surface (Figure 5.7b) to make sure the data we use to extract the pulse shape is from the first path and not from a reflected path.

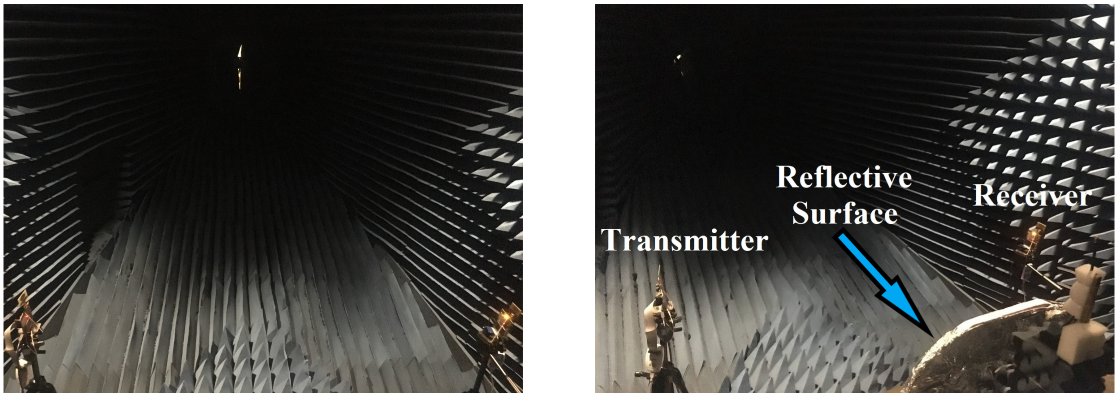


(a) Line of Sight (b) Line of Sight with Controlled Reflection

Figure 5.7: Using anechoic chamber to extract pulse shape

Figure 5.8 shows pulse shapes extracted from the first path in CIR data collected in the chamber. As expected, the width of pulse is different using different PGDelays in both channel 2 and channel 7.

**Pulse Shape Adjustment.** Even though Figure 5.8 shows the different width of pulses, the amplitudes of pulses are approximately equal which makes them not practical to be used as templates in matched filter. To mitigate this problem, we adjust those pulse shapes to make sure the area under each pulse is equal while the width of them are different (adjusted pulse shape). We change the amplitude of pulses to make pulses equal in the area. Figure 5.8 shows the pulse templates after the adjustment. In summary, the core of RAPSI is to utilize different pulse shapes during transmission and utilizing these pulses as templates for standard matched filtering to detect distorted CIR and also extract the first path from it.

#### 5.2.2.2 Using Random Pulse Shapes

UWB nodes can communicate with each other using different pulse shapes. In other words, different pulse shapes typically do not have much impact on the ranging or communication capabilities of UWB nodes. Our proposed interference avoidance

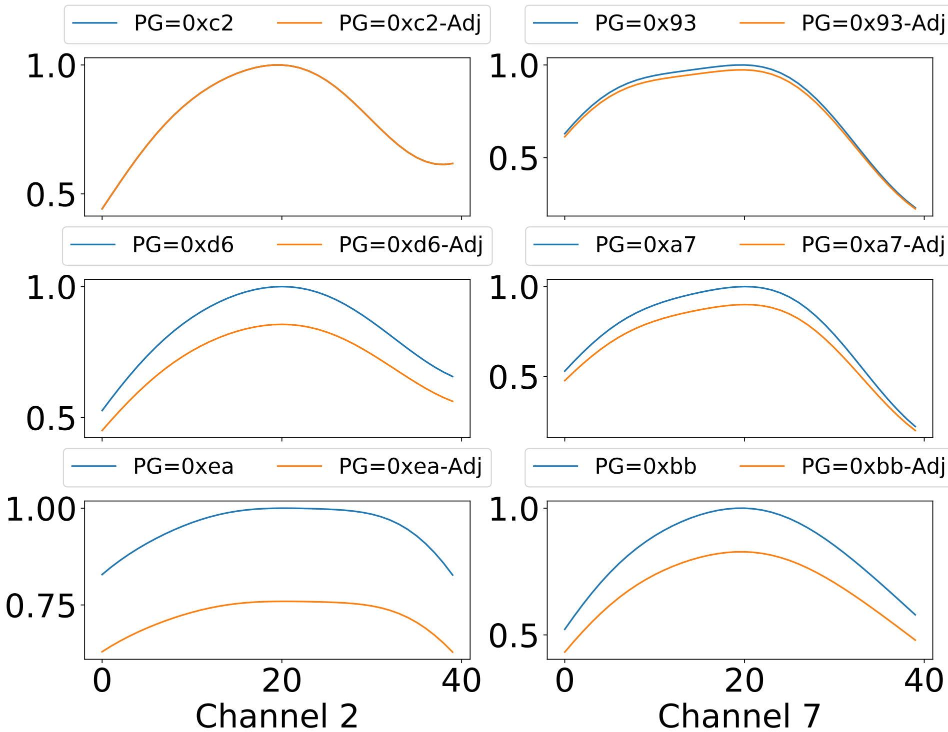


Figure 5.8: Pulse shapes across different PGDelay values

technique (RAPSI) is the combination of adding random delays and also random pulse shapes in UWB ranging. Since pulse shapes do not need to match between sender and receiver of UWB message, the sender can randomly choose a pulse shape and send its data using that pulse shape. The sender should include the pulse shape code (1 Byte) in its message. The receiver upon receiving this pulse shape code can both detect and also mitigate the ranging error caused by interference.

#### 5.2.2.3 Detect the Existence of Interference

Our technique for detection of interference is based on the hypothesis that match filter output will not match with the first path from CIR in the packets retrieved under interference.

**Algorithm 2** Proposed Interference Detection Technique

$Th_{Detection} \leftarrow$ Interference Detection Threshold
$CIR \leftarrow$ Channel Impulse Response Extracted from Received Packet
$PGDelay_{target} \leftarrow$ Sender's PGDelay Encoded in the Payload
$PulseShape \leftarrow$ Pulse shape based on $PGDelay_{target}$
$MatchedCIR \leftarrow$ Call MatchFilter($CIR$,$PulseShape$)
$MaxCorIndex \leftarrow$ Index of Maximum Value in ($MatchedCIR$)
$FPIndex \leftarrow$ Index of First Path in ($CIR$)
**if** $abs(MaxCorIndex - FPIndex) \geq Th_{Detection}$ **then**
  Return $True$
**else**
  Return $False$
**end if**

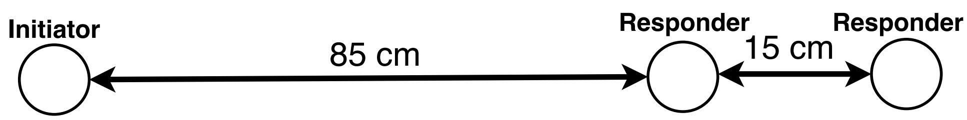


Figure 5.9: Experimental setup to verify proposed interference detection technique

To verify our hypothesis, we conducted a simple experiment. We placed one EVB1000 board as initiator node and two other EVB1000 boards as responders (Figure 5.9). The initiator node sends a broadcast message and each responder upon the reception, replies after a constant time (190 $\mu$s) using DW1000's delayed send functionality. In delayed send mode, DW1000 copies the data to its internal buffer and on the designated time ($\pm 8ns$) it just sends the data. Since two responders are 15 cm away from each other, two arriving paths should be visible at receiver as two consecutive pulses.

Following above mentioned setup, we are able to create an interference scenario. We conducted this experiment on both channel 2 and 7 while two responders were using different PGDelay values then we applied our interference detection technique on the collected CIR (Average of 1000 Packets). Figure 5.10 shows the matched filter result after applying the filter on the retrieved CIR.

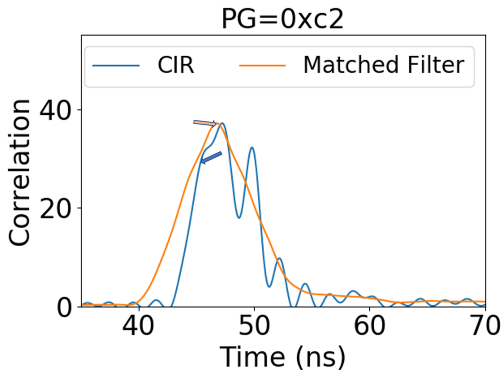


(a) Channel 2

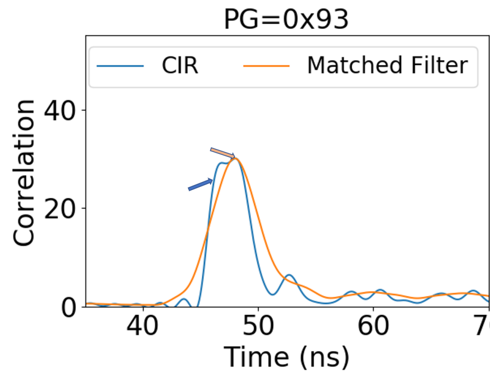


(b) Channel 7

Figure 5.10: Detect the wideband interference from CIR - peak of matched filter output (orange arrow) $\neq$ first path of CIR (blue arrow)

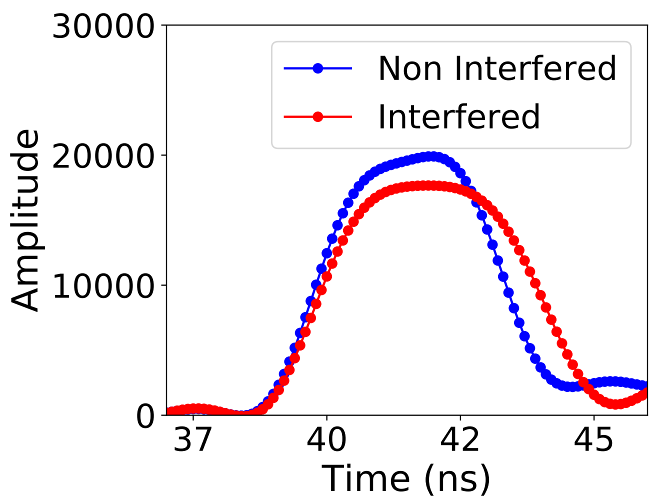


Figure 5.11: Wider first path shape under interference

On both channels, there is a gap between the first path of CIR and the peak of matched filter output. We utilize this difference as an indicator of wideband interference impact on the UWB packet which causes the ranging error. Basically, if captured packets are impacted by wideband interference, interfering signals overlap with original first path signal and increase the width of the first path pulse. Figure 5.11 shows validity of our hypothesis. Figure 5.11 shows the first path pulse width with and without interference on channel 7. This observation is the building block of our interference detection and mitigation technique.

**Algorithm 3** Proposed Interference Mitigation Technique

$Th_{mitigate} \leftarrow$ Interference Mitigation Threshold
$FP_{Org} \leftarrow$ Original First Path
$FP_{Adj} \leftarrow$ Adjusted First Path
$CIR \leftarrow$ Channel Impulse Response from Received Packet
$PGDelay_{target} \leftarrow$ Sender's PGDelay from the Payload
$PulseShape \leftarrow$ Pulse shape based on $PGDelay_{target}$
$MatchedCIR \leftarrow$ Call MatchFilter($CIR$,$PulseShape$)
**if** $InterferenceExists$ **then**
  $FP_{Adj} \leftarrow$ First index in which $MatchedCIR_{index} \geq Th_{mitigate} * max(MatchedCIR)$
  Return $FP_{Adj}$
**else**
  Return $FP_{Org}$
**end if**

Our interference detection solution is described in Algorithm 4. The detection threshold value has been measured using trial and error technique to be 5 which means if the difference between path with maximum CIR value and index of maximum output of matched filter is bigger than the detection threshold (5), it can be classified as distorted CIR and range estimation which used that packet has been done under interference. As mentioned earlier, the CIR has been up-sampled to 10 times before calling interference detection algorithm.

#### 5.2.2.4 Mitigate Impact of Interference

After detecting the packets which are impacted by interference, we adjust the range measured using those packets because using those packets as-is for ranging could result in incorrect time of flight measurement. Our hypothesis here is if nodes use different pulse shapes, the location of the first path can be adjusted using matched filter technique. To evaluate the feasibility of this idea, we used the same set up as previous experiment (Figure 5.9). In this experiment, we collected data on channels 2 and 7. On channel 2, one of the responders (target) used 0xC2 (194) as PGDelay

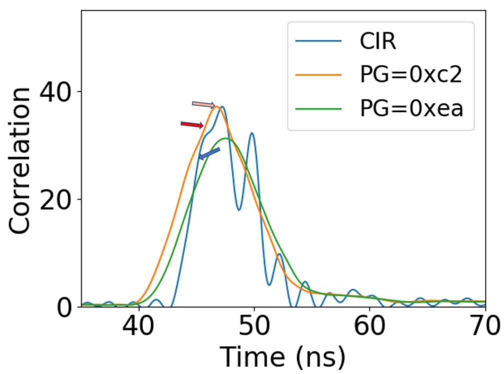


(a) Channel 2 - Intended PGDelay = 0xc2

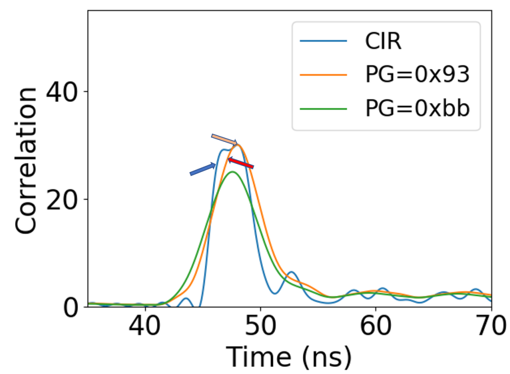


(b) Channel 7 - Intended PGDelay = 0x93

Figure 5.12: Intended pulse template has higher correlation values. First path can be adjusted from matched filter output. (blue arrow = first path detected by DW1000, orange arrow = matched filter output peak- red arrow = adjusted first path)

value while the other one (interferer) used 0xD6 (214). On channel 7, the target node used 0x93 (147) as PGDelay and interferer used 0xA7 (167). Figure 5.12 shows the result of applying matched filter with different templates (pulse shapes) on the captured CIR (Average of 500 Packets).

The correlation values on the intended pulse shape (0xc2 on channel 2 and 0x93 on channel 7) are significantly higher ($\approx 10\% - 17\%$) than the correlation values for other templates. If the receiver knows the PGDaley value used by sender, instead of searching inside the CIR, it can search the output of matched filter and extract the first path.

Overall, our experiments support the feasibility of using different pulse shapes to detect and mitigate the impact of non-cooperative UWB interference on UWB-based ranging. Algorithm 3 summarizes our mitigation algorithm. Using trial and error, we found that the suitable value for mitigation threshold in algorithm 3 is 0.85 which means after calculating the match filter output from CIR, the adjusted path is the first path whose correlation value is higher than 85% of peak of correlation values.

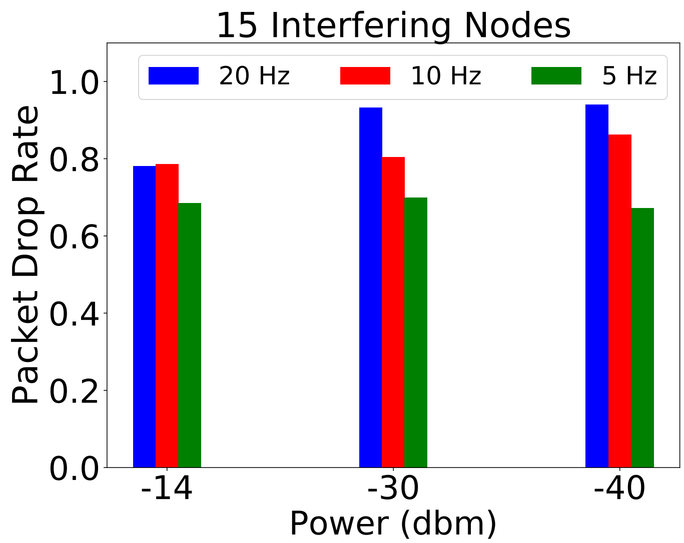


Figure 5.13: Impact of changing transmission power to avoid interference

## 5.3 Evaluation

In this section, through extensive data collection from real world scenarios, we evaluate the effectiveness of our proposed approach to detect wideband interference and also remove its impact on the range estimation (first path detection)

### 5.3.1 Performance of Interference Avoidance Techniques in IEEE 802.15.4-11

The IEEE 802.15.4-11 standard defines a few adjustable parameters (table 2.1) in UWB physical layer aiming to avoid wideband interference in UWB communication. In this section, we evaluate the effectiveness of utilizing UWB physical layer settings to avoid interference.

**Reducing Transmission Power to Avoid Interference.** In this experiment, we placed two EVB1000 nodes (ranging nodes) 12 m apart while different number (4, 8, 15) of Radino32 nodes (interfering nodes) broadcast messages with different (5 Hz,

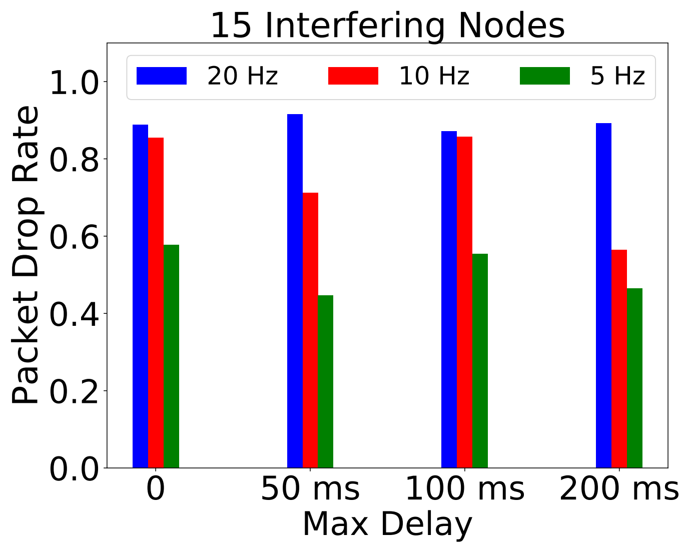


Figure 5.14: Impact of adding random delay to avoid wideband interference

10 Hz, 20 Hz) rates but with the same physical layer configurations as ranging nodes. Ranging nodes transmit with maximum possible transmission power(-30 dBm) and interfering nodes transmit with different levels of transmission power (-14 dBm, -30 dBm and -40 dBm). We want to study the impact of lowering interfering nodes' transmission power on avoiding the interference.

Figure 5.13 shows that lowering the transmission power is not a reliable way to avoid the interference in dense networks. In addition, in general, localization/tracking applications, long range performance is desired and lowering transmission power decreases the ranging performance.

**Utilizing Random Delay to Avoid Interference.** Carrier sensing techniques are considered challenging in UWB due to the limited maximum transmission power in UWB signals (To avoid interfering with narrow-band devices). IEEE 802.15.4-11 suggests ALOHA as the main technique for UWB MAC layer which sends data without checking the availability of medium. One potential improvement to pure ALOHA could be adding random delays before sending data. In this section, we

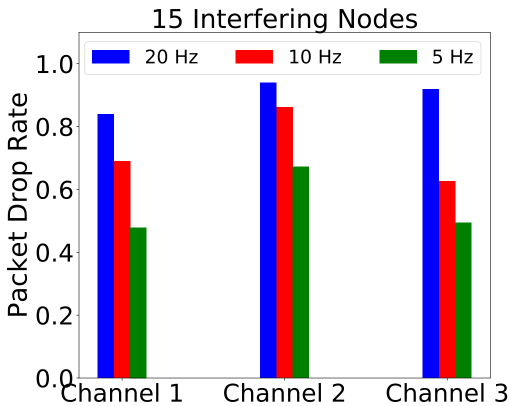


(a) Drop Rates

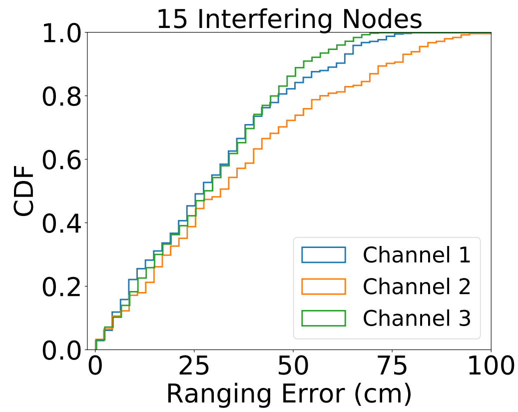


(b) Ranging Error

Figure 5.15: Packet drop and ranging error with ranging nodes (channel 2) and interfering nodes using different frequency channels (channels 1 and 3). (Channel 1=3494.4 MHz, Channel 2= 3993.6 MHz, Channel 3= 4492.8 MHz)

evaluate the effectiveness of adding random delays to UWB transmissions to avoid the wideband interference. The experiment setup is as those in the previous section, but this time we change the maximum possible random delay before sending packets and measure the packet drop rates. Each node selects a random value between 0 to max delay value and sends its data after that time interval. The maximum delay is determined by the packet sending rate. For example, for 20 Hz packet sending rate maximum random delay is 50 ms, for 5 Hz packet sending rate the maximum random delay can go up to 200 ms. Figure 5.14 shows the packet drop rates under different delays.

As shown in Figure 5.14, in some cases, adding a random delay decreases the packet drop rates but at the cost of increasing total delay of ranging application. Overall, our results indicate that nodes can utilize the maximum possible random delay to decrease the chance of interference but the improvements come at the cost of the total delay added to ranging applications. In Figure 5.14, with 20 Hz broadcasting interference, adding random delay does not change the packet drop rates due to the large number of interfering packets.

**Channel Hopping to Avoid Interference.** One of the standard ways in interference avoidance techniques is using different settings at physical layer to minimize or avoid collision between packets transmissions. In this section, we evaluate the impact of changing the UWB physical layer setting to avoid the collision. Easiest parameter to change and keep the ranging performance the same, is changing the communication channel (center frequency) of UWB signals. IEEE standard defines 16 channels for UWB communication and DW1000 chip support 6 of them. Figure 5.15 shows the drop rates and ranging errors in the experiment in which two nodes that are 12 meters apart are running ranging algorithm on channel 2, while 15 other nodes are creating traffic on other channels (channel 1 and channel 3). We kept other parameters of UWB physical layer the same in all the experiments.

Figure 5.15a shows that changing the channel does not reduce the drop rate significantly and also as Figure 5.15b reports, ranging errors are high even when the interfering nodes are communicating on different channels. This could be due to inter-channel interference between UWB channels as reported in previous studies [11]

**Changing the Preamble Length to Avoid Interference.** Other UWB physical layer setting which can be changed to increase the resilience to interference is preamble length. In this experiment, we changed the length of preamble on ranging nodes and also interfering nodes and measured the performance of ranging. The results are reported in Figure 5.16. Generally increasing the length of preamble in ranging nodes compared to interfering nodes increases the resilience to interference. Using 4096 symbols as preamble length for ranging and 64 samples as preamble length for interfering nodes achieved the lowest packet drop rate. Although longer preamble increases the performance of ranging, it increases the power consumption and transmission time which leads to a higher chances of interference.

**Changing the PRF to Avoid Interference.** Pulse repetition frequency is

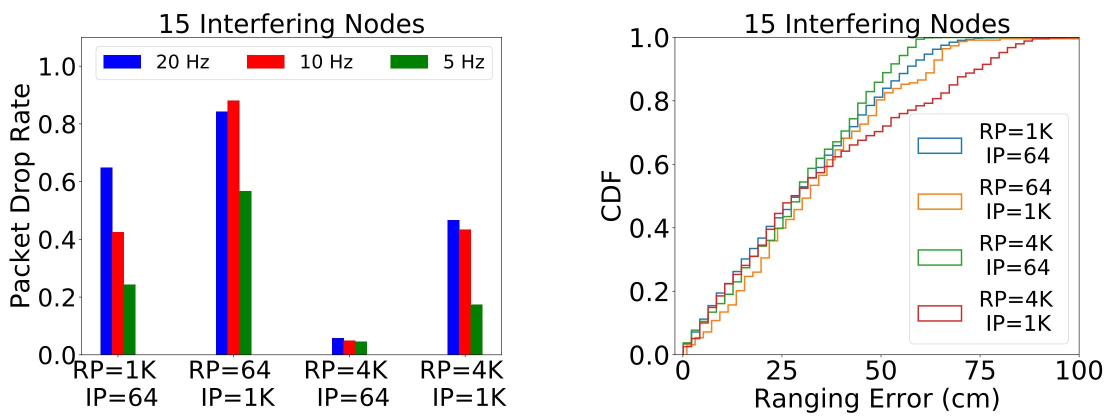


(a) Drop Rates

(b) Ranging Error

Figure 5.16: Packet drop and ranging error with ranging nodes and interfering nodes using different preamble lengths. RP=ranging node's preamble length. IP=interfering node's preamble length.

another parameter in the UWB physical layer. In this experiment, we evaluate two scenarios. In the first scenario, the ranging nodes use PRF 64 MHz while interfering nodes use 16 MHz PRF. In the second experiment, ranging nodes switch to 16 MHz and interfering nodes use PRF 64 MHz.

This is one of our most interesting findings. As shown in Figure 5.17, using different PRFs significantly reduces the likelihood of collision between nodes (Maximum packet drop of 6%). Figure 5.17 also suggests that higher PRF improves the ranging performance and resilience to interference.

**Changing the Preamble Code to Avoid Interference.** IEEE 802.15.4 defined different preamble codes per channel to avoid the interference. Figure 5.18 shows the packet drop rates while ranging nodes and interfering nodes use different preamble codes.

As expected, using different preamble codes reduces the chance of interference.

Overall, based on our experiments, using different PRFs and Preamble codes seems to be the most effective way to avoid the interference but DW1000 only supports two

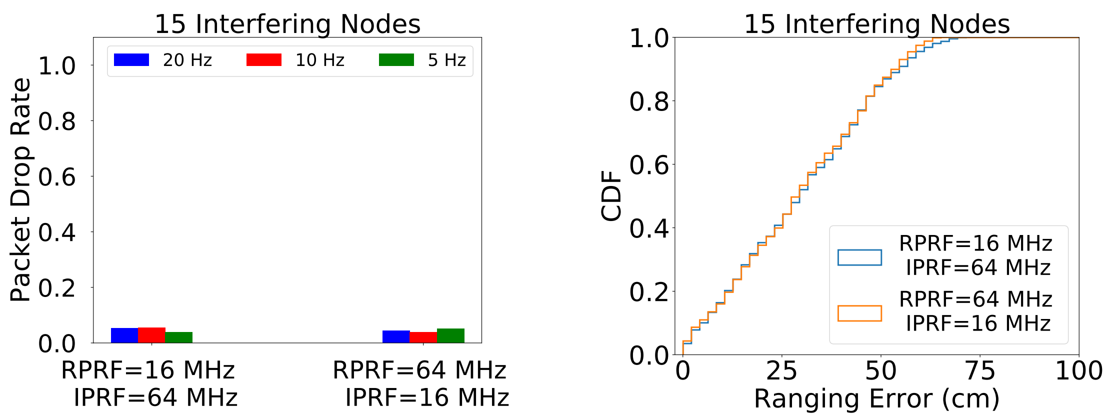


(a) Drop Rates

(b) Ranging Error

Figure 5.17: Packet drop and ranging error with ranging nodes and interfering nodes using different PRF values. RPRF=ranging node's PRF. IPRF=interfering node's PRF. The maximum drop rate was 6%.

different PRF values (16 MHz and 64 MHz) and maximum of 4 different preamble codes per channel per PRF which limits the scalability of above interference avoidance techniques. In addition, for successful UWB communication, PRF and preamble code between sender and receiver should match. Otherwise the receiver is not able to decode the received messages. This fact significantly limits the applicability of these kinds of techniques in real world localization/tracking applications since in normal localization technique, all the Tags use the same set of Anchor nodes and they all should use the same PRF and preamble code to be able to communicate. On the other hand, RAPSI just changes the pulse shape which does not impact the communication link between UWB nodes.

### 5.3.2 Accuracy of RAPSI for Interference Detection

In this section, we evaluate the accuracy of RAPSI in detecting wideband interference. In this experiment, 2 EVB1000 nodes are placed 12 m apart and run two way ranging algorithm and another 15 Radino32 nodes generate traffic using the same

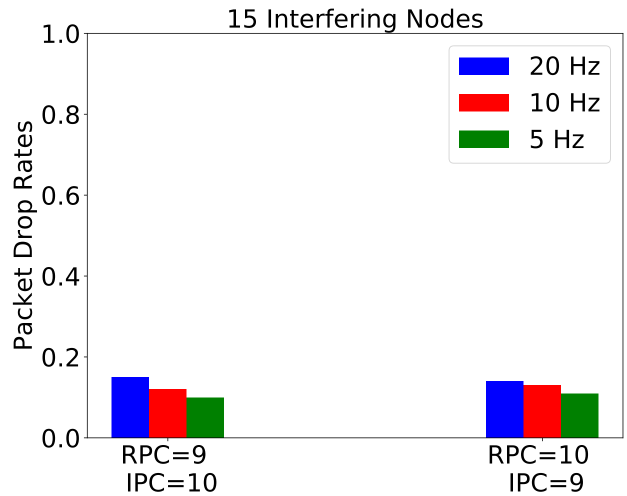


Figure 5.18: Packet drop and ranging error with ranging nodes and interfering nodes using different preamble codes. RPC= ranging node's preamble code. IPC=interfering node's preamble code

physical layer setting but using random delays and also random pulse shapes. One of our assumption here is since the location of ranging nodes are constant during the experiments, additional ranging error after activating interfering nodes, is due to the interference. To evaluate the accuracy of the proposed interference detection technique, we used amount of ranging error as an indicator of interference existence. If the ranging error estimated using a packet is higher than normal error(error when all the interfering nodes are off), we mark the packet as interfered packet. We calculated minimum and maximum of ranging error observed in our dataset and divided the error range into 10 equal size bands. Next, in each error band, we walked through all the interfered packets with error range in that specific band and measured the probability of classifying an interfered packet (ranging packet impacted by interference) as correct packet (False Negative) by our interference detection algorithm. The results are summarized in Figure 5.19.

In most cases, our proposed solution (RAPSI) is able to detect the packets which are received under interference with very small false negative rates (below 20% to

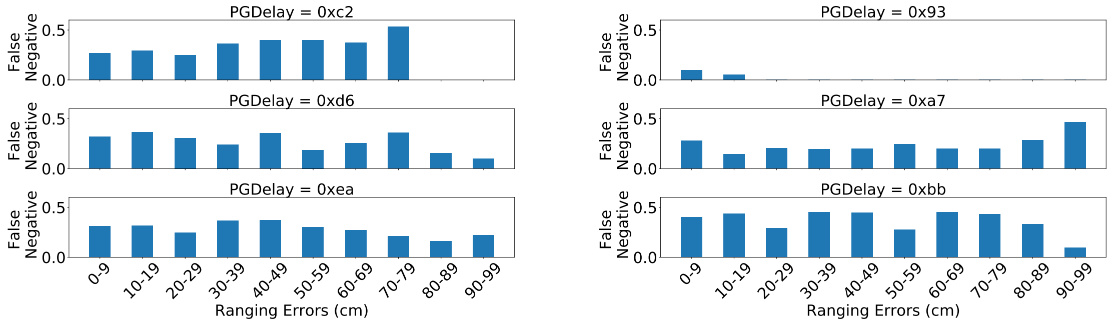


(a) Channel 2, PRF = 64 MHz, Preamble Len = 1024, Data rate = 110 Kbps

(b) Channel 7, PRF = 64 MHz, Preamble Len = 1024, Data rate = 110 Kbps

Figure 5.19: False negative values for distinguishing interfered packets from correct packets using RAPSI

%30). We achieved almost the same results with 6.8 Mbps data rate. On average on more than 75% of the cases, our technique accurately classifies corrupted ranging packets by investigating CIR and looking for the best match for designated pulse shape. We also looked at packets which were not impacted by interference and measured the false positive values (marking the packet as interfered while it is not). In average our interference mitigation technique has false positive values below 5%.

### 5.3.3 Effectiveness of RAPSI for Interference Mitigation

Next we evaluate the effectiveness of RAPSI to mitigate the impact of interference on ranging errors. We used the data collected from previous section and used our proposed technique to adjust ranging errors due to the existence of wideband interference. The results are summarized in Figure 5.20.

Regardless of bandwidth (channel 2 with 500 MHz and channel 7 with 1 GHz), our proposed interference mitigation technique is able to significantly reduce the ranging error caused by wideband interference. Based on the results from our extensive experiments, the proposed method in average reduces the ranging error by 30% to 40%

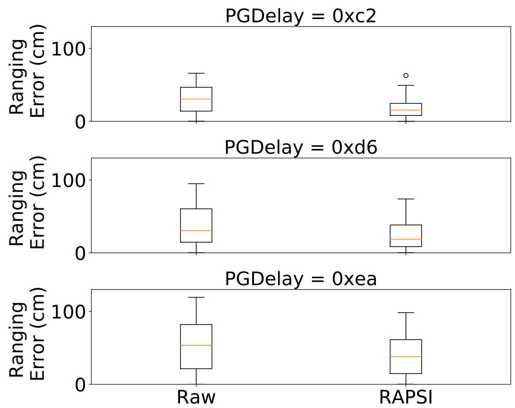


(a) Channel 2, PRF = 64 MHz, Preamble Len = 1024, Data rate = 110 Kbps

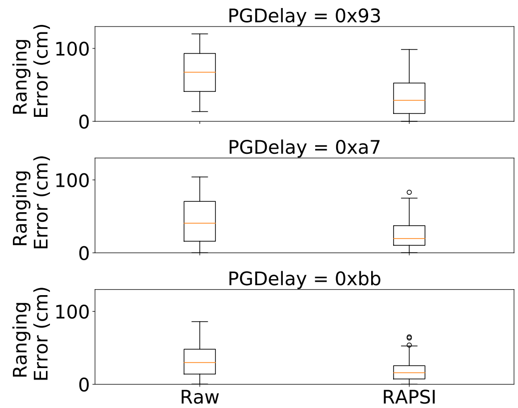


(b) Channel 7, PRF = 64 MHz, Preamble Len = 1024, Data rate = 110 Kbps

Figure 5.20: Ranging error with and without RAPSI. With RAPSI, the error is lower because RAPSI adjusts the first path using match filter

depending on the bandwidth of the channel. Higher bandwidth channels show better interference detection and mitigation on average.

## 5.4 Discussion

Time Difference of Arrival (TDoA) and Angle of Arrival (AOA) techniques reduce the localization traffic since the Tag can send one blink message for each location estimation but the chance of interference still is high in more dense networks in low data rates like 110 Kpbs. In these approaches the localization is happening in Anchor side which means these techniques are usually suitable for tracking applications and not the navigation applications. Both TDoA and AOA techniques require very accurate synchronization between anchors which may increase network traffic and chances of interference.

Changing the value of PGDelay alters the output pulse shape. Our experiments in different real world scenarios show that to be able to reliably differentiate pulse shapes, the minimum difference between two selected PGDelay values should be 5. Since PGDelay is a one byte register, on each frequency channel (DW1000 supports 6 frequency channels), $255 \div 5 = 51$ distinguishable PGDelay values are available which means our protocol can support up to 51 nodes in one area. To make sure the output signal does not violate regulatory restrictions, the TX power is tuned based on the PGDelay value.

## 5.5 Conclusions

In this work, we studied the likelihood of wideband interference from non-cooperative UWB nodes in ranging applications. We showed, in applications with low location update rates, there is a high chance of UWB interference. We also measured the impact of this wideband interference on UWB-based ranging applications. Finally, we proposed a simple yet effective technique to detect and mitigate the impact of wideband interference on ranging. Our extensive experiments in real world scenarios show the effectiveness of our proposed technique to both detect and mitigate the error caused by non-cooperative UWB nodes.

# Chapter 6

# Simultaneous Communication and Ranging in UWB

One of the physical layers covered by the IEEE 802.15.4 standard is Ultra-wideband (UWB) communication, which supports high data rate (up to 27 Mbps) communication alongside with centimeter-level ranging capability.

The ranging capability of UWB signals has recently been investigated by both research and industry, which has led to very accurate indoor localization solutions, but communication capability of UWB based LR-WPANs has not received much attention.

One common application of wireless sensor networks (WSN) is for monitoring physical events (temperature, humidity, and movement, etc.) in environments through network of sensors. In some of the applications, a mobile sink moves around the building and collects data from the deployed sensors. Accurate ranging and localization can enable lots of location-based services in sensor network applications. In current systems, UWB nodes are added to existing wireless systems to provide an accurate ranging capability to WSN.

The network traffic on today's Low Rate Wireless Personal Area Networks (LR-WPAN) can be divided into two categories: ranging traffic and non-ranging traffic. In the applications which require both communication and localization, separate hardware and software parts are responsible for each of the tasks. In other words, one chip/software reads the sensor values and reports it through WiFi or Bluetooth to the sink. In addition, a UWB chip, runs simple ranging applications and using time of flight measurement, estimates the distance between two nodes.

Existing solutions suffer from being complicated (different hardware/ software modules need to be assembled) and also high network traffic and duty cycle (handling both ranging traffic and non-ranging traffic). To be more specific, each location estimation in minimum requires at least 5 to 8 packets to be exchanged between nodes which consumes power, reduces network lifetime, and increases interference.

In our work, we investigate the possibility of using existing non-ranging traffic to estimate the distance between sender and receiver in the scenarios with high non-ranging traffic and also the feasibility of piggybacking non-ranging information (e.g., sensing application data) over ranging packets in the scenarios with low non-ranging traffic and high location update rate requirements. In the end, we propose our adaptive scheduler algorithm to optimize the ranging/non-ranging traffic by piggybacking of information which reduces the complexity of the hardware and also significantly reduces the network overhead and duty cycle.

Our contributions in this work can be summarized as the following:

- Investigate the feasibility of using existing network traffic to estimate the range
- Study the feasibility of piggybacking of non-ranging information such as sensing

application data on ranging packets.

- Propose an efficient adaptive scheduler algorithm to reduce the network overhead by utilizing existing traffic and piggybacking of information

- Evaluated our proposed algorithm over real deployment and using typical traffic on standard network stacks for low rate personal area wireless networks (LR-WPAN)

## 6.1 Related Work

### 6.1.1 Ranging in IEEE 802.15.4-11

IEEE 802.15.4-11 standard [9] suggests the following procedures for ranging. First, the application asks for ranging services from MAC layer. MAC layer increases the preamble length from its default value (to improve the ranging performance) and informs the designated receiver about new preamble length. Both sender and receiver should agree on new preamble length before starting the ranging session. Ranging will be conducted through acknowledgment packets. During ranging session, the MAC layer attaches turn around time (TX-to-RX) for all the received packets before sending them up to the higher layers. The application will inform the MAC layer to exit from ranging session and stop timestamping the packets. MAC layer informs the receiver and reduces the preamble length to its default value.

This approach is only useful for single-sided ranging which suffers from clock drift problem which leads to less accurate ranging [73]. It is also based on acknowledgment packets which increases the network traffic. The standard does not provide any further details about ranging process and ranging rates.

### 6.1.2 Traffic Reduction Techniques in Wireless Networks

One of the key techniques to improve network throughput is reducing the number of broadcast packets. RPL [81] is a standard routing protocol for Internet of Things and WSN applications. One of the main components of RPL is Trickle timer [52]. The Trickle algorithm benefits from simple suppression mechanism and also transmission point selection technique which allows Trickle's communication rate to scale logarithmically with density [52]. Trickle algorithm is not efficient in highly mobile networks and in [66] some improvements on Trickle timer has been suggested to make it more practical in mobile sensor networks.

The idea of piggybacking of packets on networks to reduce traffic overhead has been tried before. For instance, acknowledgment packets are one of the most obvious candidates for piggybacking and studies [44] showed the effectiveness of this technique in network performance improvements. Some studies [51] show up to 40% improvement in throughput by piggybacking acknowledgment messages to data messages but the improvement depends on available network traffic and the maximum delay the application can tolerate. The Nagle's algorithm [67] also tries to reduce traffic by delaying the sending of new data if any previously transmitted data on the connection still have not been acknowledged.

In summary, despite all the previous works have been done in wireless sensor networks to reduce the network traffic, to the best of our knowledge, there is no prior work that studies the coexistence of ranging and non-ranging traffic in UWB based networks.

## 6.2 Design

In this section, we explain the building blocks of our proposed technique for Simultaneous Ranging and Communication (SRAC) in UWB networks. First, we talk about our observation in two-way ranging algorithm which leads us to design two modes for ranging: active ranging and passive ranging. Finally we elaborate the scheduler algorithm in SRAC.

#### 6.2.0.1 Two Way Ranging

As mentioned in previous sections, UWB physical layer is able to accurately timestamp the arrival of the first path and estimate the time of flight. There are different algorithms which utilize these timestamps to estimate the distance between two nodes.

Double-sided two-way ranging (DS-TWR) is one of the most common range estimation techniques used in UWB localization. The overall procedure for double-sided two way ranging is shown in Figure 6.1 in which device A starts the transmission and device B replies to that message. Upon reception of B's response, device A again sends another message to B. All the communications are precisely timestamped by devices. The estimated $\hat{T}_{prop}$ can be calculated as shown in formula 6.1 [59]:

$$\hat{T}_{prop} = \frac{(T_{round_1} \times T_{round_2} - T_{reply_1} \times T_{reply_2})}{(T_{round_1} + T_{round_2} + T_{reply_1} + T_{reply_2})} \tag{6.1}$$

In formula 6.1, $T_{round_1}$ is the time it takes from sending first packet by device A to the time that device A received the reply message from device B. $T_{round_2}$ is the interval between the moment device B replies to device A's message to the moment that device B receives the reply message from device A. $T_{reply_1}$ is the time between reception of A's first message at B and the time B's reply leaves the antenna. $T_{reply_2}$

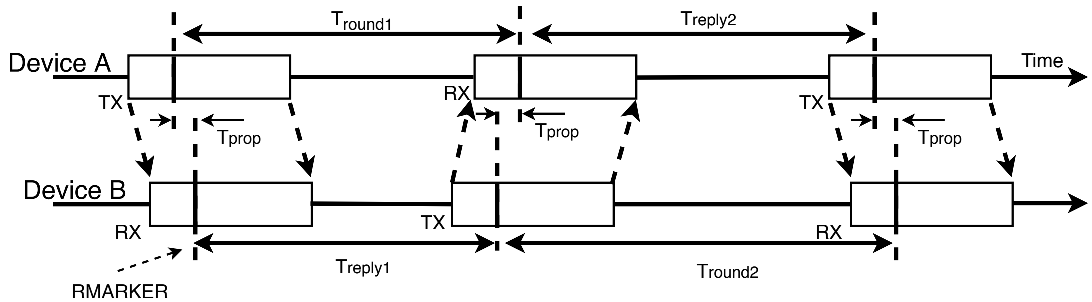

Figure 6.1: Double sided two way ranging technique

is time between receiption of B's reply at A and sending A's reply to that message.

let's assume device A runs $k_A$ times faster than its default frequency and device B runs $k_B$ times faster than its frequency.

$$\hat{T}_{prop} = \frac{(k_A T_{round_1} \times k_B T_{round_2}) - (k_A T_{reply_1} \times k_B T_{reply_2})}{(k_A T_{round_1} + k_B T_{round_2} + k_A T_{reply_1} + k_B T_{reply_2}} \tag{6.2}$$

After small back of the envelope calculation using formula 6.2, estimated propagation time would be:

$$\hat{T}_{prop} = \frac{2T_{prop} k_A k_B}{k_A + k_B} \tag{6.3}$$

finally the error in time of flight estimation can be written as formula 6.4

$$error = \hat{T}_{prop} - T_{prop} = \hat{T}_{prop} \times (1 - \frac{k_A + k_B}{2k_A k_B}) \tag{6.4}$$

#### 6.2.0.2 Resilience to Clock Drift

One of the key ideas in our work can be inferred from formula 6.4 in which the time of flight estimation error is not dependent to the $T_{reply1}$ or $T_{reply2}$ which means the response messages (from device B and A) do not necessarily have to be sent immediately. Our hypothesis is existing network traffic (sensor reports or routing information) can be utilized for ranging without sending any specific ranging packet.

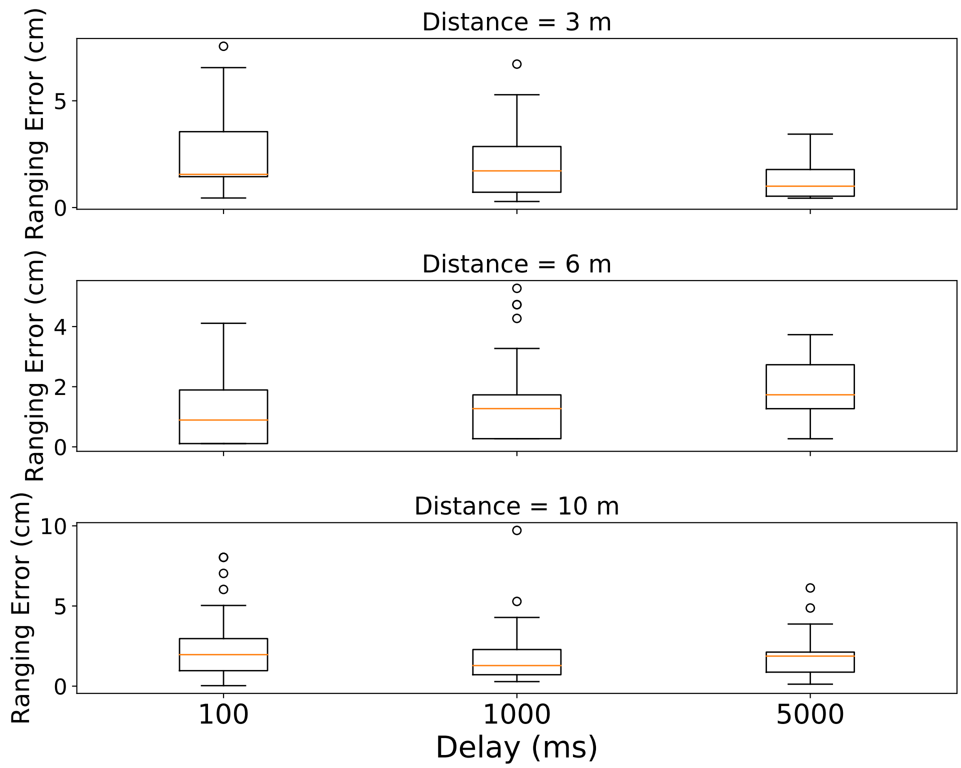


Figure 6.2: Ranging error with different $T_{reply}$ times. Increasing $T_{reply}$ does not increase the ranging error

To verify our hypothesis, we conducted a simple experiment. We placed two UWB-enabled chips (EVB1000 nodes [6]) in three different distances (3 m, 6 m, and 10 m) and used double sided two way ranging to estimate the distance between the two nodes. In each experiment, we increased the $T_{reply}$ time and measured the ranging error. The results are reported in Figure 6.2. As shown in Figure 6.2, as we increase the $T_{reply}$ time in two way ranging (which also leads to an increase in $T_{round}$ time), the observed ranging error does not change. This observation follows our expectation and proves the validity of our hypothesis.

Another interesting result from Figure 6.2 is the fact that increasing distance will not significantly change the error even during long delays. As it is mentioned in formula 6.4 $T_{prop}$ has direct relationship with the error but the speed of light in air is approximately $3 \times 10^8$ which means the UWB pulse travels almost 30 cm in each nanosecond. Even if the distance of two nodes is around 100 m the total $T_{prop}$ is around 300 ns which causes errors less then few millimeters in ranging.

This observation relaxes the requirement for immediate reply in two-way ranging algorithm. In our work, we leverage this observation to add ranging capability to sensor network applications using their existing traffic.

### 6.2.1 Passive Ranging

In passive ranging, we utilize existing network traffic to estimate the distance between nodes. Each packet contains precise timing information which helps the receiver to estimate the distance between sender and receiver of the packets.

In passive ranging, upon reception of each packet from the neighbor, the packet's sequence number and the reception timestamp is stored in the local memory. Each outgoing packet with the destination address of one of the already seen neighbors contains reply times ($T_{LastTX} - T_{LastRx}$) and delay times ($T_{CurrentTX} - T_{LastRX}$) which are calculated from packets received or overheard from neighbors. It also includes the $LastTX$ sequence number which is the last sequence number sender node has sent to target neighbor and $LastRx$ which is the last sequence number sender node has received from target neighbor. Having sequence numbers and reply and delay times, each node can calculate its distance to its neighbors.

For broadcast messages, the procedure is almost the same with a slight difference. The broadcast packet contains information from all the neighbors the node has received a packet from them in the past.

Since the size of reply time and delay time does not impact the ranging error (formula 6.4) the age of timestamps in each node's local memory does not impact ranging performance. The node could have received a packet from its neighbor 20 seconds ago and now it is sending a message to that node or broadcasting a message to all the neighbors. Upon reception of this message, the receiving neighbor can calculate its distance to the sending node.

### 6.2.2 Active Ranging

In the high mobility networks, the non-ranging traffic may not be enough for frequent ranging resulting in low rate of location updates to the applications. In this situation, SRAC switches from passive ranging to active ranging. During active ranging double sided ranging is conducted through sequence of 3 messages. The first packet is called poll message and it is a broadcast message (sent by initiator). All the recipients of poll packet immediately reply to poll message with response message which includes their calculated delay time for responding to poll message ($Response_{TX} - Poll_{RX}$). Upon reception of response messages from at least 3 responders at initiator, it sends out another broadcast message (final message) which includes initiator's reply time ($Response_{RX} - Poll_{TX}$) and delay time ($Final_{TX} - Response_{RX}$). After receiving the final message, the responder nodes calculate second reply time ($Final_{RX} - Response_{TX}$) and finally are able to calculate time of flight and their distance to initiator node. The fourth message which is an optional message is sent from responders to the initiator with calculated distance of each responder to the initiator.

During active ranging phase, SRAC piggybacks the non-ranging traffic over ranging packets. We call this case active ranging since in active ranging mode the primary traffic of the network is ranging and the non-ranging traffic has lower priority. All the non-ranging traffic will be stored in the queue and upon the availability of next

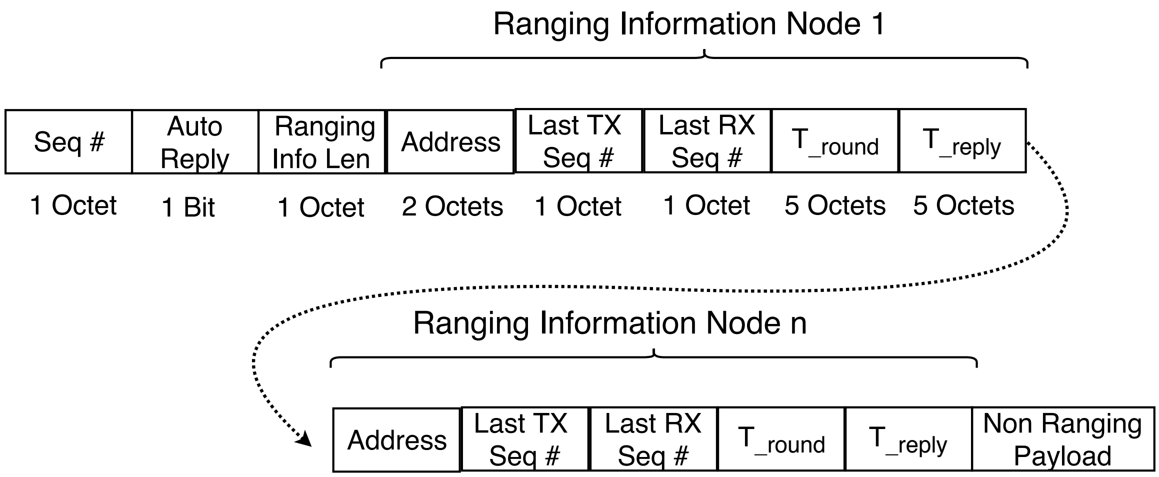


Figure 6.3: SRAC's proposed packet format

ranging packet, the non-ranging data is piggybacked over ranging packets.

### 6.2.3 SRAC:Simultaneous Ranging and Communication

We propose an adaptive scheduler to decide about active or passive ranging modes based on network conditions. In this section, we explain in details all the components of SRAC.

#### 6.2.3.1 SRAC's Packet Format

To run double sided two way ranging, time information needs to be exchanged between each pair of nodes. Figure 6.3 shows our proposed packet format to be used in SRAC.

As illustrated in Figure 6.3, each packet starts with one octet *sequence number* and 1 bit indicator of *auto reply*. In active ranging mode, poll and response messages require immediate reply which means auto reply bit has to be set in those packets. Receiver of a packet with auto reply flag on, should immediately reply to that message and include ranging timestamps. The next octet is *Ranging info Len* which determines the size of ranging information. In broadcast messages, the sender includes timestamps for all the previously seen neighbors. In unicast messages *Ranging info Len* field has a value of one. Next, ranging information for each neighbor starts. The first 2 octets are short *Address* of the neighbor. *Last TX Sequence Number* is the last sequence number sent by the sender to the target node and *Last RX Sequence Number* is the last sequence number received from target address by sender node. $T_{round}$ is $T_{lastRX} - T_{lastTX}$ and $T_{reply}$ is $T_{TX} - T_{lastRX}$. After ranging information the packet can have non-ranging (e.g., application) data which can vary in length.

#### 6.2.3.2 Scheduler Algorithm

SRAC utilizes both active and passive ranging. In this section, we propose an adaptive scheduler which switches between active and passive ranging based on network condition. Our algorithm considers the following parameters to decide about suitable ranging mode:

- Window Size: Scheduler constantly monitoring both ranging and non-ranging traffic. It uses windowing average to calculate recent traffic rates. Windows size determines the length of window to be used for averaging.

- Maximum Delay - NonRanging: Maximum delay the non-ranging traffic can tolerate. For instance, a simple temperature sensor which reports every 10 seconds has the maximum delay of 10 seconds or router solicitation message which has expiration time of 30 seconds should be sent before its expiration.

- Ranging Rate: The interval for estimating the distance between neighbors. It depends on the location update rate required by the application and network mobility. In slightly mobile networks low ranges like 2 range estimations per second should be enough while in more mobile networks ranging rate could go up to 10 or 20 Hz.

- Movement Threshold: In some applications, the ranging rate can change depending on the mobility of the network. This threshold can be defined to increase the ranging rate in movements higher than this threshold.

- Buffer Size: In active ranging mode, the non-ranging traffic can be stored in the internal buffer while it is waiting for the next ranging packet. the large buffer size is an indicator of high non-ranging traffic and triggers the SRAC to switch to passive ranging.

Our scheduler algorithm minimizes the network traffic while satisfying all the application and network constraints:

$$\begin{aligned} \text{minimize} \quad & Ranging_{Traffic} + NonRanging_{Traffic} \\ \text{subject to} \quad & Ranging_{Rate} \geq Min_{Ranging_{Rate}} \\ & NonRanging_{Delay} \leq Max_{NonRanging_{Delay}} \\ & Buffer_{Size} \leq Max_{Buffer_{Size}} \end{aligned} \tag{6.5}$$

Algorithm 4 summarizes the SRAC algorithm.

As summarized in algorithm 4, SRAC runs in a while loop. Every $Window_{size}$, scheduler calculates the ranging rate and non-ranging traffic rate. It also updates minimum ranging rate based on average movement. The algorithm switches to minimum rate (ranging or non-ranging) based on measured values if this switch does not violate other constraints like maximum tolerable delay by non-ranging applications and minimum ranging rate.

**Algorithm 4** SRAC

$Delay_{Max} \leftarrow$ Maximum Non-Ranging Delay
$RR_{Min} \leftarrow$ Default Minimum Ranging Rate
$Th_{mov} \leftarrow$ Movement Threshold
$Window_{size} \leftarrow$ Widowing Average Size
$Buffer \leftarrow$ Buffer to Store Non-Ranging Traffic
**while** TRUE **do**
  **if** $Movement \geq Th_{Mov}$ **then**
    Increase $RR_{Min}$
  **end if**
  $R_{Ranging} \leftarrow$ Calculate Ranging Rate
  $R_{NonRanging} \leftarrow$ Calculate NonRanging Rate
  **if** $R_{Ranging} \leq R_{NonRanging}$ **then**
    **if** $Delay_{Max} \leq \frac{1}{R_{Ranging}}$ *and* $len(Buffer) \leq MaxBuffer$ **then**
      Switch to Active Ranging
    **else**
      Switch to Passive Ranging
    **end if**
  **else**
    **if** $R_{NonRanging} \geq RR_{Min}$ **then**
      Switch to Passive Ranging
    **else**
      Switch to Active Ranging
    **end if**
  **end if**
  Sleep for $Window_{size}$
**end while**

### 6.2.4 Ranging as a Service for WSN Applications

One of the key contributions of our work is analyzing the feasibility of using existing network traffic for ranging. Network traffic in our work has a general definition, it could be packets from a simple sensor which is reporting sensed temperature (few bytes) to the central sink (cluster head) every 10 seconds or it can be packets from an IPv6 enabled IoT device which supports a CoAP [77] server and answers the HTTP requests from other devices. Another example could be mesh of UWB-enabled nodes which are using RPL [81] and Trickle [52] algorithms for routing dissemination process over IEEE 802.15.4 MAC layer.

SRAC improves on the efficiency of ranging service on UWB networks by combining UWB's ranging and communication capabilities.

#### 6.2.4.1 OS Jitter & DW1000 Delayed Send

One concern about developing ranging service in embedded operating systems, is the impact of delay and jitter added by operating system to ranging. To recap, one of the critical points of centimeter level ranging in UWB systems is picoseconds level timestamping of send and receive events. For accurate ranging, we need to know the exact moment the signal left the antenna and the exact moment the first path received by the antenna. In reception, DW1000 timestamps the exact reception moment but for sending, it provides the concept of delayed send. During delayed send phase, a near future sending time (designated send time) is calculated and written on DW1000 registers. Once the internal timer of DW1000 chip arrives close enough ($designated\,timestamp - antenna\,delay$) to designated send time (40 bit value,15.6 picoseconds granularity) , the chip starts sending the signal.

In our work, we utilize delayed send feature to avoid the delay and jitter added by

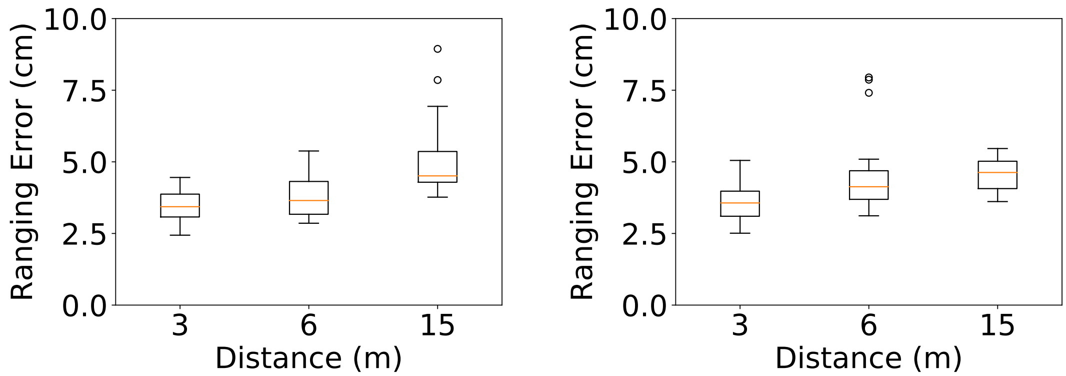

(a) Without SRAC

(b) With SRAC

Figure 6.4: Ranging error with and without SRAC. Piggybacking of ranging information does not change the accuracy of ranging.

operating system and network stack. Our experiments show if we set send timestamp around 5 ms after the time that application layer provides the outgoing data, it will leave enough gap for operating system to copy the message to DW1000's buffer and arm the chip to send the packet.

## 6.3 Performance Evaluation

We evaluate SRAC in two phases. In the first phase, over the set of controlled experiments, we evaluate the performance of SRAC for reducing network traffic by switching between active and passive ranging modes while meeting application constraints. In the second phase, we show the applicability of SRAC on different sensor network applications.

### 6.3.1 Implementing SRAC as a Network Service

To evaluate the performance of SRAC, we decided to implement SRAC as part of existing network stacks which are developed for embedded systems and Internet of

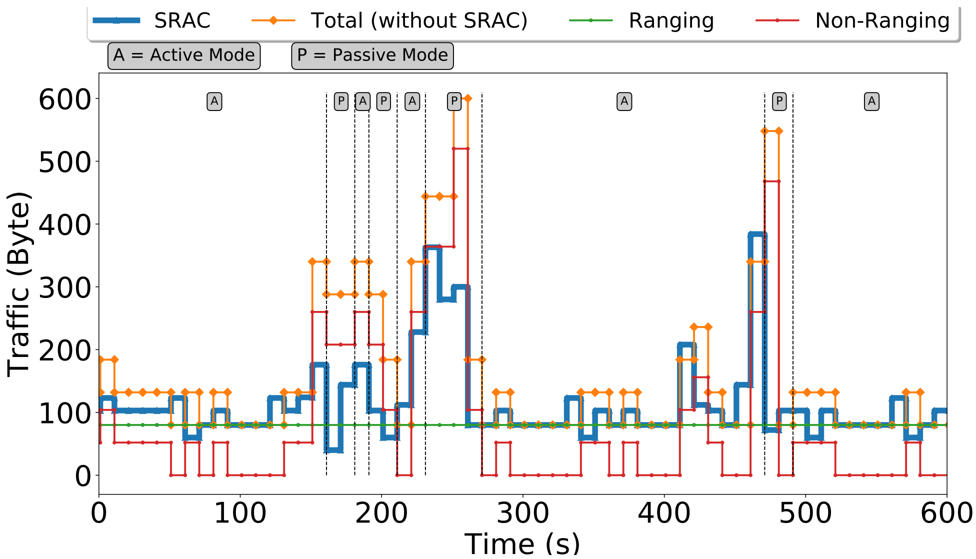


(a) 6 m Distance between Ranging Pairs

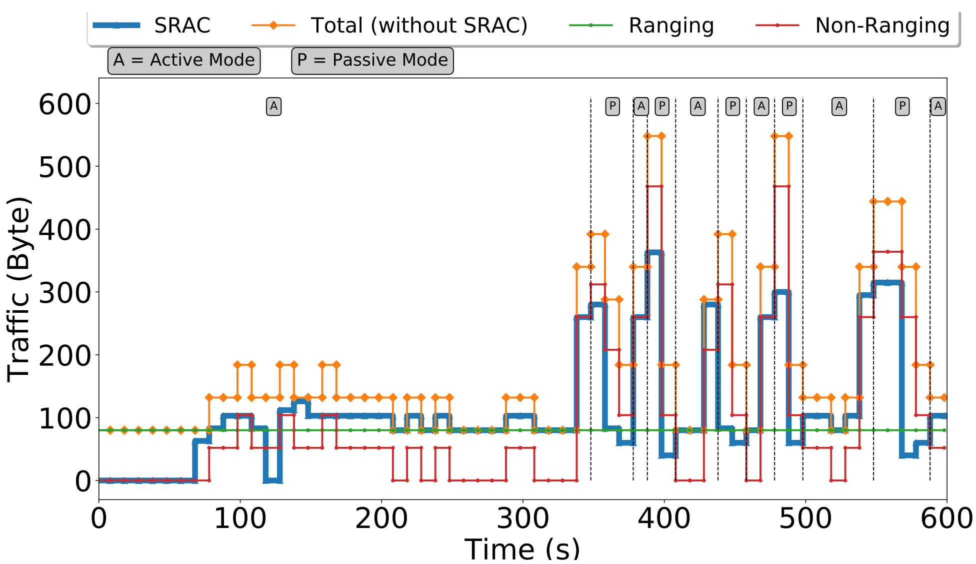


(b) 3 m Distance between Ranging Pairs

Figure 6.5: Traffic generated by SRAC. Traffic is measured in 10s intervals. SRAC adaptively switches between active and passive modes and piggybacks traffic. (Total = Ranging Traffic + Non-Ranging Traffic).

Thing applications.

Our hypothesis is that ranging can be implemented as a service provided by network stack alongside with other network services. Usually, embedded network stacks are part of embedded operating systems. We chose RIOT [21] operating system to implement SRAC. RIOT has smaller memory footprint compared to other embedded operating systems and also supports multi-threading and benefits from modular design [15]. We implemented UWB radio driver for RIOT and integrated it into the RIOT's core.

To implement passive ranging, we modified the send functionality of network driver. Whenever there is a packet to send (non-ranging traffic), and the mode is passive, the ranging information will be added to the outgoing packet but if the mode is active, the packet will be stored in a queue waiting for next outgoing ranging packet.

Since RIOT supports multi-thread programming we developed active ranging as a separate thread. The active ranging thread takes the ranging interval as input and periodically conducts ranging (broadcast poll message, receive responses and send final message). During transmission of ranging packet, it checks the internal buffer for any queued message and piggybacks the ranging packet with non-ranging traffic.

The scheduler thread monitors the ranging and non-ranging traffics and based on our proposed algorithm 4 decides about the ranging mode.

### 6.3.2 Controlled Experiments: How Effective is the SRAC?

#### 6.3.2.1 Experiment Setup

DW1000 [4] is one of the most popular UWB-enabled radio ICs which is already being used in many commercial UWB-based indoor localization solutions [12, 19]. In our experiments, we use Radino32 [13] platform which combines an STM32L151 [16] micro-controller with the DW1000 chip.

In this phase of evaluation, we placed two Radino32 nodes in three different distances (3 m, 6 m, and 15 m) and ran SRAC on both of them which by default is in active ranging mode (1 ranging every 5 seconds). Also during the experiment, there is a random UDP traffic generated by the application layer (Using RIOT's UDP server/client package). The maximum delay that non-ranging applications can tolerate is 2 seconds in this experiment. Both nodes report ranging results and packet dump of sent and received packets over serial port. In each distance, we collected data for 10 minutes.

#### 6.3.2.2 Ranging Accuracy

First metric to evaluate is the accuracy of ranging conducted by SRAC. Figure 6.4b shows the average errors in range estimation in each experiment. It can be seen in Figure 6.4b that regardless of active or passive mode running on the devices, the ranging error never exceeds a few centimeters (10 cm). As we expected even long ranging interval (5 seconds) does not have any impact on the ranging performance.

We also conduct the same set of experiments but this time just running simple ranging application between a pair of UWB nodes. The ranging errors are shown in Figure 6.4a. Comparing Figure 6.4a and 6.4b the difference between errors is less than 1 cm which proves that SRAC does not increase the ranging errors.

#### 6.3.2.3 Traffic Reduction

In this section, we show the ranging and non-ranging traffic during previous experiments at 3 m and 6 m distances. Figure 6.5 shows the ranging, non-ranging, total (ranging + non-ranging) and SRAC (real traffic sent by physical layer) traffic observed during the experiment. The windows size in scheduler algorithm in this experiment has been set to 10 seconds which means the scheduler algorithm always calculates the average traffic over the last 10 seconds to decide about the ranging modes. The reported values in Figure 6.5 are also traffic measured in each windows (10 seconds). Since in this experiment both nodes are static, the ranging traffic is always on default values (once every 5 seconds).

As shown in Figure 6.5, the proposed solution adapts to the network changes and reduces network traffic. In Figure 6.5 the total line shows the amount of traffic would have been sent by physical layer if SRAC was not there and the SRAC line, shows the traffic sent by physical layer after SRAC piggybacked either ranging traffic over non-ranging traffic or visa-versa.

Figure 6.5 also shows the proposed scheduler algorithm is effectively changing the mode based on the network condition shortly after sudden changes to the non-ranging traffic.

To quantify the amount of traffic reduction achieved by SRAC, we calculated traffic reduction ($TrafficReduction = \frac{Total_{traffic} - SRAC_{traffic}}{Total_{traffic}}$) for intervals of 10 seconds and plotted the CDF of the savings in Figure 6.6.

As shown in Figure 6.6, for almost 50% of the times the amount of traffic reduction achieved by SRAC is bigger than 40%. In 75% of the times, the amount of reduction is higher than 25%.

#### 6.3.2.4 Time Delay in SRAC

To achieve network traffic reduction, our scheduler may have to queue the packets. Queuing may lead to an increase in the transmission delay in non-ranging traffic.

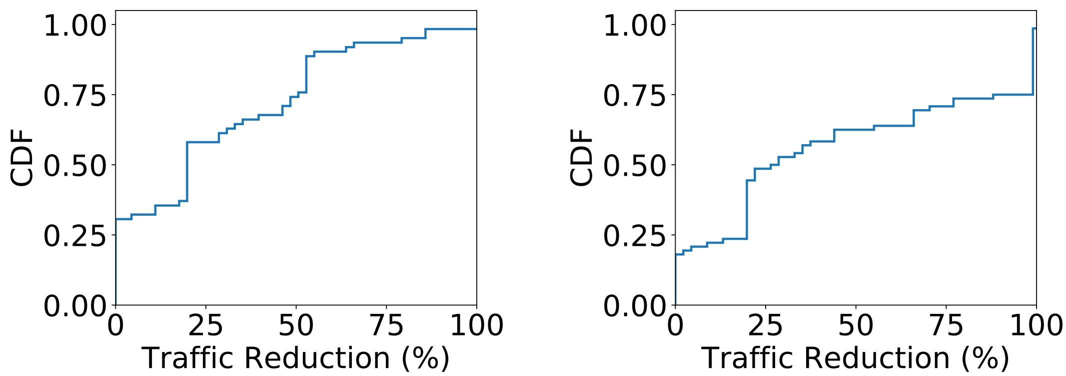


(a) 6 m Distance

(b) 3 m Distance

Figure 6.6: SRAC achieves more than 40% traffic reduction in 50% of times.

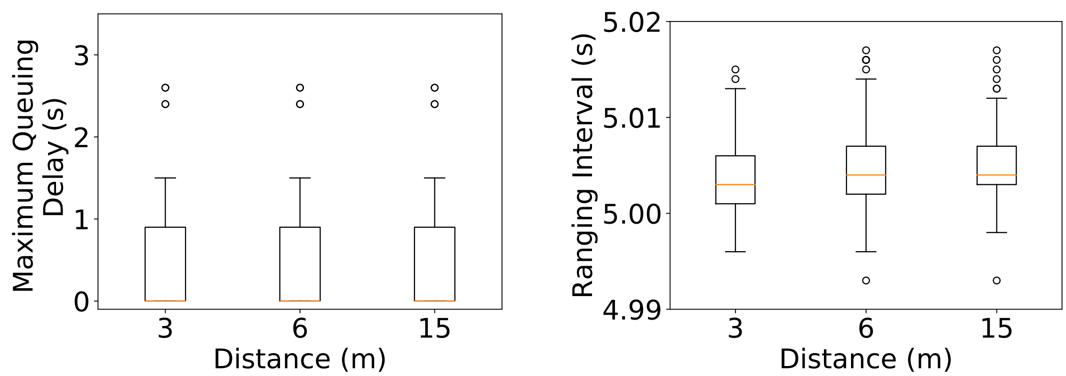


(a) Maximum Queue Time

(b) Ranging Update Intervals

Figure 6.7: Time delay in SRAC. SRAC does not violate time constraints in ranging and non-ranging applications

Figure 6.7a shows the delay faced by packets during the experiments. The added delay is reasonably low considering amount of saving on network traffic.

We also measured the time difference between every two consecutive range estimations to make sure the ranging update interval is never below the minimum acceptable ranging rate. The calculated intervals are reported in Figure 6.7b.

As shown in Figure 6.7b, the time interval between two consecutive ranging updates never exceeds 5.2 seconds which shows the fact that SRAC keeps its promise to meet application constraints (20 ms of delay can be tolerated by ranging applications).

Overall, SRAC achieves significant ($\approx$ 40%)traffic reductions and reduces the air time. Reduced air time reduces the chance of interference in UWB networks.

### 6.3.3 Uncontrolled Experiments: Is SRAC applicable in existing WSN applications?

Mesh networks in combination with IPv6 can connect local area networks to the Internet and turn the local network to real Internet of Things. In the second phase of our evaluations, over a set of uncontrolled experiments,we show applicability of our solution to add ranging to UWB networks using existing traffic. The idea here is to have ranging enabled UWB mesh networks which are able to simultaneously transfer application data and estimate their distance to neighbor nodes. In other words, we wanted to know the scenarios in which SRAC is applicable and can it save significant traffic in real world applications?

Many applications can benefit from accurate distance measurement between nodes and being able to track/localize mesh members. Mobile sensor and ad-hoc networks can directly benefit from accurate ranging. Location aware routing [54] and mobile sink sensor networks [35] can be named as a few examples.

#### 6.3.3.1 Experiment Setup

To evaluate the performance of proposed solution in IPv6 enabled mesh networks, we set up network of 12 UWB-enabled nodes (Radino32) in a corridor (3.5 m $\times$ 20 m). They are all running RPL protocol (implemented by RIOT operating system) over 6LoWPAN [65] and IEEE 802.15.4 MAC Layers. In the physical layer our implemented UWB driver (SRAC) is running. Figure 6.8b shows our setup in the corridor.

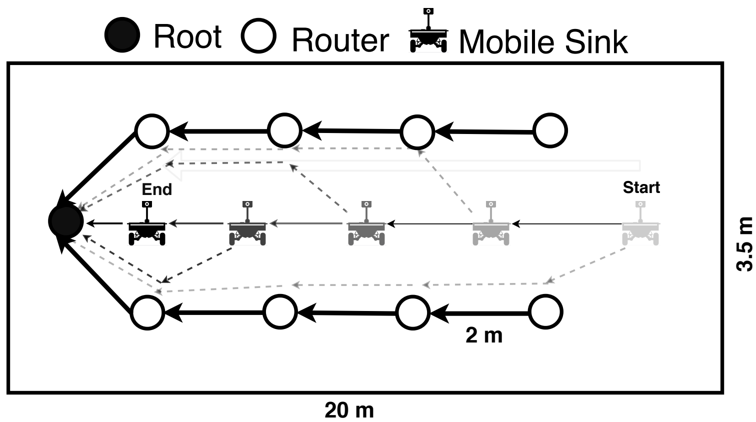


(a) DODAG created by RPL.

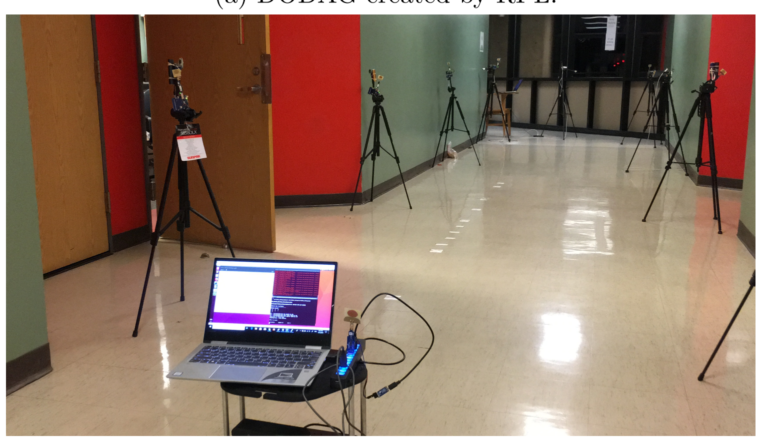

(b) Deployed UWB Mesh Network

Figure 6.8: UWB mesh network experiment setup.

The deployed network has one root and 11 RPL routers. As shown in Figure 6.8a, root and 10 of the nodes are in static locations but the 12th node is mounted on top of a robot. We configure transmission power of UWB nodes to create multi-hop network so that RPL forms the DODAG (Destination Oriented Directed Acyclic Graph) shown in Figure 6.8a. The robot travels from starting point which is 4 hops away from the root to the end point in which the root is within transmission range of the mobile node. During the travel, every 3 m, mobile node stops for 1 minute and again resumes the move. During the move from start to end point, mobile node generates a UDP traffic with constant rate and sends it to the root of DODAG over multihop network. During stop times, the mobile node looks for new parent (node which is closer to the root) and updates its next hop accordingly. Localization is also running on the Robot.

We conducted this experiment several times by changing different parameters to measure SRAC's performance on different scenarios. The experiment parameters are listed in table 6.1. First parameter is speed of robot which impacts the minimum acceptable ranging rate for SRAC. We are interested to know the location of the robot every 5 cm movement which means if the robot moves with 10 cm per second speed, the minimum acceptable ranging rate would be 2 updates per second. The second parameter is the UDP traffic generated by mobile node. We use three sources of application traffic in our experiments: first from a camera that takes video at 5 frames per second, second from a sound sensor that generates data at 1 KBps, and third from a sensor kit that generates data at 20 Bps. The last parameter is responsiveness of RPL. In our experiments, we test two different settings for RPL which we call them fast and slow RPL. The main difference between fast and slow RPL is how fast the RPL reacts to network changes which largely determines total traffic generated by RPL protocol. During all the experiments, all the nodes are using the same physical

Table 6.1: Settings of Uncontrolled Experiments with Mobile Robot

| Parameter | Value |
|---|---|
| Robot Speed (cm per second) | 10, 30, 70 |
| Traffic | Video (100 KBps), Sound (1 KBps), Sensor Kit (20 Bps) |
| Fast RPL | $I_{min} = 64ms, I_{max} = 17m, K = 3$ |
| Slow RPL | $I_{min} = 1024ms, I_{max} = 4h, K = 7$ |

layer settings (Frequency = Channel 2 (3494 MHz), Preamble Length = 1024, PRF = 16 MHz, Data rate = 6.8 Mbps). All the nodes are deployed at a height of 120 cm from the ground and have clear line of sight to each other. The surrounding walls are wooden and there is no blocking by obstacles during the experiments.

Table 6.2: Traffic Reductions Achieved by SRAC in Uncontrolled Experiments

(a) Fast RPL

| Speed \ Traffic | Video | Sound | Sensor Kit |
|---|---|---|---|
| 10 | 0.49% | 32.21% | 12.52% |
| 30 | 1.47% | 41.57% | 5.49 % |
| 70 | 3.37% | 23.40% | 2.49% |

(b) Slow RPL

| Speed \ Traffic | Video | Sound | Sensor Kit |
|---|---|---|---|
| 10 | 0.30% | 27.32% | 8.07% |
| 30 | 1.31% | 35.05% | 3.54% |
| 70 | 2.07% | 20.1% | 1.34% |

#### 6.3.3.2 Traffic Reductions by SRAC in Uncontrolled Experiments

In table 6.2, the overall traffic (Bytes) reductions achieved by SRAC are summarized. It can be seen from table 6.2 that savings as high as 41% can be achieved by SRAC which proves the effectiveness of proposed technique.

As can be seen in table 6.2 in applications with extremely low or high traffic (sensor kit/video) the percentage of traffic reductions are not that significant which is reasonable considering the ratio of ranging traffic over non-ranging traffic. We have to mention, in all numbers reported in table 6.2, the number of bytes required

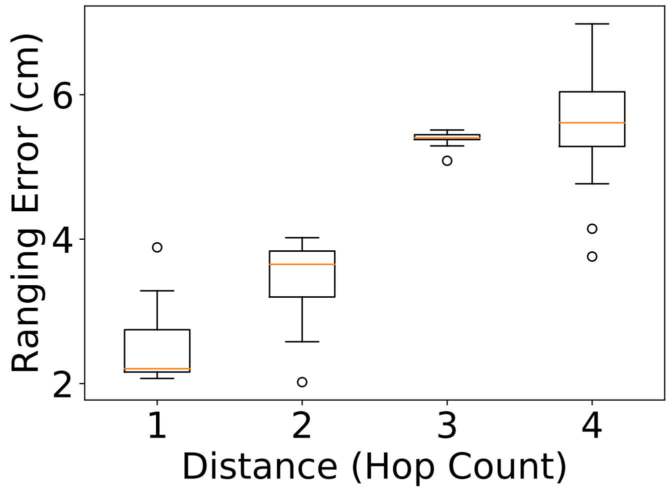


Figure 6.9: Ranging error observed by mobile robot in uncontrolled experiments

by SRAC to include time information have been included which means during all the scenarios SRAC leads to traffic reduction and the overhead proposed by SRAC to the network is negligible.

#### 6.3.3.3 Ranging Accuracy

Figure 6.9 reports ranging errors during uncontrolled experiments which shows the maximum observed ranging error during our uncontrolled experiments is less than 7 cm and the average error is around 5 cm which is comparable with average ranging accuracy reported by state of the art UWB based indoor localization solutions [60].

## 6.4 Discussion

Reducing traffic is important in low rate-wireless personal area network but it is more important in the context of ranging performance. Our experiments show that even in the small network of UWB nodes (8 nodes) with 5 ranging per second per node

, there is high chance of interference (50%). This interference from non-cooperative UWB nodes increases the packet drop rates and in the case of successful reception of packet, the ranging error increases significantly (60 cm on average). The observations from our small experiment emphasize the importance of reducing network traffic to reduce chance of interference.

Our approach is mostly practical in mesh networks with moderate mobility. In highly mobile networks, the non-ranging traffic will not be enough and our solution goes to active ranging mode which is still better than having both ranging and non-ranging traffics. Since, in active mode, non-ranging traffic will be piggybacked over ranging traffic.

One of the interesting implications of providing ranging service over mesh networks is the ability to estimate distance over several hops. In other words, the target does not need to be in direct contact with all the anchors. Only contacting one anchor can provide location information about other anchors which can be used for localization. The only modification to existing RPL protocol would be including location information from neighbors inside DAO messages. The major benefit would be saving extra ranging traffic.

## 6.5 Conclusion

In this work, we showed that two way ranging does not require the reply packets to be sent immediately. We utilize this feature and study the feasibility of using existing network traffic for ranging instead of having separate traffic for ranging. We showed the feasibility of piggybacking ranging information over normal network traffic to reduce the ranging overhead in UWB networks. We also investigated the possibility of utilizing ranging traffic for communication purposes and reducing overall network traffic.

Based on observed results, we proposed a simple yet effective scheduling algorithm which simultaneously sends non-ranging and ranging information embedded in existing network traffic. We developed our proposed solution on RIOT which is an open source embedded system and evaluated the effectiveness of our proposed solution. Our evaluations show 40% reduction in overall network traffic after using our proposed adaptive scheduler.

# Chapter 7

# Conclusion

In this dissertation, we studied the scalability of existing UWB-based indoor localization techniques and provided practical solutions to improve improve the robustness, scalability, and applicability of UWB networks in indoor environments. We analyzed four basic problems related to scalability of UWB networks and proposed simple yet effective techniques to address them. To be specific, we made the following contributions:

**Adaptively Changing Physical Layer Setting**. We studied the impact of each of the parameters in the UWB physical layer on ranging performance. Based on the observed impact, we proposed our technique to adaptively change physical layer setting for best ranging performance while maintaining application requirements in terms of energy and delay.

**Single Anchor UWB Localization**. Most of existing UWB-based indoor localization techniques require line of sight access to at least three anchors for accurate estimation of the target's location in a 2D setting. We proposed single anchor UWB indoor localization based on unique fingerprints generated from UWB signals. Our technique can locate the target in a $20cm \times 20cm$ square with 0.96 F1 score. Our technique can be combined with existing solutions and can locate the target even in scenarios where it is not possible to have three anchors.

**Interference Resilience: Random Pulse Shape Identification**. We study the possibility of UWB interference in common settings and applications and how that interference impacts ranging performance. We propose simple yet effective techniques to detect the ranging impacted by interference and mitigate the impact of interference on ranging. Our technique can reduce 50% of errors due to the interference.

**Simultaneous Ranging and Communication in UWB Networks**. Most of the focus on today's research in UWB networks is about their ranging capability. We study the feasibility of combining ranging traffic with non-ranging traffic in UWB networks to expand the applicability of UWB radios to non-ranging applications. We propose our scheduler to monitor existing traffic and piggyback either ranging traffic over non-ranging traffic or vice-versa depending on the setting that will reduce network overhead. Our evaluation showed 20% reduction in total traffic in UWB networks while running both ranging and non-ranging applications.

## 7.1 Looking forward

UWB-based indoor localization is becoming a standard approach as time passes and researchers resolve most of its challenges. Very accurate localization results alongside with reliable and robust deployments make the UWB networks more popular. Millimeter-wave and 5G are relatively new topics and gaining more attention. Lessons learned from UWB indoor localization can be applied to those standards and help to have more global indoor localization solutions. One of the key challenges for UWB networks is the availability of chips that support these signals. The 5G standard is almost there and would be on all the cellphones in a few years from now. Based on the high frequency and larger bandwidth available on 5G networks, one potential line of research would be to investigate the feasibility of accurate ranging on 5G networks and to apply localization techniques from the UWB world to 5G.

# Bibliography


[1] Ciholas indoor localization solution. https://www.ciholas.com/. Accessed: 2019-04-08.

[2] Decawave indoor localization solution. https://www.decawave.com/products/trek1000. Accessed: 2019-04-08.

[3] DW1000 data sheet. https://www.decawave.com/wp-content/uploads/2018/09/dw1000_datasheet_v2.17.pdf. Accessed: 2019-04-08.

[4] DW1000 radio ic. https://www.decawave.com/product/dw1000-radio-ic/. Accessed: 2019-04-08.

[5] EVB1000 board data sheet. https://www.decawave.com/wp-content/uploads/2018/09/evk1000kit_description.pdf. Accessed: 2019-04-08.

[6] EVB1000 boards by decawave. https://www.decawave.com/product/evk1000-evaluation-kit/. Accessed: 2019-04-08.

[7] EVB1000 evaluational kit. https://www.decawave.com/products/evk1000-evaluation-kit. Accessed: 2019-04-08.

[8] Fourier resampling. https://docs.scipy.org/doc/scipy-0.18.1/reference/generated/scipy.signal.resample.html. Accessed: 2019-04-08.

[9] IEEE 802.15.4-11 standard. http://www.ieee802.org/15/pub/TG4.html. Accessed: 2019-04-08.

[10] Incircuit radino32 data sheet. https://wiki.in-circuit.de/images/6/63/305000092A_radino32_DW1000.pdf. Accessed: 2019-04-08.

[11] Inter channel interference in DW1000. https://www.decawave.com/sites/default/files/aph010_dw1000_inter_channel_interference.pdf. Accessed: 2019-04-08.

[12] Pozyx indoor localization solution. https://www.pozyx.io/Documentation/faq. Accessed: 2019-04-08.

[13] Radino32 board. https://wiki.in-circuit.de/index.php5?title=radino32_DW1000. Accessed: 2019-04-08.

[14] Redpoint indoor localization solution. https://www.redpointpositioning.com/products-services/. Accessed: 2019-04-08.

[15] RIOT, the friendly operating system for the internet of things. https://www.riot-os.org/. Accessed: 2019-04-08.

[16] Stm32l1 datasheet. https://www.st.com/resource/en/datasheet/cd00277537.pdf. Accessed: 2019-04-08.

[17] Time domain indoor localization solution. https://timedomain.com/products/pulson-440/. Accessed: 2019-04-08.

[18] Turtlebot. http://www.turtlebot.com/. Accessed: 2019-04-08.

[19] Uniset indoor localization system. http://www.unisetcompany.com/sequitur-family-en. Accessed: 2019-04-08.

[20] Alohanet. https://en.wikipedia.org/wiki/ALOHAnet. Accessed: 2019-04-08.

[21] E. Baccelli, C. Gündoğan, O. Hahm, P. Kietzmann, M. S. Lenders, H. Petersen, K. Schleiser, T. C. Schmidt, and M. Wählisch. Riot: an open source operating system for low-end embedded devices in the iot. *IEEE Internet of Things Journal*, 2018.

[22] O. Bialer, D. Raphaeli, and A. J. Weiss. Efficient time of arrival estimation algorithm achieving maximum likelihood performance in dense multipath. *IEEE Transactions on Signal Processing*, 60(3):1241–1252, 2012.

[23] N. Carey. Establishing pedestrian walking speeds. *Karen Aspelin, Portland State University*, 1(01), 2005.

[24] G. Caso, M. T. Le, L. De Nardis, and M.-G. Di Benedetto. Performance comparison of wifi and uwb fingerprinting indoor positioning systems. *Technologies*, 6(1):14, 2018.

[25] C.-C. Chong, F. Watanabe, and M. Z. Win. Effect of bandwidth on uwb ranging error. In *WCNC 2007*, pages 1559–1564. IEEE, 2007.

[26] P. Corbalán and G. P. Picco. Concurrent ranging in ultra-wideband radios: Experimental evidence, challenges, and opportunities. 2018.

[27] D. Dardari, A. Conti, U. Ferner, A. Giorgetti, and M. Z. Win. Ranging with ultrawide bandwidth signals in multipath environments. *Proceedings of the IEEE*, 97(2):404–426, 2009.

[28] C. Di Franco, A. Prorok, N. Atanasov, B. Kempke, P. Dutta, V. Kumar, and G. J. Pappas. Calibration-free network localization using non-line-of-sight ultra-wideband measurements. In *IPSN'17*. IEEE, 2017.

[29] DW1000 power calculator. `https://www.decawave.com/sites/default/files/dw1000productpowercalc/`. Accessed: 2019-04-08.

[30] DW1000 technical detail by decawave co. `https://www.decawave.com/product/dw1000-radio-ic/`. Accessed: 2019-04-08.

[31] R. Faragher and R. Harle. Location fingerprinting with bluetooth low energy beacons. *IEEE journal on Selected Areas in Communications*, 33(11):2418–2428, 2015.

[32] M. Flury and J.-Y. Le Boudec. Interference mitigation by statistical interference modeling in an impulse radio uwb receiver. In *IEEE International Conference on Ultra-Wideband (ICUWB 2006)*, number LCA-CONF-2006-017, 2006.

[33] M. Flury, R. Merz, and J.-Y. Le Boudec. Synchronization for impulse-radio uwb with energy-detection and multi-user interference: Algorithms and application to ieee 802.15. 4a. *IEEE Transactions on Signal Processing*, 59(11):5458–5472, 2011.

[34] M. Ghasemlou, S. N. ESFAHANI, and V. V. TABATABA. An improved method for toa estimation in th-uwb system considering multipath effects and interference. 2014.

[35] N. Ghosh and I. Banerjee. Application of mobile sink in wireless sensor networks. In *Communication Systems & Networks (COMSNETS), 2018 10th International Conference on*, pages 507–509. IEEE, 2018.

[36] B. Großwindhager, C. A. Boano, M. Rath, and K. Römer. Concurrent ranging with ultra-wideband radios: From experimental evidence to a practical solution. In *2018 IEEE 38th International Conference on Distributed Computing Systems (ICDCS)*, pages 1460–1467. IEEE, 2018.

[37] B. Großwindhager, C. A. Boano, M. Rath, and K. Römer. Enabling runtime adaptation of physical layer settings for dependable uwb communications. In *19th IEEE Intl. Symp. on a World of Wireless, Mobile and Multimedia Networks (WoWMoM'18*, June 2018.

[38] B. Großwindhager, M. Rath, J. Kulmer, S. Hinteregger, M. Bakr, C. A. Boano, K. Witrisal, and K. Römer. Demo abstract: Uwb-based single-anchor low-cost indoor localization system. 2017.

[39] I. Guvenc and Z. Sahinoglu. Low complexity toa estimation for impulse radio uwb systems. *IEEE Journal on Selected Areas in communication*, 2005.

[40] M. Heydariaan, H. Mohammadmoradi, and O. Gnawali. Toward Standard Non-line-of-sight Benchmarking of Ultra-wideband Radio-based Localization. In *CPS-Bench '18*, 2018.

[41] IEEE 802.15.4. https://standards.ieee.org/findstds/standard/802.15.4-2011.html. Accessed: 2019-04-08.

[42] G. Ismail and S. Zafer. Threshold-based toa estimation for impulse radio uwb systems. In *2005 IEEE International Conference on Ultra-Wideband*, pages 420–425, Sept 2005.

[43] A. R. Jimnez and F. Seco. Comparing decawave and bespoon uwb location systems: Indoor/outdoor performance analysis. In *2016 International Conference on Indoor Positioning and Indoor Navigation (IPIN)*, pages 1–8, Oct 2016.

[44] M. Jonsson and K. Kunert. Towards reliable wireless industrial communication with real-time guarantees. *IEEE Transactions on Industrial Informatics*, 5(4):429–442, Nov 2009.

[45] B. Kempke, P. Pannuto, B. Campbell, and P. Dutta. Surepoint: Exploiting ultra wideband flooding and diversity to provide robust, scalable, high-fidelity indoor localization. In *SenSys'16*, pages 137–149, New York, NY, USA, 2016. ACM.

[46] K. Kikuta and A. Hirose. Interference mitigation in uwb receivers utilizing the differences in direction of arrival and power spectrum density. In *Microwave Conference (APMC), 2015 Asia-Pacific*, volume 1, pages 1–3. IEEE, 2015.

[47] K. Kikuta and A. Hirose. Direction-of-arrival estimation of ultra-wideband signals in narrowband interference environment based on power inversion and complex-valued neural networks. *Neural Processing Letters*, 47(3):921–933, 2018.

[48] H. Kim. Double-sided two-way ranging algorithm to reduce ranging time. *IEEE Communications letters*, 13(7), 2009.

[49] N. F. Krasner. Interference mitigation for positioning systems, Aug. 22 2017. US Patent 9,739,872.

[50] J. Kulmer, S. Hinteregger, B. Großwindhager, M. Rath, M. S. Bakr, E. Leitinger, and K. Witrisal. Using decawave uwb transceivers for high-accuracy multipath-assisted indoor positioning. In *IEEE Communications Workshops 2017(ICC Workshops)*, pages 1239–1245. IEEE, 2017.

[51] T.-H. Lee, Y.-W. Kuo, Y.-W. Huang, and Y.-H. Liu. To piggyback or not to piggyback acknowledgments? In *Vehicular Technology Conference (VTC 2010-Spring), 2010 IEEE 71st*, pages 1–5. IEEE, 2010.

[52] P. Levis, T. Clausen, J. Hui, O. Gnawali, and J. Ko. The trickle algorithm. Technical report, 2011.

[53] C. Li, H.-B. Li, and R. Kohno. Performance evaluation of ieee 802.15. 4 for wireless body area network (wban). In *Communications Workshops, 2009. ICC Workshops 2009. IEEE International Conference on*, pages 1–5. IEEE, 2009.

[54] W.-H. Liao, J.-P. Sheu, and Y.-C. Tseng. Grid: A fully location-aware routing protocol for mobile ad hoc networks. *Telecommunication systems*, 18(1-3):37–60, 2001.

[55] W. Liu, H. Ding, X. Huang, and Z. Liu. Toa estimation in ir uwb ranging with energy detection receiver using received signal characteristics. *IEEE Communications Letters*, 16(5):738–741, 2012.

[56] J. Luo and H. Gao. Deep belief networks for fingerprinting indoor localization using ultrawideband technology. *International Journal of Distributed Sensor Networks*, 12(1):5840916, 2016.

[57] T. Lyu. *Threshold Selection Based on the SNR in Time of Arrival Localization System*. PhD thesis, Oregon State University, 2016.

[58] M. Mati. *Identification & Mitigation of NLOS Information for UWB based Indoor Localization*. PhD thesis, University of Windsor (Canada), 2016.

[59] M. McLaughlin and B. Verso. Asymmetric double-sided two-way ranging in an ultrawideband communication system, Mar. 1 2018. US Patent App. 15/500,633.

[60] Microsoft indoor localization competition, 2018. `https://www.microsoft.com/en-us/research/event/microsoft-indoor-localization-competition-ipsn-2018/`. Accessed: 2019-04-08.

[61] H. Mohammadmoradi and O. Gnawali. Study and mitigation of non-cooperative uwb interference on ranging. In *EWSN*, 2019.

[62] H. Mohammadmoradi, M. Heydariaan, and O. Gnawali. Uwb physical layer adaptation for best ranging performance within application constraints. In *Proceedings of the 2Nd International Conference on Smart Digital Environment*, ICSDE'18, pages 119–126, New York, NY, USA, 2018. ACM.

[63] H. Mohammadmoradi, M. Heydariaan, and O. Gnawali. Srac: Simultaneous ranging and communication in uwb networks. In *2019 International Conference on Distributed Computing in Sensor Systems (DCOSS)*. IEEE, 2019.

[64] H. Mohammadmoradi, M. Heydariaan, O. Gnawali, and K. Kim. Uwb-based single-anchor indoor localization using channel impulse response. In *Proceedings of the Workshop on Computing, Networking and Communications (CNC 2019)*, 2019.

[65] G. Mulligan. The 6lowpan architecture. In *Proceedings of the 4th workshop on Embedded networked sensors*, pages 78–82. ACM, 2007.

[66] S. Murali and A. Jamalipour. Mobility-aware energy-efficient parent selection algorithm for low power and lossy networks. *IEEE Internet of Things Journal*, pages 1–1, 2018.

[67] J. Nagle. Congestion control in ip/tcp internetworks. *ACM SIGCOMM Computer Communication Review*, 14(4):11–17, 1984.

[68] N. Nasios and A. G. Bors. Variational learning for gaussian mixture models. *IEEE Transactions on Systems, Man, and Cybernetics, Part B (Cybernetics)*, 36(4):849–862, 2006.

[69] B. Oded, R. Dan, and W. Anthony. Two-way range estimation utilizing uplink and downlink channels dependency. *IEEE Transactions on Signal Processing*, 62(7):1619–1633, April 2014.

[70] Y. Qin, D. Wang, J. Li, R. Liu, and Z. Lu. Cs-based narrowband interference estimation and suppression for uwb system. In *2018 13th APCA International Conference on Control and Soft Computing (CONTROLO)*, pages 75–79. IEEE, 2018.

[71] J. Romme, J. H. C. van den Heuvel, G. Dolmans, G. Selimis, K. Philips, and H. de Groot. Measurement and analysis of uwb radio channel for indoor localization in a hospital environment. In *2014 IEEE International Conference on Ultra-WideBand (ICUWB)*, pages 274–279, Sept 2014.

[72] D. K. Rout and S. Das. Multiple narrowband interference mitigation using hybrid hermite pulses for body surface to external communications in uwb body area networks. *Wireless Networks*, 23(2):387–402, 2017.

[73] Z. Sahinoglu and S. Gezici. Ranging in the ieee 802.15.4a standard. In *2006 IEEE Annual Wireless and Microwave Technology Conference*, pages 1–5, Dec 2006.

[74] Z. Sahinoglu and I. Guvenc. Multiuser interference mitigation in noncoherent uwb ranging via nonlinear filtering. *EURASIP Journal on Wireless Communications and Networking*, 2006(2):67–67, 2006.

[75] S. Sharma, V. Bhatia, and A. Gupta. Sparsity-based narrowband interference mitigation in ultra wide-band communication for 5g and beyond. *Computers & Electrical Engineering*, 64:83–95, 2017.

[76] S. Sharma, A. Gupta, and V. Bhatia. Impulse noise mitigation in ir-uwb communication using signal cluster sparsity. *IEEE Communications Letters*, 22(3):558–561, 2018.

[77] Z. Shelby, K. Hartke, and C. Bormann. The constrained application protocol (coap). Technical report, 2014.

[78] X. Shen, M. Guizani, R. C. Qiu, and T. Le-Ngoc. *Ultra-wideband wireless communications and networks*. John Wiley & Sons, 2007.

[79] S. Shi, S. Sigg, and Y. Ji. Probabilistic fingerprinting based passive device-free localization from channel state information. In *VTC'16*, pages 1–5. IEEE, 2016.

[80] TREK1000 by decawave co. http://www.decawave.com/products/trek1000. Accessed: 2019-04-08.

[81] T. Winter, P. Thubert, A. Brandt, J. Hui, R. Kelsey, P. Levis, K. Pister, R. Struik, J. P. Vasseur, and R. Alexander. Rpl: Ipv6 routing protocol for low-power and lossy networks. Technical report, 2012.

[82] R. Yang and H. Zhang. Rssi-based fingerprint positioning system for indoor wireless network. In *LSMS'14*, pages 313–319. Springer, 2014.

[83] Z. Yang, Z. Zhou, and Y. Liu. From rssi to csi: Indoor localization via channel response. *ACM Computing Surveys (CSUR)*, 46(2):25, 2013.